APR 19 '46

UNITED STATES DEPARTMENT OF COMMERCE

Journal of Research

of the

National Bureau of Standards

Vol. 36, No. 2 February 1946

CONTENTS

RP	TITLE AND AUTHOR	Page
1693.	Heat capacity of a two-phase system, with applications to vapor corrections in calorimetry. Harold J. Hoge.....[Price 5 cents]	111
1694.	A method for determining small amounts of gold, and its use in ascertaining the thickness of electrodeposited gold coating. W. Stanley Clabaugh.....[Price 5 cents]	119
1695.	Purification and properties of 29 paraffin, 4 alkylcyclopentane, 10 alkylcyclohexane, and 8 alkylbenzene hydrocarbons. Alphonse F. Forziati, Augustus R. Glasgow, Jr., Charles B. Willingham, and Frederick D. Rossini.....[Price 5 cents]	129
1696.	Effect of some added materials on dicalcium silicate. Edwin S. Newman and Lansing S. Wells.....[Price 10 cents]	137
1697.	Reproducibility of the lead electrode and the electromotive force of the lead stick-lead amalgam cell at 0° to 60° C. Roger G. Bates, Murray Edelstein, and S. F. Acree.....[Price 5 cents]	159
1698.	Engine tests with producer gas. Frederic A. Middleton and Clarence S. Bruce.....[Price 5 cents]	171
1699.	Phase equilibrium relations in a portion of the system Na_2O-CaO-Al_2O_3-SiO_2. Kenneth T. Greene and R. H. Bogue.[Price 10 cents]	185

The articles listed may be purchased separately (see cover page II) at the prices stated

A monthly periodical of pure and applied science published by our National Government

Journal of Research
of the
National Bureau of Standards

The January 1946 issue of the JOURNAL OF RESEARCH of the National Bureau of Standards began the thirty-sixth semiannual volume of this periodical. Fundamental researches in progress in the Bureau's laboratories are reported in this JOURNAL. If you are interested in new developments in science and technology you should receive the JOURNAL. If you are not already a subscriber, you are invited to send in your subscription.

Technical News Bulletin

This is a monthly publication containing short articles reporting progress of work in the Bureau laboratories, abstracts of papers that appear in the JOURNAL OF RESEARCH, accounts of scientific and technical meetings in which the Bureau has taken part, a list of all publications by members of the staff, and other items within the Bureau's fields. The BULLETIN is designed primarily to give a general and timely review of the activities of the Bureau in brief form. It is a prompt and reliable source of official information. If you have not already subscribed for the BULLETIN, you are invited to do so.

ANNUAL SUBSCRIPTION	Price	
	United States, Canada, Cuba, Mexico, Newfoundland, Republic of Panama	Other countries
JOURNAL OF RESEARCH of the National Bureau of Standards:		
12 monthly issues (2 volumes), paper covers	$3.50	$4.50
Bound volume (½ year, 1 volume), blue buckram	3.00	3.50
Technical News Bulletin, 12 monthly issues	.50	.70

Research Papers, reprinted individual articles appearing in the JOURNAL OF RESEARCH, are available from the Superintendent of Documents shortly after appearance of monthly issues of the JOURNAL.

Address orders only to
Superintendent of Documents, U. S. Government Printing Office
Washington 25, D. C.

UNITED STATES DEPARTMENT OF COMMERCE
HENRY A. WALLACE, Secretary
NATIONAL BUREAU OF STANDARDS
E. U. CONDON, Director

✦

Journal of Research

of the

National Bureau of Standards

✦

Volume 36, Number 2

February 1946

[Published with approval of the Director of the Budget]

UNITED STATES
GOVERNMENT PRINTING OFFICE
WASHINGTON : 1946

For sale by the Superintendent of Documents, U. S. Government Printing Office
Washington 25, D. C. - Price 30 cents, $3.50 per year on subscription

The prices of the separate Research Papers appearing in this JOURNAL are given on the front cover page. If 100 or more copies of any separate are ordered, a discount of 25 percent is allowed. Those who desire copies of separate Research Papers should send their orders and remittances without delay to the Superintendent of Documents, U. S. Government Printing Office, Washington 25, D. C. Research Papers are not printed from electrotypes, and usually no more reprints can be had when the first and only printing is exhausted.

MATHEMATICAL TABLES

A list of the mathematical tables now obtainable from the National Bureau of Standards is printed on pages 3 and 4 of the JOURNAL cover. New tables will be announced from time to time as they become available. An order blank is available on the last page of this issue.

U. S. Department of Commerce National Bureau of Standards

RESEARCH PAPER RP1693

Part of Journal of Research of the National Bureau of Standards, Volume 36, February 1946

HEAT CAPACITY OF A TWO-PHASE SYSTEM, WITH APPLICATIONS TO VAPOR CORRECTIONS IN CALORIMETRY

By Harold J. Hoge

ABSTRACT

A formula is derived that gives the heat capacity of a system composed of solid or liquid in equilibrium with saturated vapor in terms of the specific heat of the condensed phase and certain auxiliary data. This formula is valid throughout the entire range from 0 to 100 percent of vapor, and at the latter extreme reduces to a well-known relation between the specific heats of saturated liquid and saturated vapor.

The formula is applied to the calculation of vapor corrections in calorimetry. Its advantage lies in the fact that the correction is expressed as a single term that may be readily transformed with Clapeyron's equation, yielding two alternative correction formulas.

Vapor corrections to the heat capacity and to the heat of fusion are summarized and tabulated for four different experimental procedures in calorimetry.

CONTENTS

	Page
I. Introduction	111
II. Heat capacity of a two-phase system	112
III. Vapor correction to the heat of fusion	114
IV. Application to calorimetry	115
V. Summary of formulas and required data	116
VI. Definitions and symbols	117
VII. References	118

I. INTRODUCTION

A solid or liquid having an appreciable vapor pressure will partially vaporize when placed in a closed calorimeter. The presence of vapor, which changes both in volume and density as the temperature is changed, makes it necessary in such cases to apply a vapor correction to heat-capacity data. The size of the correction varies with the degree of filling of the calorimeter. In practice it seldom exceeds 3 or 4 percent of the heat capacity of the solid or liquid, but under unusual conditions has been reported to be as large as 20 percent [1].*

Osborne and Van Dusen [2] appear to have been the first to give a detailed mathematical treatment of the problem of vapor corrections. Their equations are given in the Handbuch der Experimentalphysik [3] and seem to have been widely adopted. In 1924 Osborne [4, 5] gave a new treatment of the problem of vapor corrections based on the practice of making duplicate calorimetric runs, one with a large and the other with a small amount of material in the calorimeter. He appears to have been the first to use this method, which has

* Figures in brackets indicate the literature references at the end of this paper.

several advantages, among which are the elimination both of the effect of material in the filling tube and the effect of strain on the heat capacity of the calorimeter. Others who have discussed vapor corrections, either incidentally or in detail include Babcock [6], Awbery and Griffiths [7], and Bennewitz and Splittgerber [8].

All the correction formulas given by these authors are mathematically and physically correct, but some are unnecessarily complicated. Nowhere has it been clearly brought out that the correction can always be expressed in two alternative forms, one of which is in terms of latent heats, the other in terms of vapor pressures. The present paper is an attempt to clarify the situation, and to present in their simplest form the equations needed for making the vapor correction in any ordinary calorimetric experiment. It is thought that these correction formulas may help to eliminate the unnecessary work that is sometimes done when vapor pressure data are first used to compute latent heats, the latent heats then being used in a vapor correction formula. In such a calculation the specific volume of the vapor appears twice, once in Clapeyron's equation, and again in computing x, the fraction of the material in the vapor phase. If incorrect vapor volumes are used, incorrect latent heats are obtained, but this error is exactly compensated by the error in x, so that the vapor correction is independent of the assumed vapor volume. It seems unlikely that investigators have been generally aware of this fact.

The starting point in the derivation given below is an equation for the entropy of a two-phase system. This considerably shortens the derivation as compared with the conventional approach of accounting for all the energy supplied, and yields the results directly in the desired form without the necessity of combining terms. The suggestion that the problem be treated from the entropy standpoint was made by Harold W. Woolley, and it was this point of view that led to equation 5.

II. HEAT CAPACITY OF A TWO-PHASE SYSTEM

Consider a mass M [1] of material confined in a volume, V, and partially vaporized, so that there are M_g grams of gas in equilibrium with M_c grams of condensed phase, which may be either solid or liquid. This system has a definite heat capacity, provided the volume, V, is a definite function of temperature, for if this is the case, the state of the system is completely defined by the temperature. The pressure in the system is always the vapor pressure of the material. We wish to find an expression for the heat capacity of this system. This is most easily done by finding an expression for the total entropy of the system, and finally converting this expression by differentiation into an equation giving the desired heat capacity.

Let s_g and s_c be the entropies per unit mass of saturated vapor and saturated condensed phase, respectively. Then the total entropy of the system is

$$S=M_c s_c+M_g s_g$$
$$=Ms_c+M_g(s_g-s_c). \tag{1}$$

[1] Symbols are defined as they appear, and a table of symbols used is given at the end of this paper.

Since $s_g - s_c$ is the entropy of vaporization per unit mass it is equal to l/T, where l is the heat of vaporization per unit mass, so that

$$S = Ms_c + M_g l/T. \tag{2}$$

The quantity $M_g l/T$ may be considered an "excess" entropy, since it represents the difference between the entropy of the actual system and that of the corresponding system with no vapor phase. Putting $S' = M_g l/T$ we have

$$S = Ms_c + S' \tag{3}$$

and differentiating with respect to T

$$\frac{dS}{dT} = M\frac{ds_c}{dT} + \frac{dS'}{dT}. \tag{4}$$

Now for any reversible absorption of heat $dS = \delta Q/T = CdT/T$. Hence we may substitute $dS/dT = C/T$ and $ds_c/dT = c_c/T$, where C is the heat capacity of the two-phase system and c_c is the heat capacity of unit mass of saturated condensed phase. This gives

$$C = Mc_c + T\frac{dS'}{dT}, \tag{5}$$

which is the basic formula for the heat capacity of a two-phase system.

The next problem is to evaluate $S' \equiv M_g l/T$. The mass of vapor, M_g, can be expressed in terms of the total mass, M, the total volume, V, and the specific volumes of vapor and condensed phase, v_g and v_c, as follows:

$$\begin{aligned} V &= M_c v_c + M_g v_g \\ &= Mv_c + M_g(v_g - v_c), \end{aligned}$$

whence

$$M_g = \frac{V - Mv_c}{v_g - v_c}. \tag{6}$$

The excess entropy is therefore

$$S' = \frac{M_g l}{T} = \frac{l}{T}\frac{V - Mv_c}{v_g - v_c}. \tag{7a}$$

The quantity $l/[T(v_g - v_c)]$ is by Clapeyron's equation equal to dp/dT, the slope of the vapor-pressure curve. This substitution gives an alternative expression for excess entropy.[2]

$$S' = \frac{dp}{dT}(V - Mv_c). \tag{7b}$$

Equations 5, 7a, and 7b, permit c_c, the specific heat of saturated condensed phase to be calculated from C, the heat capacity of the two-phase system, and certain auxiliary data, which may be either l, V, v_g, and v_c; or dp/dT, V, and v_c. When these formulas are used to make vapor corrections they will ordinarily be applied to systems whose vapor fraction, or dryness ($=M_g/M$) is between 0 and 10 per-

[2] A shorter but less obvious method of getting equations 7a and 7b is to note that S' is the change in entropy when the volume occupied by the material is increased from Mv_c to V at constant temperature, so that $S' = (\partial S/\partial V)_T(V - Mv_c)$. Since, by Maxwell's relation $(\partial S/\partial V)_T = dp/dT$, we have 7b at once and 7a may be obtained from 7b by use of Clapeyron's equation.

cent. They are valid, however, throughout the whole range from 0 to 100 percent dryness. For the limiting case of 100 percent dryness, 5 and 7a yield a well-known relation between the heat capacities of saturated vapor and saturated liquid. For this particular case, $V=Mv_g$, so that S' is simply Ml/T, and 5 is

$$C=Mc_g=Mc_e+T\frac{d}{dT}\left(\frac{Ml}{T}\right),$$

where c_g is the heat capacity per gram of saturated vapor. Since M is independent of T, this reduces to the usual form

$$c_g-c_e=T\frac{d}{dT}\left(\frac{l}{T}\right). \tag{8}$$

III. VAPOR CORRECTION TO THE HEAT OF FUSION

When a melting point or other first-order transition is encountered in a two-phase system, special formulas are needed for making the vapor correction. The simplest way to obtain these is to start with equation 3, the equation for the entropy of the two-phase system, $S=Ms_e+S'$. Let the subscript "a" refer to the system just before the transition starts (solid-gas) and let the subscript "b" characterize it at the end of the transition (liquid-gas). The change in entropy during melting is, by equation 3,

$$S_b-S_a=M(s_{eb}-s_{ea})+S'_b-S'_a. \tag{23}$$

If Q is the measured quantity of heat supplied during the process, then $Q/T=S_b-S_a$. Likewise, $s_{eb}-s_{ea}$, the difference in specific entropies of the two condensed phases, is l_f/T, where l_f is the heat of fusion per gram. Making these substitutions and multiplying by T gives

$$Q=Ml_f+T(S'_b-S'_a). \tag{24}$$

The excess entropies may be evaluated with the formulas previously developed. If 7a is used,

$$S'_b-S'_a=\left[\frac{lV-Mv_e}{T\ v_g-v_e}\right]_a^b, \tag{25}$$

while if 7b is used,

$$S'_b-S'_a=\left[\frac{dp}{dT}(V-Mv_e)\right]_a^b \tag{26}$$

When evaluating these expressions it should be remembered that the only quantities having the same value at both limits are V, M, T, and v_g.

The vapor correction to the heat of fusion may be considered to be made up of two parts. One part is due to the fact that M_g is not zero, and hence not all of the total mass M takes part in the process of melting. The other is due to the fact that M_g generally changes a little one way or the other owing to a difference between v_{ea} and v_{eb}. This causes the absorption or liberation of the heat of vaporization of a small amount of material.

IV. APPLICATION TO CALORIMETRY

Use of the formulas derived above in making vapor corrections is a straightforward procedure that need not be discussed in detail. The vapor correction is not made until after the calculation of the gross, tare, and net heat capacities. In calculating both the gross and the tare heat capacities it may be necessary to apply a curvature correction [reference 9, p. 79]. After this correction has been applied it is convenient to tabulate the gross and tare heat capacities at 5-degree intervals and to subtract one table from the other to obtain the net heat capacity. The vapor correction is then applied to the net heat capacity.

The working formulas for this purpose depend on the type of experiment. Four different types of experiment may be considered, characterized by the presence or absence of a filling tube that contains a small part of the calorimetric charge, and by whether the tare charge is zero or a mass of material M_2, which is small compared to the gross charge M_1 but sufficient to fill the system with saturated vapor at all temperatures.

In the next section the appropriate formulas for each of the four types of experiment are tabulated. The quantities which must be known in order to evaluate the formulas are also listed. These are divided into two groups: the basic data, which are required regardless of the vapor correction; and the auxiliary data, which are needed only to evaluate the vapor correction. For one type of experiment, formulas are given which contain M_t, the mass of material in the filling tube. These formulas may be derived by treating the vapor in the tube as an ideal gas. The problem is essentially the same as that of correcting for the gas in the capillary of a gas thermometer [10]. In order that the filling tube shall contain only vapor, it is of course necessary that no part of it shall have a temperature lower than that of the calorimeter proper.[3]

In calculating the vapor correction, the derivative dE/dT must always be calculated, and in many cases the derivative dp/dT also. A procedure which has been found satisfactory for this purpose is to tabulate E (or p) at 5-degree intervals and to calculate $\Delta E/\Delta T$ for each interval. The values of $\Delta E/\Delta T$ are ordinarily sufficiently good approximations to the values of dE/dT at the midpoints of the intervals. Where greater accuracy is desired, formulas such as that of Rutledge [11], which are based on polynomial approximations of higher degree may be used.

The author acknowledges valuable discussions with M. S. Van Dusen, of the Bureau's Pyrometry Section.

[3] Osborne and his coworkers have for certain experiments used a filling tube that is at all times filled with liquid. This requires the opposite condition—that no part of the tube shall have a temperature higher than that of the calorimeter proper.

V. SUMMARY OF FORMULAS AND REQUIRED DATA

For definitions of terms and symbols, see section VI.

Type 1. Gross charge: M
Tare charge: 0
Filling tube: No

$$\begin{cases} c_e = \dfrac{C_{net} - T dS'/dT}{M} \\ l_t = \dfrac{Q - T(S'_b - S'_a)}{M} \\ \text{Basic data: } C_{net},\ M,\ T,\ Q \end{cases}$$

$$\begin{cases} S' = \dfrac{l}{T}\dfrac{V - Mv_e}{v_g - v_e} \\ \text{Auxiliary data: } l_a,\ l_b,\ V,\ v_{ca},\ v_{cb},\ v_g \end{cases}$$

or

$$\begin{cases} S' = \dfrac{dp}{dT}(V - Mv_e) \\ \text{Auxiliary data: } (dp/dT)_a,\ (dp/dT)_b,\ V,\ v_{ca},\ v_{cb}. \end{cases}$$

Type 2. Gross charge: M_1
Tare charge: M_2
Filling tube: No

$$\begin{cases} c_e = \dfrac{C_{net} - Td(S'_1 - S'_2)/dT}{M_1 - M_2} \\ l_t = Q_{net} - T\dfrac{[(S'_1 - S'_2)_b - (S'_1 - S'_2)_a]}{M_1 - M_2} \\ \text{Basic data: } C_{net},\ M_1 - M_2,\ T,\ Q_{net}, \end{cases}$$

$$\begin{cases} S'_1 - S'_2 = -\dfrac{l}{T}\dfrac{(M_1 - M_2)v_e}{v_g - v_e} \\ \text{Auxiliary data: } l_a,\ l_b,\ v_{ca},\ v_{cb},\ v_g. \end{cases}$$

or

$$\begin{cases} S'_1 - S'_2 = -\dfrac{dp}{dT}(M_1 - M_2)v_e \\ \text{Auxiliary data: } (dp/dT)_a,\ (dp/dT)_b,\ v_{ca},\ v_{cb}. \end{cases}$$

Type 3. Gross charge: M_1
Tare charge: M_2
Filling tube: Yes

The temperature distribution in the tube must be the same in the tare run as in the gross run. With this precaution, the quantities M_t and dM_t/dT drop out of the working equations, which become identical with those for an experiment of type 2.

Type 4. Gross charge: M
Tare charge: 0
Filling tube: Yes

$$\begin{cases} c_c = \dfrac{C_{net} - T dS'/dT - l dM_t/dT}{M - M_t} \\ l_t = \dfrac{Q - T(S'_b - S'_a)}{M - M_t} \\ \text{Basic data: } C_{net},\ M,\ T,\ Q. \end{cases}$$

$$\begin{cases} S' = \dfrac{l}{T}\dfrac{V - (M - M_t)v_c}{v_g - v_c} \\ \text{Auxiliary data: } l_a,\ l_b,\ V,\ v_{ca},\ v_{cb},\ v_g \end{cases}$$

or

$$\begin{cases} S' = \dfrac{dp}{dT}[V - (M - M_t)v_c] \\ \text{Auxiliary data: } (dp/dT)_a,\ (dp/dT)_b,\ V,\ v_{ca},\ v_{cb} \end{cases}$$

also

$$\begin{cases} M_t = p\dfrac{W}{R}\sum_1 \dfrac{V_1}{T_1} \\ \dfrac{dM_t}{dT} = \dfrac{W}{R}\left[\dfrac{dp}{dT}\sum_1 \dfrac{V_1}{T_1} + p\dfrac{}{dT}\sum_1 \dfrac{V_1}{T_1}\right] \\ \text{Auxiliary data: } p,\ V_1,\ T_1,\ dp/dT. \end{cases}$$

VI. DEFINITIONS AND SYMBOLS

Calorimeter.—That part of the apparatus which contains the material and participates in absorbing the measured power input.
Charge.—Mass of material in the calorimeter and filling tube.
Filling tube.—Tube extending from the calorimeter to outside the apparatus. Contains a small part of the total charge during measurements.
Gross heat capacity.—Heat capacity of calorimeter plus a large charge M_1.
Tare heat capacity.—Heat capacity of calorimeter with no charge, or with a small charge M_2.
Net heat capacity.—Gross heat capacity minus tare heat capacity.

C=heat capacity
c=specific heat (heat capacity per unit mass)
l=heat of sublimation, vaporization or fusion per unit mass
M=mass of charge contained in calorimeter and filling tube
p=pressure, equal to vapor pressure of material at temperature T
Q=heat absorbed during a transition such as melting
R=gas constant
S=entropy
S'=excess entropy of a system, as compared with the same mass of saturated condensed phase
s=entropy per unit mass
T=absolute temperature of calorimeter and contents
V=volume of the calorimeter

v=volume per unit mass
W=molecular weight of the material
x=fraction of the material in the vapor phase, sometimes called dryness.

SUBSCRIPTS

a=pertaining to the form stable below a transition
b=pertaining to the form stable above a transition
c=condensed phase, solid or liquid
f=pertaining to fusion
g=gaseous phase
i=pertaining to the ith element of volume of the filling tube
t=pertaining to the filling tube
1=corresponding to the gross charge M_1
2=corresponding to the tare charge M_2.

VII. REFERENCES

[1] A. Eucken and E. Schröder, Low temperature caloric measurements on a few fluorides (BF_3, CF_4, SF_6), Z. physik. Chem. [B] **41,** 307–319 (1938).
[2] Nathan S. Osborne and Milton S. Van Dusen, Specific heat of liquid ammonia, Bul. BS **14,** 397–432 (1918) S313.
[3] A. Eucken, Hand. Experimentalphysik **8,** part 1, p. 291–294 (1929).
[4] Nathan S. Osborne, Calorimetry of saturated fluids, J. Opt. Soc. Am. & Rev. Sci. Instr. **8,** 519–540 (1924).
[5] Nathan S. Osborne, Calorimetry of a fluid, BS J. Research **4,** 609–629 (1930) RP168.
[6] Henry A. Babcock, The specific heat of ammonia, Proc. Am. Acad. Arts Sci. **55,** 323–409 (1920).
[7] J. H. Awbery and Ezer Griffiths, The specific heat of liquid CH_3Cl, Proc. Phys. Soc. **52,** 770–776 (1940).
[8] K. Bennewitz and E. Splittgerber, Investigations in the critical region. I. Specific heat of CO_2 near the critical point, Z. physik. Chem. **124,** 49–65 (1926).
[9] N. S. Osborne, H. F. Stimson, T. S. Sligh, Jr., and C. S. Cragoe, Specific heat of superheated NH_3 vapor, BS Sci. Pap. **20,** 65–110 (1925) S501.
[10] Harold J. Hoge and Ferdinand G. Brickwedde, Establishment of a temperature scale for the calibration of thermometers between 14° and 83° K, J. Research NBS **22,** 351–373 (1939) RP1188.
[11] George Rutledge, A reliable method of obtaining the derivative function from smoothed data of observation, Phys. Rev. **40,** 262–8 (1932).

WASHINGTON, October 24, 1945.

U. S. Department of Commerce National Bureau of Standards

RESEARCH PAPER RP1694

Part of Journal of Research of the National Bureau of Standards, Volume 36, February 1946

A METHOD FOR DETERMINING SMALL AMOUNTS OF GOLD, AND ITS USE IN ASCERTAINING THE THICKNESS OF ELECTRODEPOSITED GOLD COATINGS

By W. Stanley Clabaugh

ABSTRACT

This paper presents a method for the determination of the thickness of gold electroplate, using a punch and die to obtain samples of known small area. Amounts of gold up to 10 micrograms (0.010 mg), corresponding to a thickness of 0.00050 mm (0.00002 in.) or less on 1 mm² (0.00155 in.²) of surface, are determined directly by means of the color produced with *o*-tolidine. Results are reported for thicknesses of gold plate on experimentally plated samples and on commercially plated products.

CONTENTS

	Page
I. Introduction	119
II. Colorimetric determination of small amounts of gold by means of *o*-tolidine	120
1. Preparation and stability of the reagent solution of *o*-tolidine and of dilute solutions of gold	120
2. Preparation and measurement of the color of the *o*-tolidine–gold solution	121
III. Application of the colorimetric method to the determination of the thickness of electrodeposited gold plate	123
1. Method of obtaining sample of known small area	123
2. Application to experimentally plated samples	124
3. Application to commercially plated objects	126

I. INTRODUCTION

Many articles of jewelry, such as watchcases, rings, lockets, earrings, tie clasps, ornamental and emblematic buttons, coverings for knife handles, brushes, combs, and insignia for the armed forces, are electroplated with gold. The thickness of the gold may vary from less than one-millionth to more than one ten-thousandth of an inch.

The calculation of the thickness of gold depends on the measurement of a given area, the determination of the total gold on this area, and the known density of gold (19.3). The deposit of gold, usually nonuniform, even on plane surfaces, is still less uniform on curved surfaces, so that the thickness determined by this method is only an average value. The application of this procedure is difficult, because of the uneven contour of the surface, the small size of many articles, and the small amount of gold involved. One square centimeter (0.155 in.²) of surface plated with 0.00025 mm (0.00001 in.) of gold contains only 0.49 mg of gold. The need exists, therefore, for a precise method that can be applied to a small measured area. By means of a suitable die an area of 1 mm² can usually be cut out from some portion of a commercially electroplated article, and the quantity

of gold involved will generally fall within the limits that can be conveniently determined colorimetrically.

II. COLORIMETRIC DETERMINATION OF SMALL AMOUNTS OF GOLD BY MEANS OF *o*-TOLIDINE

The reagent, *o*-tolidine, 3,3′-dimethylbenzidine, reacts with chloroauric acid, $HAuCl_4$, to produce a yellow color. This reaction, which is not new, has been investigated by Pollard.[1] The development of the color depends on the oxidation of the *o*-tolidine, and, consequently, any oxidizing substances, such as ferric ion or chlorine, must be rigidly excluded.

With the visual method of comparison, amounts of gold up to about 8 micrograms (0.008 mg) in 25 ml of solution can be determined, and with a spectrophotometer, as much as 10 micrograms in the same volume. Because the yellow color is unstable, freshly prepared color standards must be used in the visual comparisons, but they are not required in the spectrophotometric method after the relation between concentration and percentage transmittance is determined; hence the latter method is more convenient for routine tests.

1. PREPARATION AND STABILITY OF THE REAGENT SOLUTION OF *o*-TOLIDINE AND OF DILUTE SOLUTIONS OF GOLD

The *o*-tolidine used in the colorimetric determination of gold should be free from impurities that effect the color developed by the reaction. Purification of the commercial product was found necessary to eliminate unidentified impurities that caused the characteristic yellow color to fade rather quickly. A reagent of sufficient purity can easily be prepared by recrystallizing the commercial grade of *o*-tolidine from 2-*N* sulfuric acid. A boiling solution of 2-*N* sulfuric acid is saturated with *o*-tolidine, filtered while hot through porous porcelain or a glass frit to remove insoluble impurities and any undissolved *o*-tolidine, and allowed to cool to room temperature. The *o*-tolidine sulfate that crystallizes is removed by filtration and recrystallized twice more from 2-*N* sulfuric acid. Filter paper should not be used because of the danger of introducing organic matter, which has a deleterious effect on the subsequent development of the yellow color. The final product should be a nearly pure white powdery or finely crystalline mass.

The reagent solution is prepared by saturating *N* sulfuric acid with the purified *o*-tolidine sulfate and diluting 1 volume of the saturated solution with 19 volumes of *N* sulfuric acid. Both the saturated solution and the diluted solution are stable for long periods of time, hence the preparation of fresh reagent solution for each series of determinations is unnecessary.

Standard solutions, containing 1.0 microgram (0.001 mg) of gold per milliliter, were prepared by dissolving 0.1000 g of pure gold, diluting to 1 liter, and then diluting 10 ml of this solution to 1 liter. In each case the liter of solution contained 60 ml of concentrated hydrochloric acid and 40 ml of concentrated nitric acid. The above quantities of acids were added to prevent the separation of gold from such dilute solutions. Experience showed that solutions so prepared remained stable and constant with respect to the gold content.

[1] W. B. Pollard, Bul. Inst. Mining Met., No. 223, 8 p. (1923).

2. PREPARATION AND MEASUREMENT OF THE COLOR OF THE o-TOLIDINE–GOLD SOLUTION

A definite amount of the standard gold solution (in the range 0.5 to 10.0 micrograms of gold) was placed in a 50-ml beaker and evaporated nearly to dryness on the steam bath. A drop of aqua regia was added, and evaporation to complete dryness was accomplished by impinging on the surface of the solution a jet of purified air. Evaporation on the steam bath alone usually caused some reduction of the chloroauric acid to aurous chloride or metallic gold. No such reduction occurred when the beaker was held in the hand and the stream of air was used.

To the completely air-dried residue of chloroauric acid 25 ml of the *o*-tolidine reagent was added, and the resulting solution was trans-

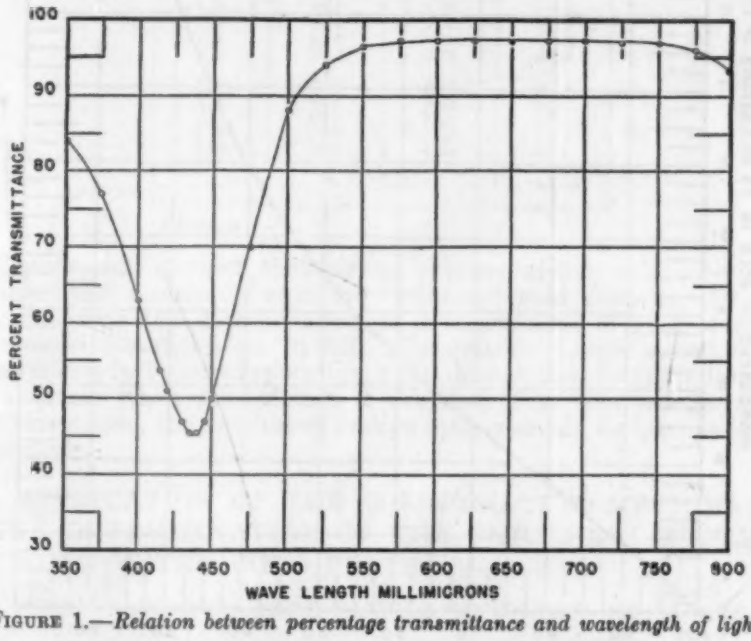

FIGURE 1.—*Relation between percentage transmittance and wavelength of light.*

ferred to a 25-ml cell for measurement of the percentage transmittance of light by means of a spectrophotometer. The instrument used was a Coleman Universal Spectrophotometer, model 11. The 25-ml cells were cylinders 50.0 mm long.

When the *o*-tolidine solution was added to the dry residue of chloroauric acid, a yellow color developed, the intensity of which reached a maximum in 1 to 3 minutes and remained stable for 10 to 30 minutes. As extensive experience showed that evaporation either of small or large quantities of aqua regia, in the manner described above, left no oxidizing material, 25 ml of the *o*-tolidine reagent was used directly as the solution in the "blank cell."

The relation between percentage transmittance and wavelength of light is shown in figure 1. The solution was found to have a minimum transmittance of light at a wavelength of 437 millimicrons.

The relation between percentage transmittance at 437 millimicrons and the weight of gold contained in 25 ml of solution is shown in figure 2.

The reproducibility of the calibration curve was established by using aliquot portions of independently prepared standard gold

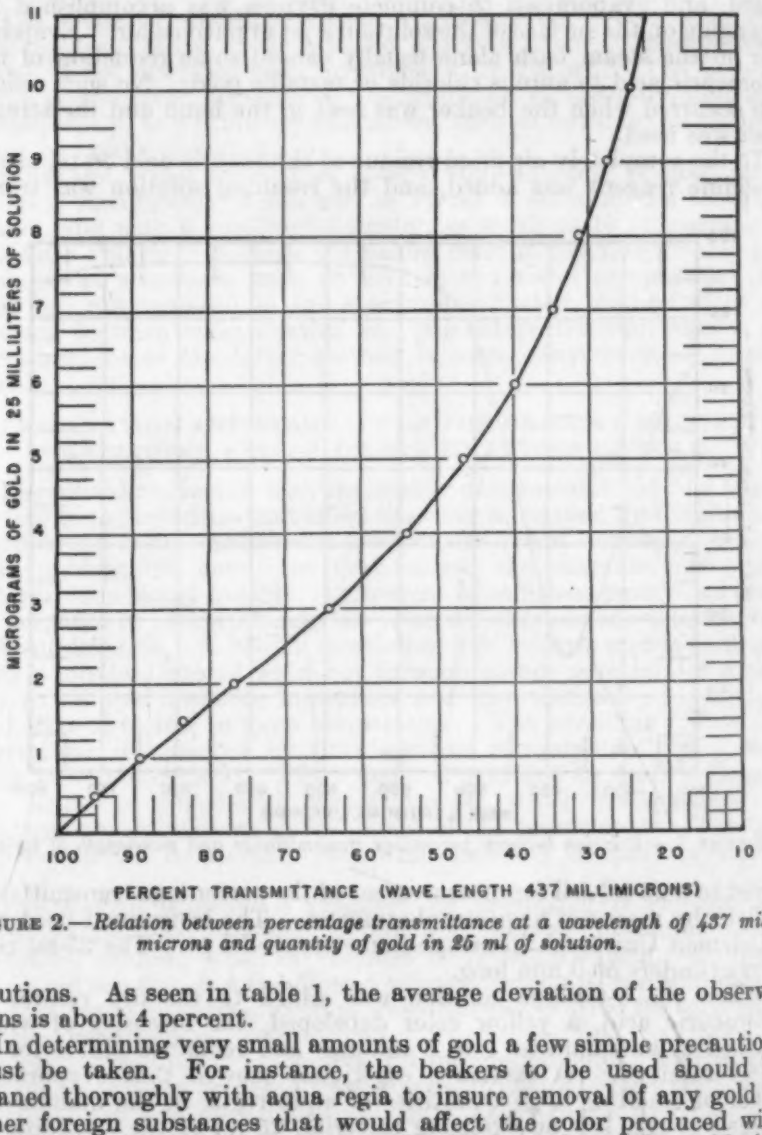

FIGURE 2.—*Relation between percentage transmittance at a wavelength of 437 millimicrons and quantity of gold in 25 ml of solution.*

solutions. As seen in table 1, the average deviation of the observations is about 4 percent.

In determining very small amounts of gold a few simple precautions must be taken. For instance, the beakers to be used should be cleaned thoroughly with aqua regia to insure removal of any gold or other foreign substances that would affect the color produced with *o*-tolidine. As the determination of gold depends on the oxidation of *o*-tolidine by gold in its tervalent condition, it is necessary to maintain the gold in this state of valency until the *o*-tolidine solution

is added. Simple evaporation of gold solutions causes reduction of some of the chloroauric acid to aurous chloride or metallic gold, but experience has shown that no such reduction occurs if a jet of purified air is used to obtain final dryness. The impurities, ammonia, hydrogen sulfide, and dust, commonly in the air can easily be removed by passing the air through concentrated sulfuric acid, Ascarite, and a fritted-glass filter.

TABLE 1.—*Reproducibility of the calibration curve*

Gold taken	Transmittance, 437 millimicrons	Gold determined	Error
Micrograms	*Percent*	*Micrograms*	*Percent*
1.20	85.0	1.30	+3.1
1.20	86.2	1.20	−4.8
1.58	80.0	1.70	+7.6
1.58	81.0	1.60	+1.3
2.37	70.2	2.52	+6.3
2.37	71.2	2.43	+2.5
2.99	65.8	2.92	−2.3
3.24	61.0	3.35	+3.4
3.24	61.0	3.35	+3.4
4.38	51.8	4.33	−1.1
			[1]±3.58

[1] Average.

Experiments showed that silver, copper, nickel, and zinc, the metals most commonly used for "coloring" gold deposits, did not interfere with the determination of 5 micrograms of gold, even if present in quantities up to 500 micrograms. Larger amounts of these metals leave, on evaporation, a salt deposit that makes it difficult to ascertain when the solution is evaporated to complete dryness. For this reason, the amount of foreign metals should be kept as small as possible.

III. APPLICATION OF THE COLORIMETRIC METHOD TO THE DETERMINATION OF THE THICKNESS OF ELECTRODEPOSITED GOLD PLATE

1. METHOD OF OBTAINING SAMPLE OF KNOWN SMALL AREA

To utilize the foregoing colorimetric method to determine the thickness of gold plating, areas of 1.00 mm^2 (0.00155 in.^{2}) [2] were cut from experimental gold-plated brass sheets. The punch and die used for this operation was designed and constructed by Charles W. Hyder, of this Bureau, and is shown diagrammatically in figure 3. The punch was designed to cut samples from specimens whose total thickness was $\frac{1}{32}$ inch or less.

To remove the gold coating from its affixed base metal layer, the sample cut out by the punch was treated in a 50-ml beaker with from 0.5 to 1.0 ml of a diluted solution of nitric acid, composed of one volume of concentrated nitric acid and one volume of water. It was found that if the gold layer was thicker than 3 millionths of an inch,

[2] This area was calculated by Charles P. Saylor from measurements, made with a microscope, of the diameters of the pieces which were cut out and of the holes which remained.

the tiny gold disk remained intact during the acid treatment, and could be washed by decantation with water; otherwise, the gold must be collected and washed on a microfilter. A medicine dropper with a fine capillary tip was advantageous in removing the water from the beaker. The gold was then dissolved in aqua regia, and its determination was completed as previously described.

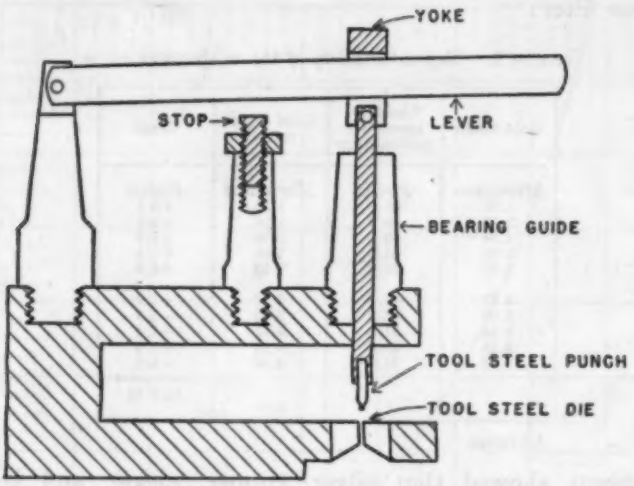

FIGURE 3.—*Diagram of punch and die used to cut samples of 1-mm² area.*

For converting the determined quantity of gold into thickness of gold layer, a graph was prepared in which the amount of gold, in terms of percentage transmittance of light at 437 millimicrons, was plotted as a function of thickness in millionths of an inch (fig. 4).

2. APPLICATION TO EXPERIMENTALLY PLATED SAMPLES

To prepare the experimental plates, flat sheets of brass approximately 7 cm (2.76 in.) by 8 cm (3.15 in.) were plated on one side with gold by Frances H. Colbert, of this Bureau, under conditions to produce a relatively uniform layer. The average thickness was calculated from the area plated and the amount of gold deposited. Table 2 reports the results obtained by taking from 2 to 5 samples from near the center of each plate and shows that the values determined in this region agreed well with the calculated value for thicknesses up to 0.000005 in.

For layers of greater thickness significant variations are observed between the values determined at the center of the plates and average thicknesses calculated from the areas of the plates and the amounts of gold deposited. As these variations greatly exceed the limits of accuracy of the microdetermination, the values obtained at the centers of the plates must be considered as representing more correctly the actual thickness of the gold layer in the region tested.

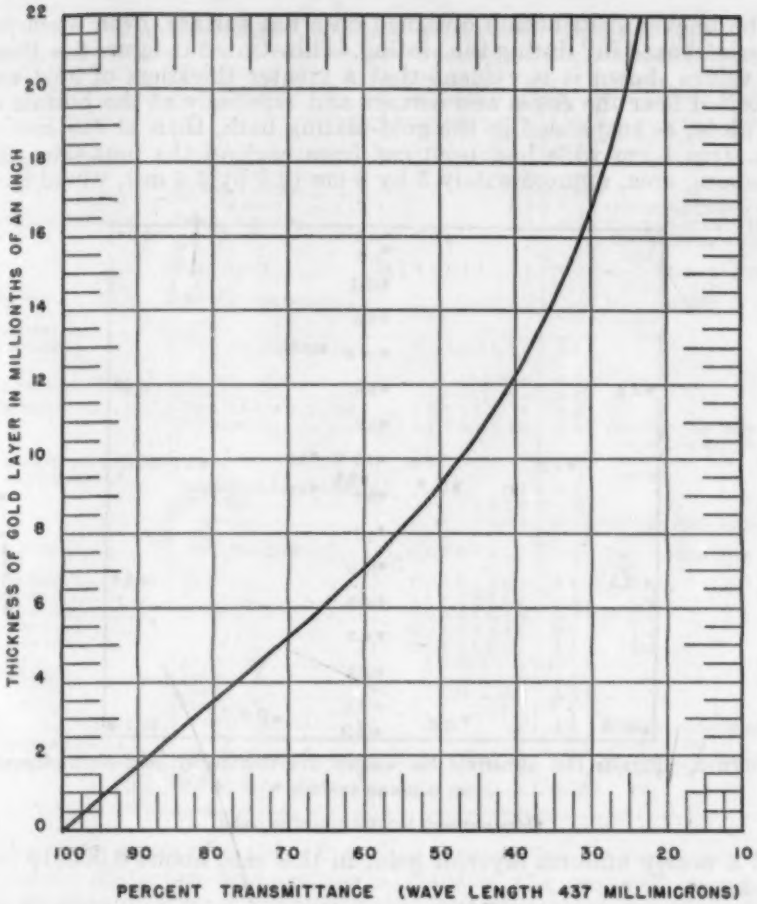

FIGURE 4.—*Graph for converting amount of gold per 1-mm² area (in terms of percentage transmittance at a wavelength of 437 millimicrons) to thickness of gold layer.*

TABLE 2.—*Comparison of thickness of gold layer determined near center of specimen and the average thickness calculated from the area plated and the amount of gold deposited*

Plate number	Thickness of gold, millionths of an inch						
	Determined						Calculated from weight of deposit
	1	2	3	4	5	Average	
1	1.5	1.5	----	----	----	1.5	1.0
2	3.2	2.5	2.2	2.2	2.5	2.5	2.5
3	4.5	4.4	4.4	4.1	4.0	4.3	4.3
4	4.5	4.4	4.4	4.5	4.7	4.5	4.5
5	6.9	6.1	5.9	6.9	6.9	6.5	8.6
6	8.2	8.0	8.4	8.4	8.3	8.3	10.6
7	9.5	9.0	9.0	9.4	----	9.2	11.0
8	20.0	21.5	20.5	20.0	20.5	20.5	25.0

The uneven distribution obtained on a flat surface, even when the plate is "boxed in" during the plating, is illustrated in figure 5. From the values shown it is evident that a greater thickness of gold was deposited near the edges and corners and especially at the bottom of the plate, as suspended in the gold-plating bath, than at the center. If a strip 1 cm wide had been cut from each of the four sides, the remaining area, approximately 5 by 6 cm (2.0 by 2.4 in.), would have

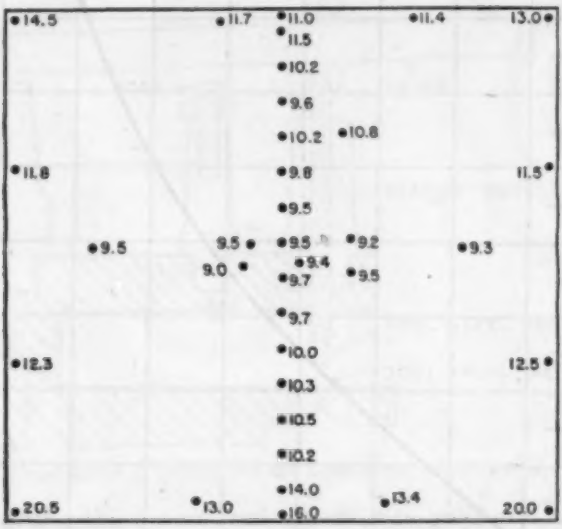

FIGURE 5.—*Results that illustrate the uneven distribution of gold electrodeposited on a plane surface.*

[Measurements in millionths of an inch.]

had a nearly uniform layer of gold, in this case about 0.000010 inch thick.

3. APPLICATION TO COMMERCIALLY PLATED OBJECTS

To apply the method of testing to commercially plated objects, 16 prewar gold-plated articles of jewelry were obtained through the courtesy of Byron L. Shinn, counsel, Jewelers' Vigilance Committee, and W. H. Blake, associate secretary, New England Manufacturing Jewelers' & Silversmiths' Association. Some of the articles were labeled "electroplated precious metal," some "24K fine gold finish", and some bore no identification as to whether they were gold plated or not.

The results of determination of thickness of the gold layer are given in table 3.

TABLE 3.—*Thickness of gold on commercially plated articles*

Article	Portions tested	Thickness of gold (millionth of an inch)	Avg	Remarks
1. Ladies compact	Top, bottom, sides			Was not gold plated.
	End clamps	1.6, 1.4	1.5	
	Tongue of clasp	3.1, 3.5	3.3	
2. Chain watch band	Top of clasp	3.1	3.1	Contained filigree work.
	Bottom of clasp	6.2	6.2	The part of clasp that is in contact with the skin.
	Chain part	6.3, 6.9, 6.0, 7.1, 7.1	6.7	Each from a different link.
3. Earring	Each of four petals			Gold too thin to determine.
4. Earring	do			Do.
5. Tie clasp	Two samples from each side.	2.5, 3.2, 3.7, 3.0	3.1	
6. Sport watch chain	Swivel	13.5, 15.0	14.2	
	Chain	10.7, 11.0	10.8	
7. Tie clasp	Two sides of front bar	7.5, 7.3, 7.7, 7.8	7.6	
8. Tie clasp with chain and monograms.	Monograms	2.5, 2.5, 1.9, 1.9	2.2	Two samples from one letter; one sample from each of two other letters.
	Monogram bar holder	2.7	2.7	
	Shirt bar	1.5, 2.0	1.8	
	Chain	1.0, 0.8	0.9	Samples from each end of chain.
9. Tie clasp	Front and back	5.0, 6.0, 4.0, 5.7	5.2	Two samples from each side.
10. Tie clasp	do	7.0, 6.0, 4.2, 4.5	5.4	Do.
11. Tie clasp	do	5.5, 5.0, 3.7, 3.5	4.4	Do.
12. Collar clasp	do	3.8, 3.3, 4.0, 4.3	3.8	Do.
13. Collar clasp	do	3.0, 3.5, 4.5, 4.0	3.8	Do.
14. Collar clasp	do	4.7, 4.2, 5.0, 4.2	4.5	Do.
15. Key chain	Belt clamp	9.5, 10.5, 10.3	10.1	
	Key ring	9.5, 10.0	9.8	
	Chain	13.2, 14.3	13.8	
	Snap catch	2.7, 3.2	3.0	
	Center ornament	2.6	2.6	Attached outside of enamel cover.
16. Ladies compact	Top metal case	Less than 1.0		Metal case inside of enamel cover.
	Bottom of metal case	do		Do.

The chain parts of articles 2 and 15 were tested by measuring the respective diameters and cutting a piece of the required length to give an area of 1 mm². Articles that were too thick for the punch were ground down on one side to reduce the total thickness to less than $\frac{1}{32}$ inch, precautions being taken not to disturb the gold layer on the side to be tested.

Articles that have gold layers thicker than 20 millionths of an inch can be tested either by using a larger volume of *o*-tolidine–sulfuric acid reagent solution for dissolving the air-dried residue—or by diluting the aqua-regia solution of the gold obtained in the test and evaporating an aliquot of this solution to dryness for the colorimetric determination of the gold.

The data in tables 1 and 2 and in figure 5 show that the determination of thickness by the method described is accurate well within ±10 percent. This degree of accuracy is greater than that of the uniformity of thickness usually attained in commercial plating.

WASHINGTON, November 14, 1945.

U. S. Department of Commerce National Bureau of Standards

RESEARCH PAPER RP1695

Part of Journal of Research of the National Bureau of Standards, Volume 36, February 1946

PURIFICATION AND PROPERTIES OF 29 PARAFFIN, 4 ALKYLCYCLOPENTANE, 10 ALKYLCYCLOHEXANE, AND 8 ALKYLBENZENE HYDROCARBONS[1]

By Alphonse F. Forziati,[2] Augustus R. Glasgow, Jr., Charles B. Willingham, and Frederick D. Rossini

ABSTRACT

This report gives the results of the purification and measurements of refractive index (n_D at 20° and 25° C), density (at 20° and 25° C), boiling point and pressure coefficient of the boiling point (at 1 atm) and, except for four of the compounds, the freezing point, together with the calculated amount of impurity, of samples of 51 hydrocarbons, including 29 paraffins, 4 alkylcyclopentanes, 10 alkylcyclohexanes, and 8 alkylbenzenes.

CONTENTS

		Page
I.	Introduction	129
II.	Materials and purification	129
III.	Refractive indices	132
IV.	Densities	135
V.	Boiling points	135
VI.	Freezing points and purities	135
VII.	References	136

I. INTRODUCTION

In connection with the work of the American Petroleum Institute Research Project 6 at this Bureau on the analysis, purification, and properties of hydrocarbons, samples of 50 hydrocarbons, including 29 paraffins, 3 alkylcyclopentanes, 10 alkylcyclohexanes, and 8 alkylbenzenes, were purified in the period from March 1941 to May 1943. On these 50 compounds, plus an additional one (cyclopentane) not requiring further purification, measurements were made of the boiling point, freezing point, refractive index, and density. This paper gives the results of the purification and measurements of these properties.

II. MATERIALS AND PURIFICATION

In table 1 are given the sources of the materials from which (except for the cyclopentane supplied by M. R. Fenske, which was not further purified) the final "best" samples of the compounds were obtained by

[1] This investigation was performed at the National Bureau of Standards as part of the work of the American Petroleum Institute Research Project 6 on the Analysis, Purification, and Properties of Hydrocarbons.

[2] Research Associate on the American Petroleum Institute Research Project 6 at the National Bureau of Standards.

purification in the distillation laboratory of the API Research Project 6. As indicated by table 1, the starting materials were supplied from eight different laboratories, as follows: 24 from the API Hydrocarbon Research Project (now the API Research Project 45) at the Ohio State University, Columbus, Ohio; 15 from the API Research Project 6 at the National Bureau of Standards; 2 from the Petroleum Refining Laboratory at the Pennsylvania State College; 2 from the Ethyl Corporation, Detroit, Mich.; 2 from the Barrett Division of the Allied Chemical Corporation, New York, N. Y.; 2 from the Dow Chemical Co., Midland, Mich.; 1 from the Humble Oil & Refining Co., Houston, Tex.; and 3 as commercially available materials from the Phillips Petroleum Co., Bartlesville, Okla.

TABLE 1.—*Information on the sources of the starting materials and on the purification*

Compound	Source of starting material [a]	Purification [b]		
		Kind	Still No.	Time of distillation
PARAFFINS				
n-Pentane	Phillips	Azeotropic (methanol)	D	12/2/42 to 12/13/42
2-Methylbutane (isopentane)	do	Regular	D	3/30/43 to 4/17/43
n-Hexane	APIRP 6	Azeotropic (methanol)	H	2/14/42 to 2/26/43
2-Methylpentane	do	do	H	5/5/42 to 5/14/42
3-Methylpentane	do	do	H	5/14/42 to 5/22/42
2,2-Dimethylbutane	Phillips	do	J	1/1/43 to 1/8/43
2,3-Dimethylbutane	Penn State	do	J	7/7/42 to 7/16/42
n-Heptane	APIRP 6	do	F	12/29/42 to 1/8/43
2,2-Dimethylpentane	Ethyl	do	I	4/14/41 to 4/26/41
2,3-Dimethylpentane	do	do	I	3/31/41 to 4/11/41
n-Octane	APIHRP	Azeotropic (ethanol)	I	10/10/42 to 10/17/42
2-Methylheptane	do	do	I	7/28/42 to 8/9/42
3-Methylheptane	do	do	I	8/10/42 to 8/22/42
4-Methylheptane	do	do	I	8/24/42 to 9/5/42
3-Ethylhexane	do	do	I	7/6/42 to 7/17/42
2,2-Dimethylhexane	do	do	I	8/6/41 to 8/23/41
2,3-Dimethylhexane	do	do	I	4/28/41 to 5/9/41
2,4-Dimethylhexane	do	do	J	6/6/42 to 6/18/42
2,5-Dimethylhexane	do	do	I	6/2/42 to 6/13/42
3,3-Dimethylhexane	do	do	I	7/25/41 to 8/6/41
3,4-Dimethylhexane	do	do	J	6/25/42 to 7/6/42
2-Methyl-3-ethylpentane	do	do	I	11/4/41 to 11/26/41
3-Methyl-3-ethylpentane	do	do	I	10/16/41 to 11/3/41
2,2,3-Trimethylpentane	do	Azeotropic (methyl Cellosolve).	J	4/26/43 to 5/6/43
2,2,4-Trimethylpentane	APIRP 6	Azeotropic (ethanol)	D	12/14/42 to 12/26/42
2,3,3-Trimethylpentane	APIHRP	do	I	7/10/41 to 7/24/41
2,3,4-Trimethylpentane	do	do	I	7/17/42 to 7/28/42
n-Nonane	APIRP 6	Azeotropic (Cellosolve)	E	12/29/42 to 1/8/43
n-Decane	do	Azeotropic (butyl Cellosolve).	E	1/28/43 to 2/3/43
ALKYLCYCLOPENTANES				
Cyclopentane	Penn State	[c]		
Methylcyclopentane	APIRP 6	Azeotropic (methanol)	D	4/8/42 to 4/22/42
n-Propylcyclopentane	APIHRP	Azeotropic (methyl Cellosolve).	J	3/26/43 to 4/9/43
Isopropylcyclopentane	do	do	J	3/17/43 to 3/25/43
ALKYLCYCLOHEXANES				
Cyclohexane	Barrett	Regular	D	3/8/43 to 3/29/43
Methylcyclohexane	do	Azeotropic (methanol)	F	12/18/42 to 12/28/42
Ethylcyclohexane	APIRP 6	Azeotropic (methyl Cellosolve).	I	11/10/42 to 11/16/42
cis-1,2-Dimethylcyclohexane	APIHRP	Azeotropic (isopropanol)	J	3/3/42 to 3/19/42
trans-1,2-Dimethylcyclohexane	do	do	J	2/23/42 to 3/3/42

See footnotes at end of table.

TABLE 1.—*Information on the sources of the starting materials and on the purification*—Continued

Compound	Source of starting material [a]	Purification [b]		
		Kind	Still No.	Time of distillation
ALKYLCYCLOHEXANES—con.				
cis-1,3-Dimethylcyclohexane	APIHRP	Azeotropic (ethanol)	I	11/26/41 to 12/8/41
trans-1,3-Dimethylcyclohexane	do	do	I	1/24/42 to 2/2/42
cis-1,4-Dimethylcyclohexane	do	Azeotropic (isopropanol)	I	3/17/42 to 3/27/42
trans-1,4-Dimethylcyclohexane	do	Azeotropic (methyl Cellosolve).	J	4/29/42 to 5/12/42
n-Propylcyclohexane	APIRP 6	Azeotropic (butyl Cellosolve).	J	3/8/43 to 3/15/43
ALKYLBENZENES				
Benzene	do	Regular	E	2/4/43 to 2/18/43
Toluene	Humble	do	D	1/26/43 to 2/12/43
Ethylbenzene	APIRP 6	do	N	4/29/43 to 5/10/43
o-Xylene	do	Azeotropic (Cellosolve)	J	12/14/42 to 12/25/42
m-Xylene	do	do	I	12/14/42 to 12/24/42
p-Xylene	do	do	I	12/28/42 to 1/15/43
n-Propylbenzene	Dow	Azeotropic (butyl Cellosolve).	H	12/18/42 to 12/26/42
Isopropylbenzene	do	Azeotropic (Cellosolve)	D	12/26/42 to 1/14/43

[a] The abbreviations represent the following laboratories: APIHRP, American Petroleum Institute Hydrocarbon Research Project (now the American Petroleum Institute Research Project 45) at the Ohio State University, Columbus, Ohio. APIRP6, American Petroleum Institute Research Project 6 at the National Bureau of Standards, Washington, D. C. Penn State, Petroleum Refining Laboratory at the Pennsylvania State College, State College, Pa. Ethyl, Chemical Laboratory of the Ethyl Corporation, Detroit, Mich. Barrett, Barrett Division of the Allied Chemical & Dye Corporation, New York, N. Y. Dow, Dow Chemical Co., Midland, Mich. Humble, Humble Oil & Refining Co., Houston, Tex. Phillips, Phillips Petroleum Co., Bartlesville, Okla.

[b] See text for further details. Methyl Cellosolve is ethylene glycol monomethyl ether; Cellosolve is ethylene glycol monoethyl ether; butyl Cellosolve is ethylene glycol monobutyl ether.

Table 1 lists the kind of distillation used in the purification and the azeotrope-forming substance (if used), together with (for purposes of record) the number of the distilling column and the time during which the distillation was performed. The details of the assembly, testing, and operation of these distilling columns are given in another report [1].* Column D had a Pyrex glass rectifying section consisting of 138 bubble cap sections, each 25 mm in diameter and 20 mm in length [7], and the over-all separating efficiency was near 100 theoretical plates at total reflux. The other columns listed in table 1 had rectifying sections packed with stainless-steel helices ($\frac{3}{32}$ in. in diameter, No. 30 AWG wire) and had the following sizes of rectifying section, capacity of still pot, and approximate number of theoretical plates at total reflux: E, 25 by 2,750 mm, 3 liters, 100; F, 25 by 2,750 mm, 3 liters, 100; H, 15 by 2,700 mm, 3 liters, 110; I, 10 by 2,800 mm, 0.75 liter, 125; J, 10 by 2,800 mm, 0.75 liter, 125; N, 25 by 2,730 mm, 3 liters, 100. The distillations were performed at a reflux ratio approximately equal to the number of theoretical plates. The volumes of hydrocarbon charged for azeotropic distillation ranged from 250 ml for the compounds distilled in columns I and J to near 1,500 ml for the compounds distilled in the larger columns.

For this group of compounds, no time was available for the detailed examination of the purity, by measurement of freezing points,[3] of the

*Figures in brackets indicate the literature references at the end of this paper.

[3] In more recent work in this laboratory on the preparation of API-NBS hydrocarbons and of NBS Standard Samples in the cooperative program of the American Petroleum Institute and the National Bureau of Standards, the blending of fractions of distillate is done on the basis of measurements of freezing points of appropriate fractions of distillate [2].

distillate as a function of its volume, and the best sample was taken as an appropriately selected "heart" cut (not necessarily the middle part of the distillate) of 50 to 200 ml, comprising not more than 25 percent of the distillate. The heart cut was selected largely on the basis of refractive index and boiling point, although, as will be shown in a later report [2], this is a procedure that frequently results in the discarding of the best material. Only this best sample of each compound was subjected to measurements of properties. In each case the sample was filtered through silica gel to remove water and non-hydrocarbon impurities.

III. REFRACTIVE INDICES

The measurements of refractive index were made with a precision refractometer, by reference to three hydrocarbons [4] 2, 2,4-trimethylpentane, methylcyclohexane and toluene, for which the values of refractive index were determined on a spectrometer with hollow prism by L. W. Tilton, of the Optical Instruments Section of the National Bureau of Standards. The values for the three reference hydrocarbons were reported accurate to ± 0.00001. The reference compounds were used as follows: 2,2,4-Trimethylpentane for the paraffin hydrocarbons, methycyclohexane for the naphthene hydrocarbons, and toluene for the aromatic hydrocarbons. By this procedure, the refractometer was actually used only to determine the difference in refractive index, n_D, between the reference compound and the hydrocarbon being measured. The uncertainties of the values of refractive index, which are reported in table 2, are estimated to be as follows: Precision, ± 0.00002 to ± 0.00003; accuracy, (including the effect of impurities), ± 0.00005 to ± 0.00008.

[4] These three hydrocarbons were substantially the same as those which became available on December 1, 1944 as NBS Standard Samples of hydrocarbons certified with respect to refractive index at 20°, 25°, and 30° C at each of 7 wavelengths.

TABLE 2.—*Properties of 29 paraffin, 4 alkylcyclopentane, 10 alkylcyclohexane, and 8 alkylbenzene hydrocarbons*[a]

TABLE 2.—*Properties of 29 paraffin, 4 alkylcyclopentane, 10 alkylcyclohexane, and 8 alkylbenzene hydrocarbons* [b]

Compound	Formula	Boiling point at 760 mm Hg	Pressure coefficient of the boiling point at 760 mm dt/dP	Refractive index [a] n_D, at—		Density at [a]—		Freezing point of the actual sample in air at 1 atm	Calculated amount of impurity
				20° C	25° C	20° C	25° C		
PARAFFINS		° C	° C/mm Hg			g/ml	g/ml	° C	Mole fraction
n-Pentane	C_5H_{12}	36.073	0.03856	1.35745	1.35466			−129.751	0.0014
2-Methylbutane (Isopentane)	C_5H_{12}	27.852	.03815	1.35369	1.35084			−160.002	.0054
n-Hexane	C_6H_{14}	68.740	.04191	1.37486	1.37226	0.65937	0.65481	−95.338	.0009
2-Methylpentane	C_6H_{14}	60.271	.04141	1.37145	1.36873	.65315		−153.700	.0011
3-Methylpentane	C_6H_{14}	63.282	.04182	1.37652	1.37386	.66431	.65976		
2,2-Dimethylbutane	C_6H_{14}	49.741	.04117	1.36876	1.36595	.64916		−99.991	.0006
2,3-Dimethylbutane	C_6H_{14}	57.988	.04173	1.37495	1.37231	.66164	.65702	−128.798	.0010
n-Heptane	C_7H_{16}	98.426	.04480	1.38764	1.38517	.68367	.67949	−90.609	.0007
2,2-Dimethylpentane	C_7H_{16}	79.203	.04394	1.38217	1.37955	.67385	.66958	−123.794	.0001
3,3-Dimethylpentane	C_7H_{16}	86.069	.04510	1.39085	1.38837	.69322	.68909	−134.99(II)	.0017
n-Octane	C_8H_{18}	125.665	.04738	1.39743	1.39505	.70252	.69849	−56.806	.0004
2-Methylheptane	C_8H_{18}	117.647	.04691	1.39494	1.39257	.69792	.69392	−109.248	.010
3-Methylheptane	C_8H_{18}	118.925	.04712	1.39848	1.39610	.70582	.70175	−120.595	.006
4-Methylheptane	C_8H_{18}	117.709	.04695	1.39792	1.39553	.70463	.70055	−120.983	.0015
3-Ethylhexane	C_8H_{18}	118.534	.04719	1.40162	1.39919	.71358	.70948		
2,2-Dimethylhexane	C_8H_{18}	106.840	.04650	1.39349	1.39104	.69528	.69112	−121.232	.0018
2,3-Dimethylhexane	C_8H_{18}	115.607	.04724	1.40113	1.39880	.71214	.70809		
2,4-Dimethylhexane	C_8H_{18}	109.429	.04664	1.39534	1.39291	.70036	.69620		
2,5-Dimethylhexane	C_8H_{18}	109.103	.04646	1.39246	1.39004	.69354	.68934	−91.405	.010
3,3-Dimethylhexane	C_8H_{18}	111.969	.04741	1.40009	1.39782	.71000	.70596	−126.13	.0012
3,4-Dimethylhexane	C_8H_{18}	117.725	.04752	1.40406	1.40180	.71923	.71516		
2-Methyl-3-ethylpentane	C_8H_{18}	115.650	.04749	1.40401	1.40167	.71932	.71522	−115.050	.005
3-Methyl-3-ethylpentane	C_8H_{18}	118.259	.04844	1.40775	1.40549	.72742	.72354	−90.996	.005
2,2,3-Trimethylpentane	C_8H_{18}	109.841	.04755	1.40295	1.40066	.71602	.71207	−112.453	.007
2,2,4-Trimethylpentane	C_8H_{18}	99.238	.04651	1.39145	1.38901	.69192	.68777	−107.396	.0012
2,3,3-Trimethylpentane	C_8H_{18}	114.760	.04833	1.40750	1.40522	.72619	.72232	−101.655	.006
2,3,4-Trimethylpentane	C_8H_{18}	113.467	.04761	1.40422	1.40198	.71906	.71503	−109.248	.0016
n-Nonane	C_9H_{20}	150.796	.04965	1.40549	1.40316	.71766	.71382	−53.606	VV.003
n-Decane	$C_{10}H_{22}$	174.123	.05172	1.41189	1.40967	.73005	.72625	−20.724	VV.003

See footnotes at end of table.

TABLE 2.—*Properties of 29 paraffin, 4 alkylcyclopentane, 10 alkylcyclohexane, and 8 alkylbenzene hydrocarbons* [b]—Continued

Compound	Formula	Boiling point at 760 mm Hg	Pressure coefficient of the boiling point at 760 mm dt/dP	Refractive index [a] n_D at—		Density at—		Freezing point of the actual sample in air at 1 atm	Calculated amount of impurity
				20° C	25° C	20° C	25° C		
		° *C*	° *C/mm Hg*			*g/ml*	*g/ml*	° *C*	*Mole fraction*
ALKYLCYCLOPENTANES									0.0003
Cyclopentane	C_5H_{10}	49.262	0.04003	1.40646	1.40362	0.74538	0.74045	−93.917	.0013
Methylcyclopentane	C_6H_{12}	71.812	.04274	1.40969	1.40686	.74860	.74393	−142.468	.0033
n-Propylcyclopentane	C_8H_{16}	130.937	.04886	1.42827	1.42593	.77625	.77223	−117.402	.0028
Isopropylcyclopentane	C_8H_{16}	126.415	.04913	1.42586	1.42355	.77656	.77257	−111.462	
ALKYLCYCLOHEXANES									.0003
Cyclohexane	C_6H_{12}	80.738	.04376	1.42623	1.42354	.77855	.77389	+6.547	.0010
Methylcyclohexane	C_7H_{14}	100.934	.04671	1.42305	1.42056	.76936	.76501	−126.597	.0017
Ethylcyclohexane	C_8H_{16}	131.783	.04969	1.43304	1.43073	.78792	.78390	−111.343	.0006
cis-1,2-Dimethylcyclohexane	C_8H_{16}	129.728	.04968	1.43596	1.43358	.79627	.79222	−50.211	.004
trans-1,2-Dimethylcyclohexane	C_8H_{16}	123.419	.04951	1.42607	1.42471	.77601	.77204	−88.284	
cis-1,3-Dimethylcyclohexane	C_8H_{16}	124.450	.04910	1.43085	1.42843	.78472	.78055	−93.39	.023
trans-1,3-Dimethylcyclohexane	C_8H_{16}	120.088	.04880	1.42294	1.42063	.76603	.76196	−77.052	.015
cis-1,4-Dimethylcyclohexane	C_8H_{16}	124.321	.04921	1.42967	1.42731	.78285	.77870	−87.780	.010
trans-1,4-Dimethylcyclohexane	C_8H_{16}	119.351	.04903	1.42090	1.41853	.76254	.75835	−37.093	.004
n-Propylcyclohexane	C_9H_{18}	156.711	.05201	1.43686	1.43470	.79349	.78960	−94.864	.005
ALKYLBENZENES									.0004
Benzene	C_6H_6	80.103	.04273	1.50110	1.49790	.87903	.87368	+5.506	.0010
Toluene	C_7H_8	110.623	.04630	1.49662	1.49405	.86893	.86220	−95.032	.0046
Ethylbenzene	C_8H_{10}	136.187	.04898	1.49580	1.49319	.86696	.86258	−95.061	.0010
o-Xylene	C_8H_{10}	144.414	.04969	1.50324	1.50282	.89005	.87583	−25.225	
m-Xylene	C_8H_{10}	139.102	.04903	1.49715	1.49485	.86412	.85985	−47.976	.0029
p-Xylene	C_8H_{10}	138.348	.04918	1.49580	1.49319	.86100	.85666	+13.233	.0008
n-Propylbenzene	C_9H_{12}	159.216	.05143	1.49195	1.48950	.86198	.85776	−99.581	.0028
Isopropylbenzene	C_9H_{12}	152.393	.05076	1.49125	1.48874	.86175	.85748	−96.043	.0004

[a] For air-saturated hydrocarbon in the liquid state at 1 atmosphere.
[b] See text for uncertainties of experimental values.

IV. DENSITIES

The measurements of density were made with a density balance, the assembly, calibration, and operation of which has been described [3]. The uncertainties of the values of density, which are reported in table 2, are estimated to be as follows: Precision, ± 0.00002 to ± 0.00003; accuracy (including the effect of impurities), ± 0.00005 to ± 0.00010.

V. BOILING POINTS

The normal boiling points of these compounds were determined as part of another investigation on their vapor pressures, and the values reported in table 2 for the normal boiling point and the pressure coefficient of the boiling point at 1 atmosphere are taken directly from the report of that investigation [4]. The uncertainties in the values of the normal boiling point reported in table 2 are estimated to be as follows: Precision, ± 0.002 to $\pm 0.003°$ C; accuracy (including the effect of impurities), ± 0.005 to $\pm 0.010°$ C.

VI. FREEZING POINTS AND PURITIES

The freezing point of the actual sample of each of the compounds (except for four of the octanes) was determined from time-temperature freezing and melting curves, by using the apparatus and procedure described in another report [5]. The values of freezing points are given in table 2.

The purity of the actual sample was calculated, according to the method described in section VIII of reference [5], from the freezing point for zero impurity and values of the cryoscopic constants subsequently determined in another investigation on the preparation of API–NBS hydrocarbons [2, 6]. The calculated amount of impurity is given in table 2. From the manner of preparation and purification of these compounds, it is believed that the impurities in each case are substantially all close-boiling isomers.

Grateful acknowledgment is made to the following persons and laboratories for supplying the materials for purification listed in table 1: C. E. Boord, supervisor of the API Research Project 45 (formerly the API Hydrocarbon Research Project) at the Ohio State University, Columbus, Ohio; M. R. Fenske, supervisor of the Petroleum Refining laboratory, Pennsylvania State College, State College, Pa.; George Calingaert, director of Chemical Research, Ethyl Corporation, Detroit, Mich.; Barrett Division of the Allied Chemical & Dye Corporation, New York, N. Y.; Dow Chemical Co., Midland, Mich.; Humble Oil & Refining Co., Houston, Tex. Additional thanks are due Professor Fenske for having supplied the very pure sample of cyclopentane.

VII. REFERENCES

[1] C. B. Willingham and F. D. Rossini, API Research Project 6; National Bureau of Standards. Unpublished.
[2] A. J. Streiff, E. T. Murphy, C. B. Willingham, V. A. Sedlak, and F. D. Rossini, API Research Project 6, National Bureau of Standards. Unpublished.
[3] A. F. Forziati, B. J. Mair, and F. D. Rossini, J. Research NBS **35,** 513 (1945) RP1685.
[4] C. B. Willingham, W. J. Taylor, J. M. Pignocco, and F. D. Rossini, J. Research NBS **35,** 219 (1945) RP1670.
[5] A. R. Glasgow, Jr., A. J. Streiff, and F. D. Rossini, J. Research National Bureau of Standards **35,** 355 (1945) RP1676.
[6] A. R. Glasgow, E. T. Murphy, C. B. Willingham, and F. D. Rossini, API Research Project 6, National Bureau of Standards. Unpublished.
[7] J. H. Brunn, and W. B. M. Faulconer, Ind. Eng. Chem. Anal. Ed. **9,** 192 (1937).

WASHINGTON, September 25, 1945.

U. S. Department of Commerce National Bureau of Standards

RESEARCH PAPER RP1696

Part of Journal of Research of the National Bureau of Standards, Volume 36, February 1946

EFFECT OF SOME ADDED MATERIALS ON DICALCIUM SILICATE

By Edwin S. Newman and Lansing S. Wells

ABSTRACT

Studies of binary systems are helpful in the investigation of polycomponent systems forming industrial products, such as portland cement, dolomite refractories, or blast-furnace slags. Details are given of the application of differential heating and cooling curves to the determination of the temperature of the $\alpha \rightleftarrows \beta$ inversion of $2CaO.SiO_2$ in binary mixtures with CaO, SiO_2, Al_2O_3, MgO, Fe_2O_3, CaF_2, TiO_2, BaO, Cr_2O_3, B_2O_3, Mn_2O_3, V_2O_5, P_2O_5, Na_2O, and K_2O. These added materials, excepting CaO, lowered the temperature of the $\alpha \rightleftarrows \beta$ inversion and estimates of the limits of solid solution in α-$2CaO.SiO_2$ are given. X-ray patterns of β-$2CaO.SiO_2$ containing BaO, P_2O_5, Na_2O, or K_2O indicated the existence of solid solutions of the substitution type. Observations were made of the effectiveness of the added materials in preventing dusting, which results from the $\beta \rightarrow \gamma$ inversion of $2CaO.SiO_2$. It was found that Mn_2O_3 should be added to the list of known chemical inhibitors of dusting.

CONTENTS

		Page
I.	Introduction	137
II.	Materials and general procedure for preparing and testing mixtures	139
III.	Choice of the method of differential heating curves	140
IV.	Apparatus and procedure for obtaining differential heating and cooling curves	141
V.	Temperature of the $\alpha \rightleftarrows \beta$ inversion of $2CaO.SiO_2$	144
VI.	Effect of added materials on $2CaO.SiO_2$	150
	1. Al_2O_3, MgO, Fe_2O_3, TiO_2, and CaF_2	150
	2. $2BaO.SiO_2$ and BaO	155
	3. Cr_2O_3	155
	4. V_2O_5, P_2O_5, B_2O_3, and Mn_2O_3	155
	5. Na_2O and K_2O	156
VII.	X-ray diffraction patterns	156
VIII.	$B \rightarrow \gamma$ inversion of $2CaO.SiO_2$	157
IX.	Summary and conclusions	157
X.	References	158

1. INTRODUCTION

Dicalcium silicate, $2CaO.SiO_2$, is one of the major constituents of portland cement and is found also in blast furnace slags [1] [1] and in certain refractories developed from lime and dolomite [2]. Knowledge of the properties of $2CaO.SiO_2$ is therefore important to the users of these industrial products. It was the purpose of the present study to

[1] Figures in brackets indicate literature references at the end of this paper.

determine the behavior during heating and cooling of dicalcium silicate in binary mixtures with oxides, which either occur in ordinary industrial raw materials or have been added experimentally in the manufacture of portland cement. Such studies of simple systems are helpful in the investigation of polycomponent systems existing in industrial products.

Dicalcium silicate has three enantiotropic forms: alpha, beta, and gamma. The $\alpha \rightleftarrows \beta$ inversion has been reported as occuring at 1,420° C and the $\beta \rightleftarrows \gamma$ at 675° C [3]. An increase in volume of about 10 percent accompanies the $\beta \rightleftarrows \gamma$ inversion and causes the so-called "dusting" of dicalcium silicate and may result in a destructive expansion of materials in which it is an ingredient. Also, because gamma $2CaO.SiO_2$ has no hydraulic properties, it is not desired in portland cement clinker. Consequently, preventing the transformation of the beta to the gamma form is of industrial importance. It has been found that a number of substances prevent this transformation by entering into solid solution with dicalcium silicate. Studies of the solubility of various substances in beta dicalcium silicate are therefore valuable because of their bearing on the beta to gamma inversion. This solubility may be determined in the following way.

If the addition of a substance to a compound having two enantiotropic forms causes the formation of a solid solution the temperature of the inversion will be altered providing the solute is more soluble in one of these forms than in the other. When saturation is reached, no further change in the inversion temperature will occur upon the addition of more of the solute if the observed change is due entirely to the formation of solid solution. In this way the measurement of the temperature of the $\alpha \rightleftarrows \beta$ inversion of dicalcium silicate furnishes a means for estimating the limit of solubility of a substance in dicalcium silicate.

The addition of a substance to a compound such as dicalcium silicate may not only alter the temperature of the inversion but also cause the formation of new phases. The presence of an additional phase in a heat-treated preparation is evidence that the limit of solubility of the added substance in the compound has been exceeded at the temperature of heating. The presence of the new phase may be revealed by an inflection on the heating and cooling curves in addition to the inflection caused by the inversion.

If it is desired to know which of several inflections on a heating or cooling curve represents the inversion of the compound containing added material, it is usually necessary to examine a suitable series of such curves arranged in the order of increasing amounts of the added substance. It will then be found that the inflection caused by the inversion will become smaller, whereas the other inflections will become larger.

It is evident therefore that the temperature of the $\alpha \rightleftarrows \beta$ inversion of dicalcium silicate should be known accurately if one is to interpret properly the various inflections in heating and cooling curves. This is particularly important when the limit of solubility of a substance in dicalcium silicate is small and the temperature of the $\alpha \rightleftarrows \beta$ inversion is changed but slightly by the addition of the substance in question.

As preliminary experiments with various samples of presumably pure dicalcium silicate prepared by the authors, and also by several other investigators at the National Bureau of Standards, gave inflections in heating and cooling curves that were usually higher than the reported temperature of the $\alpha \rightleftarrows \beta$ inversion of 1,420° C [3], it was decided to study the cause of this and to obtain more information on the $\alpha \rightleftarrows \beta$ inversion before attempting to investigate the limits of solubility of various substances in dicalcium silicate as determined by the effects on the temperature of the $\alpha \rightleftarrows \beta$ inversion.

Zerfoss and Davis [4] apparently were also confronted with the question of the temperature of the $\alpha \rightleftarrows \beta$ inversion of dicalcium silicate, for they state "Much difficulty was experienced in detecting the alpha-to-beta inversion of a pure preparation of C_2S in a mineralizer-free system. Despite numerous refinements in technique, one could not attach much certainty to the recorded inversion temperature; in fact only in the presence of a mineralizer (CaF_2) were the authors able to obtain a reliable heat effect."

The first part of the present paper deals with the application of heating and cooling curves to the determination of the temperature of the $\alpha \rightleftarrows \beta$ inversion of $2CaO.SiO_2$ and of the effect of excess CaO or SiO_2 (oxide constituents of $2CaO.SiO_2$) on the temperature of this inversion. The second part of the paper deals with the effects of additions of Al_2O_3, MgO, Fe_2O_3, CaF_2, TiO_2, BaO, Cr_2O_3, Mn_2O_3, V_2O_5, P_2O_5, Na_2O, and K_2O, on the temperature of the $\alpha \rightleftarrows \beta$ inversion, the extent to which they form solid solutions with the dicalcium silicate, and their effectiveness in preventing the β to γ inversion or dusting.

II. MATERIALS AND GENERAL PROCEDURE FOR PREPARING AND TESTING MIXTURES

All the materials were of analytical reagent quality. The source of CaO was precipitated "low alkali" $CaCO_3$ which contained less than 0.042 percent of total determined impurities, including less than 0.010 percent of K and Na as sulfates and less than 0.010 percent of MgO. Silica gel with a 0.06 percent residue nonvolatile with HF was the source of SiO_2. The added substances were introduced as $Al_2O_3.3H_2O$, $Mg(OH)_2$, Fe_2O_3, CaF_2, TiO_2, $BaCO_3$, Cr_2O_3, $2CaO.B_2O_3$, Mn_2O_3, V_2O_5, H_3PO_4, Na_2CO_3, and K_2CO_3. Sufficient silica was added with the $2CaO.B_2O_3$ to react with the CaO and form $2CaO.SiO_2$.

Mixtures of $CaCO_3$ and silica gel proportioned in the molar ratio of CaO to SiO_2 of 2.00 were prepared in 100- to 200-g quantities and tumbled for 8 to 12 hr in 1-pt glass jars that contained a few wooden balls. One of these mixtures was heated for 1 hr at 1,450° C, cooled, and remixed by hand. This was repeated three times. The resulting material, largely $\gamma 2CaO.SiO_2$ as shown by microscopical examination, was reserved as a "standard" sample of dicalcium silicate and was used throughout the investigation as one of the materials to calibrate and check the thermocouples by the temperature of its β to α inversion as shown by heating curves.

Portions of about 5 g of the other mixtures of $CaCO_3$ and silica gel were heated for ½ hr at 1,440° to 1,480° C, cooled, and ground in an agate mortar. This was repeated three times. Each portion so pre-

pared was then placed in the crucible of the apparatus used for obtaining differential heating and cooling curves and heated to about 1,470° C for 1 hr. The temperature of the $\alpha \rightleftarrows \beta$ inversion was then determined. If the material did not give the desired temperature of inversion, the necessary adjustments were made on the batch material by adding very small quantities of $CaCO_3$ or silica gel. The reasons for the necessity of this procedure will be discussed subsequently.

The standardized $CaCO_3$-silica gel mixtures so prepared and tested were used in making the preparations of $2CaO.SiO_2$ with added materials. About 5 g total weight of a standardized dicalcium silicate raw mix, plus the added material, were tumbled for 2 to 4 hr in 2-oz bottles that contained a single wooden ball. These preparations were heat-treated and remixed in the same manner as that used in testing the dicalcium silicate raw mix. Heating and cooling curves were then obtained with these mixtures.

Small samples of dicalcium silicate with each of the various additions were also quenched in mercury after heating them above the $\beta \rightarrow \alpha$ inversion temperature [2] for one-half to one hour. These quenched samples were examined petrographically and X-ray patterns [3] were obtained representative of those preparations in which the beta form of the dicalcium silicate was preserved.

III. CHOICE OF THE METHOD OF DIFFERENTIAL HEATING CURVES

Time-versus-temperature curves were used in many of the previous studies of phase equilibria in silicate systems, including determinations of melting points. Rankin and Wright [3] in 1915 reported their value of 1,420° C for the temperature of the $\alpha \rightleftarrows \beta$ inversion of $2CaO.SiO_2$ obtained from such curves.

More recently differential heating curves have gained favor. One of the present authors [5] showed that differential heating curves gave an accurate location of the temperature of the $\beta \rightarrow \alpha$ inversion of $CaSO_4$. Such curves can be used also to determine melting points.

A time-temperature curve for the melting of $2CaO.B_2O_3$ is shown in the right-hand portion of figure 1 and a time-temperature curve for the $\beta \rightarrow \alpha$ inversion of a sample of $2CaO.SiO_2$ in the left-hand portion of the same figure. For comparison, the corresponding differential heating curves are also shown. It is evident from an examination of the two sets of curves that the differential heating curves give a more definite location of the temperature of change-of-phase than do curves of time versus temperature. Hence the selection of differential heating curves in the present study.

[2] In general discussions of the transformation between the alpha and beta forms the symbol $\alpha \rightleftarrows \beta$ is used to indicate the inversion without regard to the direction of change of temperature. When the temperature is raised, i. e., in heating curves, the direction of inversion is from β to α and the symbol $\beta \rightarrow \alpha$ is adopted. With falling temperature the inversion is in the reverse direction and the symbol $\alpha \rightarrow \beta$ is used.

[3] Prepared by E. Golovato and B. L. Steierman and interpreted by H. F. McMurdie.

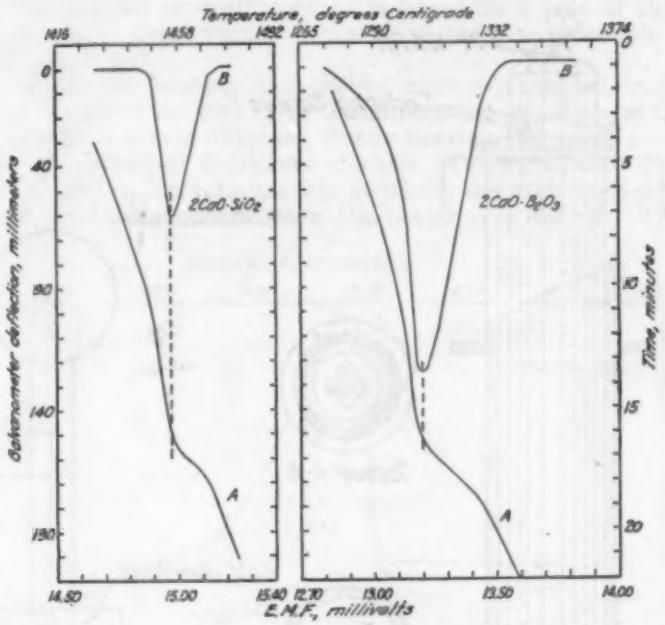

FIGURE 1.—*Time-temperature and differential heating curves for the melting of* $2CaO.B_2O_3$ *and for the* $\beta \rightarrow \alpha$ *inversion of* $2CaO.SiO_2$.

The time-temperature curves, *A*, have been rotated 90° clockwise for comparison with the differential heating curves, *B*. Dotted lines show the relation between curve *A* and the maximum deflection of curve *B*. Time-temperature deflection data for both curves were obtained in a single heating of each material. Heating rate, approximately 3 degrees centigrade per minute.

IV. APPARATUS AND PROCEDURE FOR OBTAINING DIFFERENTIAL HEATING AND COOLING CURVES

The arrangement of the crucibles and supports in the furnace used for obtaining differential heating and cooling curves is shown in detail in figure 2. The crucibles were a narrow, deep type, recommended by White [6] for the determination of melting points. They were 1 inch deep and semicircular in cross section, with a 0.25-in. radius, and held 2 to 4 g of powdered material.

The differential thermocouple, Pt:Pt–10-percent Rh, was made of wire calibrated in the Bureau's Pyrometry Section.

In obtaining the data for differential heating and cooling curves, the furnace temperature was changed at an approximately constant rate by suitable manipulation of the control [7] and of the rheostats regulating the heating current. Two rates were used, about 8.5 and 2.5 degrees centigrade/min. The faster rate was used in exploratory tests, and the slower rate in determining more exactly the temperature at which the heat effects occurred. At intervals of 1 min or less, if the deflection was changing rapidly, readings were taken of the emf of the thermocouple in contact with the sample in crucible 1 (fig. 2) and of the deflection of the galvanometer in series with thermocouple 1 and the opposed thermocouple in the reference material (corundum) in crucible 2. Seldom more than 1 second intervened between the final balancing of the potentiometer and the reading of the deflection. A

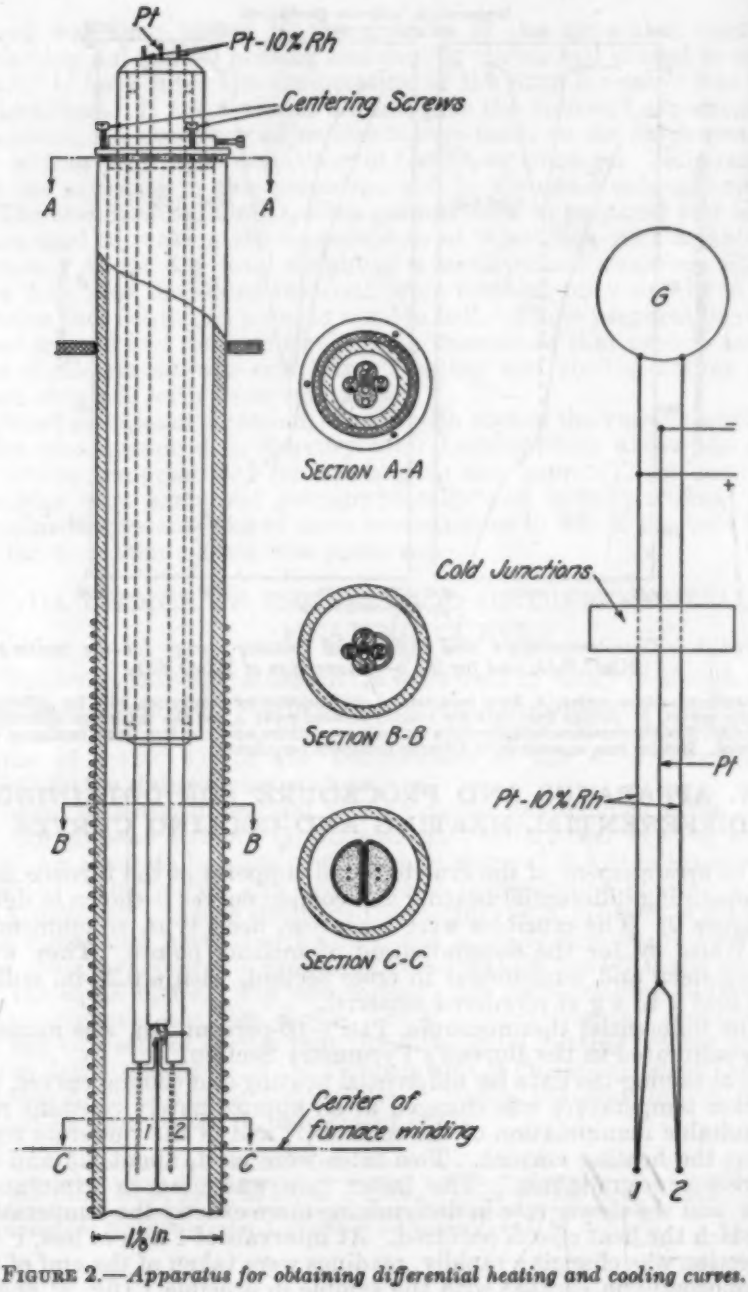

FIGURE 2.—*Apparatus for obtaining differential heating and cooling curves.*

differential heating or cooling curve is based on a plot of these galvanometer deflections versus the emf of the thermocouple in the material under test.

The differential heating and cooling curves presented in figure 3 show the effects of the two rates of temperature change and the relative positions of curves obtained during heating and cooling of a particular preparation of dicalcium silicate. Tangents were drawn to facilitate selecting the temperature at which the maximum deflection of the galvanometer occurs when the material is heated. This pro-

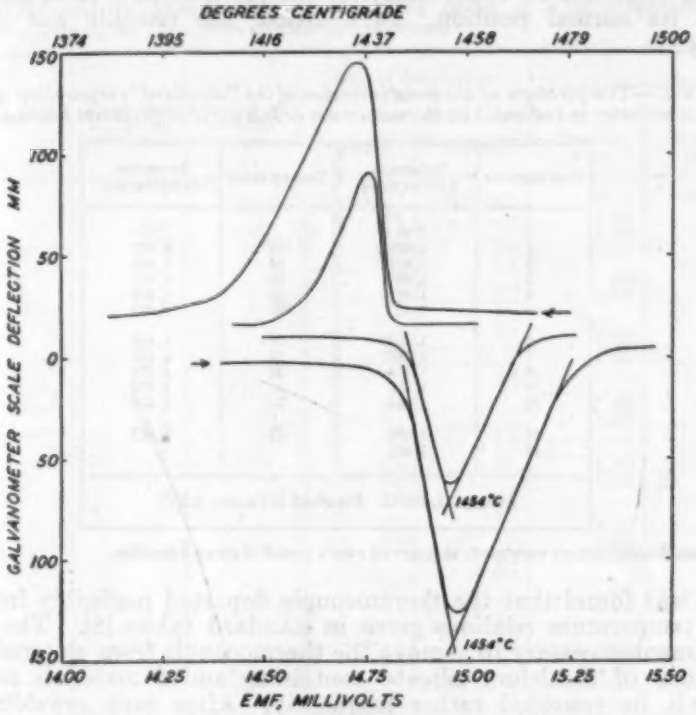

FIGURE 3.—*Differential heating and cooling curves indicating temperature of the* $\beta \rightleftarrows \alpha$ *inversion of* $2CaO.SiO_2$.

Rates of temperature change, 8.5 and 2.5 degrees centigrade per minute. Curves showing the greater deflection were obtained at the faster rate. Arrows indicate the direction of change of temperature.

cedure of drawing tangents was found to be necessary when inflections on the curves were small and poorly defined. The temperature obtained during the heating cycle was always higher than that obtained during the cooling cycle of the same sample. This difference can be attributed to superheating or supercooling of the sample, but, because of the greater tendency toward supercooling, the temperatures obtained by heating were chosen as the more reliable.

The thermocouple was checked from time to time against the melting points of K_2SO_4, $2CaO.B_2O_3$, $CaO.MgO.2SiO_2$, or $3CaO.B_2O_3$. Shifting of the thermocouple was prevented in some of the melting point determinations by means of a small platinum-wire guard clamped adjacent to the bead.

The temperature of the β to α inversion of the sample of $2CaO.SiO_2$ reserved for calibration also served as a check on the thermocouple. Table 1 gives the values of 23 determinations of the β to α inversion of this "standard" preparation of dicalcium silicate, as indicated by the maximum deflection of the differential heating curves. These determinations were made at intervals over a period of about 6 months. The average was 1,456° C, with a standard deviation of 2.2° C. The significance of this temperature will be discussed later. Dicalcium silicate was useful for the calibration because fusion did not occur, and hence there was no opportunity for the thermocouple to be displaced from its normal position. In addition, the crucible was cleaned easily.

TABLE 1.—*Temperature of the $\beta \rightarrow \alpha$ inversion of the "standard" preparation of dicalcium silicate, as indicated by the maximum deflection of differential heating curves*[a]

Test number	Inversion temperature	Test number	Inversion temperature
	°C		°C
1	1,458	13	1,455
2	1,456	14	1,461
3	1,457	15	1,457
4	1,452	16	1,458
5	1,453	17	1,459
6	1,454	18	1,459
7	1,457	19	1,455
8	1,455	20	1,454
9	1,456	21	1,452
10	1,455	22	1,456
11	1,456	23	1,453
12	1,455		
Average, 1,456°C. Standard deviation, 2.2°C.			

[a] These determinations were made at intervals over a period of about 6 months.

It was found that the thermocouple departed negligibly from the emf temperature relations given in standard tables [8]. The rough treatment necessary to remove the thermocouple from sintered preparations of dicalcium silicate containing added materials required that it be rewelded rather frequently. After each rewelding the thermocouple was recalibrated.

V. TEMPERATURE OF THE $\alpha \rightleftharpoons \beta$ INVERSION OF $2CaO.SiO_2$

As stated previously, it was found that various samples of dicalcium silicate which had been prepared by several investigators at this Bureau gave inflections in heating and cooling curves that were higher than the reported temperature of the $\alpha \rightleftharpoons \beta$ inversion of 1,420° C [3]. A total of eight batches of dicalcium silicate had been prepared and differential heating and cooling curves were obtained. Samples of all eight preparations were then carefully analyzed and the molar ratios of CaO to SiO_2 computed. Table 2 gives these molar ratios together with the percentage of R_2O_3. It also contains the values of the $\beta \rightarrow \alpha$ and $\alpha \rightarrow \beta$ inversions ascertained from the respective heating and cooling curves (fig. 4) by the method of drawing tangents, as illustrated in figure 3. The rates of heating and cooling are also given in table 2 and figure 4. It can be seen from table 2 that for each prepara-

tion the values of the $\beta \rightarrow \alpha$ inversion obtained by heating at different rates agreed very well. All of the values were above 1,420° C. For the most part the temperatures of the $\alpha \rightarrow \beta$ inversions for each preparation also checked for the different cooling rates. However, as mentioned previously, the temperature of the $\beta \rightarrow \alpha$ inversions obtained with heating curves were invariably higher than the temperatures of the $\alpha \rightarrow \beta$ inversions obtained with cooling curves.

TABLE 2.—*Temperatures of the $\beta \rightarrow \alpha$ inversion obtained by differential heating curves, and of the $\alpha \rightarrow \beta$ inversion by differential cooling curves, of eight preparations of chemically analyzed dicalcium silicate compositions*

Sample	Molar ratio CaO/SiO_2	Percentage of R_2O_3[a]	Rate of temperature change		Temperature of inversion	
			Heating	Cooling	Heating $\beta \rightarrow \alpha$	Cooling $\alpha \rightarrow \beta$
		%	°C/min	°C/min	°C	°C
1	2.00	0.20	5.0		1,455	
			0.8		1,454	
				8.4		1,439
				1.7		1,439
2	2.00	.26	5.0		1,450	
			0.8		1,447	
				8.4		1,430
				1.7		1,433
3	2.02	.16	8.4		1,456	
			0.8		1,455	
				8.4		1,438
				1.7		1,439
4	2.01	.20	8.4		1,437	
			1.7		1,437	
				8.4		1,416
				1.7		1,424
5	2.03	.20	8.4		1,442	
			1.7		1,442	
				8.4		1,427
				1.7		1,432
6	2.02	.08	8.4		1,439	
			1.7		1,439	
				8.4		1,420
				1.7		1,425
7	2.01	.14	8.4		1,435	
			1.7		1,432	
				8.4		1,423
				1.7		1,426
8	1.96	.14	8.4		[b] 1,429	
			4.2		[c] 1,432	
				4.2		1,423

[a] Uncorrected for blank of approximately 0.1 percent of R_2O_3.
[b] Second heat effect at 1,454° C.
[c] Second heat effect at 1,456° C.

If, instead of selecting the temperatures at which the maximum galvanometer deflection occurs as representing the temperature of inversion, those temperatures at which the breaks in the heating and cooling curves first started from the normal had been selected, then temperatures other than those recorded in table 2 would have been chosen. This can be seen in figure 4. In several instances, notably for preparations 4, 5, 6, and 8, the breaks in the differential heating curves started below 1,420° C. On the other hand, with these same preparations, the initial breaks in the cooling curves started considerably above 1,420° C. In only one instance (preparation 1) were the temperatures of the initial breaks in both heating and cooling curves at approximately the same temperature.

The selection of the temperature at which the breaks first start has, however, the disadvantages not only in that there is a spread in the temperature range between the initial breaks of the heating and cooling curves but also because these temperatures often occur at different temperatures at different heating and cooling rates and of the uncertainty of their location (fig. 4). Because of these difficulties it seemed advisable to choose the temperature of the maximum

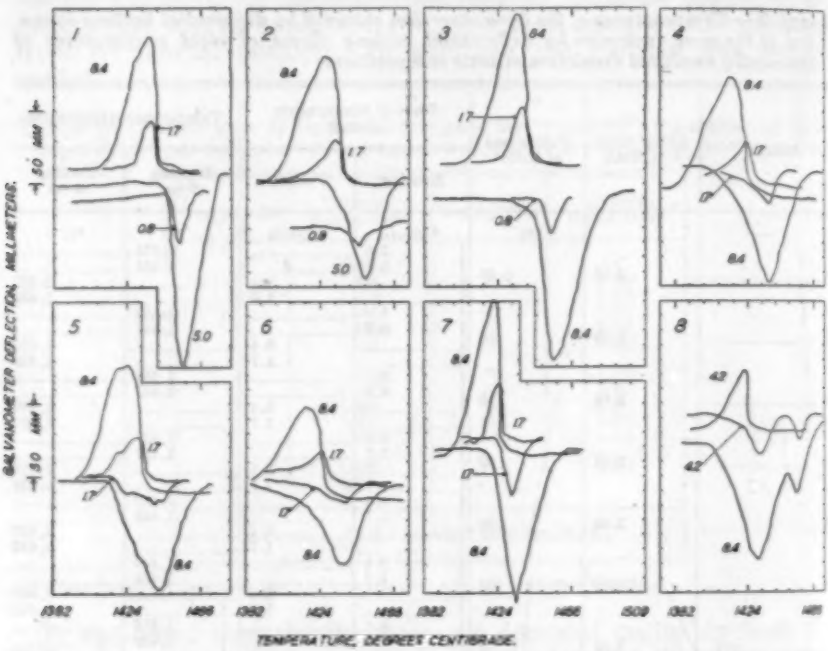

FIGURE 4.—*Differential heating and cooling curves of dicalcium silicate preparations.*

Small numerals adjacent to the curves show the rates of temperature changes in degrees centigrade per minute. Curves plotted with maximum deflection downward were obtained with increasing temperatures.

deflection of the galvanometer as the temperature of inversion and, as stated previously, to select the temperature of the $\beta \rightarrow \alpha$ inversion rather than the $\alpha \rightarrow \beta$ temperature of inversion because of the greater tendency toward supercooling than superheating. In addition, it should be recalled that the temperatures obtained by this method checked well at different heating rates (table 2).

In order to study the reason for the range in the observed $\alpha \rightleftarrows \beta$ inversion temperatures, both heating and cooling curves were obtained for a series of samples in which the CaO/SiO_2 molar ratio was varied slightly by adding CaO and SiO_2 separately to portions of a single batch of dicalcium silicate base mix.

The temperature of the $\beta \rightarrow \alpha$ inversion of this base mix, as indicated by the maximum deflection of the galvanometer, was 1,458° C, a value very close to 1,456° C, the average inversion temperature of

the "standard" sample reserved for calibration (table 1). The addition of 0.50 and 4.00 percent of CaO (table 3) did not change the $\beta \rightarrow \alpha$ inversion of the base mix. Likewise, these additions of CaO did not alter the $\alpha \rightarrow \beta$ inversion temperature. The addition of 0.12 percent of SiO_2 did not lower the $\beta \rightarrow \alpha$ inversion temperature from 1,458° C, but when the percentage was increased to 0.19, this inversion was lowered to 1,438° C. The further additions of SiO_2 (table 3) caused no further significant alteration of the temperature of the $\beta \rightarrow \alpha$ inversion. However, the addition of 1.00 percent or more of SiO_2 resulted in the appearance of a second inflection in the heating

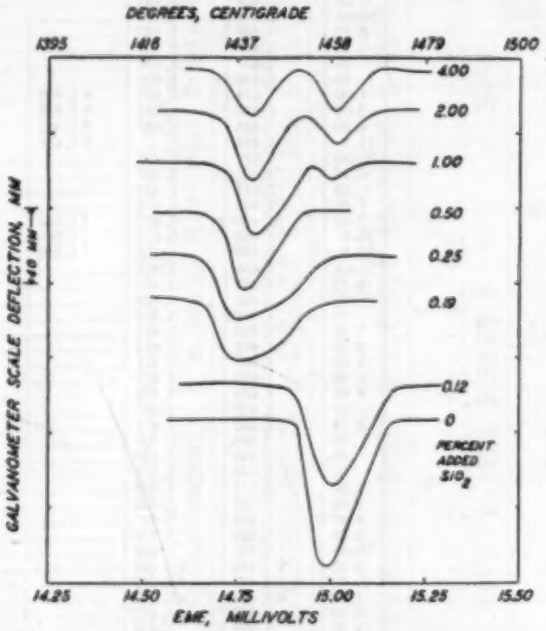

FIGURE 5.—*Differential heating curves.*

Effect of added SiO_2 on the heating curve of $2CaO.SiO_2$. The deflection at about 1,460° obtained with mixtures containing 1.00 percent or more added SiO_2 is assumed to represent melting of the $3CaO.2SiO_2$-$CaO.SiO_2$ eutectic. Heating rate 2.5 degrees centigrade per minute.

curves (fig. 5) somewhat similar to those obtained with preparation number 8 shown in figure 4 where the molar ratio of CaO to SiO_2 was 1.96 to 1. The relative sizes of the two inflections in the three upper heating curves of figure 5 demonstrate that these second heat effects do not represent the $\beta \rightarrow \alpha$ inversion temperature even though they occur at approximately 1,458° C. Presumably the additional heat effects were caused by the melting of the eutectic between $3CaO.2SiO_2$ and $CaO.SiO_2$ [3]. These second inflections did not appear on the cooling curves because the temperatures of the inflections were lowered by undercooling to coincide with that of the $\alpha \rightarrow \beta$ inversion temperature of the dicalcium silicate.

TABLE 3.—*Results of differential heating and cooling curves of* $2CaO.SiO_2$ *containing various added materials* [a]

Material added		Temperature of heat effect [b]				Dusted [c]
		Inversion of $2CaO.SiO_2$		Other phase changes		
		Heating $\beta \rightarrow \alpha$	Cooling $\alpha \rightarrow \beta$	Heating	Cooling	
Percent		°C	°C	°C	°C	
CaO	None	1,458	1,443			+
	0.05	1,458	1,443			+
	4.00	1,458	1,443			+
SiO_2	None	1,458	1,443			+
	0.12	1,458	1,442			+
	.19	1,438	1,431			+
	.25	1,437	1,430			+
	.50	1,438	1,430			+
	1.00	1,441	1,429	[d] 1,459		+
	2.00	1,440	1,424	[d] 1,460	[d] 1,437	+
	4.00	1,440	1,427	[d] 1,459	[d] 1,443	+
	11.7	1,438		[d] 1,456	[d] 1,434	+
Al_2O_3	None	1,457	1,442			+
	0.25	1,451	1,427			+
	.50	1,443	1,432			+
	1.00	1,442	1,434			+
	5.00	1,445	1,418	[f] 1,546	[f] 1,505	+
	10.0	1,442	1,412	[f] 1,548	[f] 1,510	+
	15.0	1,440	1,405	[f] 1,549	[f] 1,520	+
MgO	None	1,458	1,443			+
	0.12	1,452	1,435			+
	.25	1,446	1,427			+
	.50	1,438	1,415			+
	1.00	1,442	1,411			+
	2.00	1,441	1,412			+
	4.00	1,440	1,411			+
	5.00	1,440	1,411			+
	8.00	1,439	1,409			+
Fe_2O_3	None	1,457	1,440			+
	0.12	1,452	1,431			+
	.25	1,448	1,426			+
	.38	1,445	1,420			+
	.50	1,443	1,417			+
	1.00	1,437	1,428			+
	2.00	1,438	1,428			+
	4.00	1,434	1,425			+
	8.25	1,425	1,418			+
CaF_2	None	1,458	1,442			+
	0.25	[e] 1,456	[e] 1,441			+
	.50	[e] 1,457	[e] 1,441			+
	1.00	[e] 1,456	[e] 1,441			+
	2.00	[e] 1,442	[e] 1,427			+
	4.00	1,438	1,429			+
	8.00	1,438	1,432			+
	[b] 0.49	1,457	1,438			+
	[b] .52	1,456	1,436			+
	[b] .58	1,455	1,437			+
	[b] .70	1,438	1,427			+
TiO_2	None	1,457	1,440			+
	0.25	1,451	1,433			+
	.50	1,442	1,420			+
	1.00	1,436	1,423			+
	2.00	1,435	1,424			+
	4.00	1,434	1,424	[f] 1,386	[f] 1,367	+
	8.00	1,434	1,425	[f] 1,390		+
BaO	None	1,457	1,440			+
	1.00	1,445	1,430			+
	2.00	1,434	1,419			+
	5.00	1,402	1,388			+
	10.0	1,357	1,339			+
	20.0	1,260	1,229			+
$BaCl_2$	None	1,457	1,440			+
	1.00	1,445	1,430			+
	2.00	1,436	1,419			+
	5.00	1,408	1,387			+
	10.0	1,362	1,343			+
	20.0	1,273	1,254			+
Cr_2O_3	None	1,457	1,442			+
	0.25	1,449	1,434			+
	.50	1,438	1,413			+
	1.00	1,420	1,399			+
	1.50	1,412	1,396			+
	2.50	1,396	1,382			+
	7.50	1,402	1,374			+

See footnotes at end of table.

TABLE 3.—*Results of differential heating and cooling curves of* $2CaO.SiO_2$ *containing various added materials*[a]—Continued

Material added		Temperature of heat effect[b]				Dusted[c]
		Inversion of $2CaO.SiO_2$		Other phase changes		
		Heating $\beta \rightarrow \alpha$	Cooling $\alpha \rightarrow \beta$	Heating	Cooling	
Percent		°C	°C	°C	°C	
	None	1,457	1,442			+
	0.25	1,430	1,412			−
	.50	1,408	1,391			−
	1.00	1,387	1,367			−
B_2O_3[d]	2.00	1,355	1,339			−
	4.00	1,327	1,309	[f] 1,117	[f] 1,019	−
				[g] 1,175	[g] 1,142	−
	8.00	1,306	1,285	[f] 1,121	[f] 1,072	−
				[g] 1,177	[g] 1,100	−
	None	1,458	1,442			+
	0.12	1,455	1,439			+
	.25	1,452	1,434			−
	.50	1,446	1,424			−
Mn_2O_3	1.00	1,435	1,410			−
	2.00	1,425	1,394			−
	4.00	1,405	1,382			−
	8.00	1,385	1,352		[f] 1,288	−
				[f] 1,501	[f] 1,476	−
	None	1,457	1,440			+
	.25	1,433	1,418			+
	.50	1,428	1,406	[f] 1,453		−
	.75	1,422	1,399			−
	1.00	1,416	1,387	[f] 1,267		−
V_2O_5				[f] 1,443		−
	1.50	1,408	1,379	[f] 1,263		−
				[f] 1,447	[f] 1,399	−
	2.00	1,392	1,367	[f] 1,254		−
				[f] 1,439	[f] 1,396	−
	None	1,456	1,438			+
	1.00	1,390	1,349	[g] 1,453	[g] 1,423	−
	1.50	1,372	1,332	[g] 1,437	[g] 1,402	−
P_2O_5	2.00	1,342		[g] 1,451	[g] 1,390	−
	0.25	1,445	1,429			−
	.50	1,432	1,404			−
	4.00	1,290		[g] 1,452	[g] 1,424	−
	None	1,456	1,438			+
	[h] 0.16	1,443	1,427			+
Na_2O	[h] .39	1,425	1,412	[f] 1,288	[f] 1,237	+
	[h] .61	1,306	1,385	[f] 1,290	[f] 1,249	+
	[h] 1.32	1,346	1,335	[f] 1,292	[f] 1,252	+
	[h] 2.97		1,272	[f] 1,295	[f] 1,262	+
	None	1,456	1,438			+
	[h] 0.26	1,458	1,435			+
K_2O	[h] .26	1,450	1,431			+
	[h] .15	1,454	1,435			+
	[h] .34	1,430	1,420			+
	[h] .63	1,402	1,393			+

[a] The rate of temperature change was constant, usually about 2.5 degrees centigrade per min. The materials were added to portions of mixtures, prepared in 100- to 200-g quantities, of $CaCO_3$ and silica gel with a molar ratio CaO/SiO_2 of 2.00. Preparations were heated for ½ hr at 1,440° to 1,480° C, cooled, and ground. This was repeated 3 times. The samples were placed in the apparatus and held for 1 hr at 1,460° to 1,480° C before obtaining the heating and cooling curves.

[b] Temperatures were given by the intersection of tangents drawn to the inflections on the differential heating and cooling curves.

[c] A plus sign in the "Dusted" column indicates that the sample underwent the volume change accompanying the $\beta \rightarrow \gamma$ inversion of $2CaO.SiO_2$.

[d] Melting or freezing of the eutectic $3CaO.2SiO_2$–$CaO.SiO_2$. G. A. Rankin and F. E. Wright, Am. J. Sci. [4], **39**, 1 (1915).

[e] Incomplete dusting.

[f] Melting or freezing of the eutectic $2CaO.SiO_2$–$2CaO.SiO_2.Al_2O_3$. See reference in footnote d.

[g] Inversion temperatures disregarded because of volatility of some of the fluorine in the added CaF_2.

[h] Calculated from analysis made after the experiment. Analyses by R. B. Peppler.

[i] Unidentified.

[j] Added in combination with silica gel in molar ratio $2BaO:SiO_2$.

[k] Added as $2CaO.B_2O_3$ with silica gel in molar ratio $2CaO.B_2O_3:SiO_2$.

[l] Melting or freezing of the eutectic $2CaO.SiO_2$–$CaO.SiO_2$–$2CaO.B_2O_3$. E. P. Flint and L. S. Wells, J. Research NBS. **17**, 727 (1936) RP941.

[m] Boundary $2CaO.SiO_2$–$CaO.SiO_2$. See reference in footnote l.

[n] Invariant point $2CaO.SiO_2$–$3CaO.2SiO_2$–$7CaO.2SiO_2.P_2O_5$. R. L. Barrett, and W. J. McCaughey Am. Mineral. **27**, 680 (1942).

To summarize, one may assume that the inversion temperature of pure dicalcium silicate is 1,438° C and that a small quantity of CaO raises this temperature to 1,456° C, or, inversely, that the true inversion temperature is 1,456° C and that a small quantity of SiO_2 lowers it to 1,438° C.

Because it is difficult to determine the percentages of CaO and SiO_2 within a few hundredths of a percent by chemical analysis, it is apparent that it is preferable to adjust the $\alpha \rightleftarrows \beta$ inversion temperature of all samples of $2CaO.SiO_2$ at a fixed temperature by the addition of very small quantities of either CaO or SiO_2 rather than to depend on chemical analysis and obtain preparations which may give different inversion temperatures. As the present study was concerned with the effect of various substances on dicalcium silicate, and as the change in the $\alpha \rightleftarrows \beta$ inversion temperature was of such importance, a fixed temperature for this inversion seemed highly desirable. The reference temperature chosen was 1,456° C (table 1), the temperature of the $\beta \rightarrow \alpha$ inversion on the batch of dicalcium silicate reserved for calibration. Mixtures of $CaCO_3$ and silica gel that did not give the value of 1,456° C for the $\beta \rightarrow \alpha$ inversion with heating curves within the standard deviation of 2.2° C (table 1) were adjusted to give this temperature. It is realized that 1,456° C may not represent the true inversion temperature, and that the preparations could have been adjusted equally well to 1,438° C, the temperature obtained by the addition of small quantities of SiO_2.

VI. EFFECT OF ADDED MATERIALS ON $2CaO.SiO_2$

Attention will now be directed to the effect on dicalcium silicate of added material other than CaO and SiO_2 already discussed. Table 3 gives the temperature of the $\beta \rightarrow \alpha$ inversion of each raw mix of $2CaO.SiO_2$ obtained by heating curves and the temperature of the $\alpha \rightarrow \beta$ inversion obtained by cooling curves, as well as the effect of increasing quantities of the various added materials on these inversion temperatures. In addition, it gives the temperature of heat effects produced by phase changes other than the $\beta \rightarrow \alpha$ and $\alpha \rightarrow \beta$ inversions and the identification of certain of these with the corresponding literature references. Whether the sample underwent a volume change accompanying the $\beta \rightarrow \gamma$ inversion of $2CaO.SiO_2$ is noted in the last column.

When phase changes in addition to the $\alpha \rightleftarrows \beta$ inversion occurred with the dicalcium silicate containing added materials (Al_2O_3, TiO_2, B_2O_3, Mn_2O_3, V_2O_5, P_2O_5, and Na_2O), the shapes of the heating curves were typical of those obtained with increasing amounts of SiO_2 (fig. 5). Where additional phase changes did not occur (MgO, Fe_2O_3, CaF_2, BaO, Cr_2O_3, and K_2O) the shapes of the curves more closely resembled those for the addition of BaO shown in figure 6. The effects of the various additions are summarized graphically in figures 7, 8, 9, 10, and 11.

1. Al_2O_3, MgO, Fe_2O_3, TiO_2, AND CaF_2

It can be seen from the data of table 3 and the plot of figure 7 that Al_2O_3, MgO, Fe_2O_3, TiO_2, and CaF_2 resembled each other in their effects on the $\beta \rightarrow \alpha$ inversion in that a rather small quantity of any

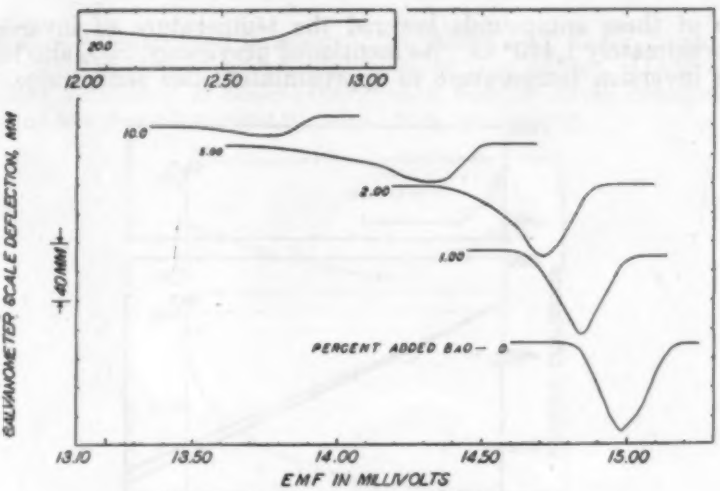

FIGURE 6.—*Differential heating curves.*

Effect of added BaO on the heating curve of $2CaO.SiO_2$. Heating rate 2.5 degrees centigrade per minute.

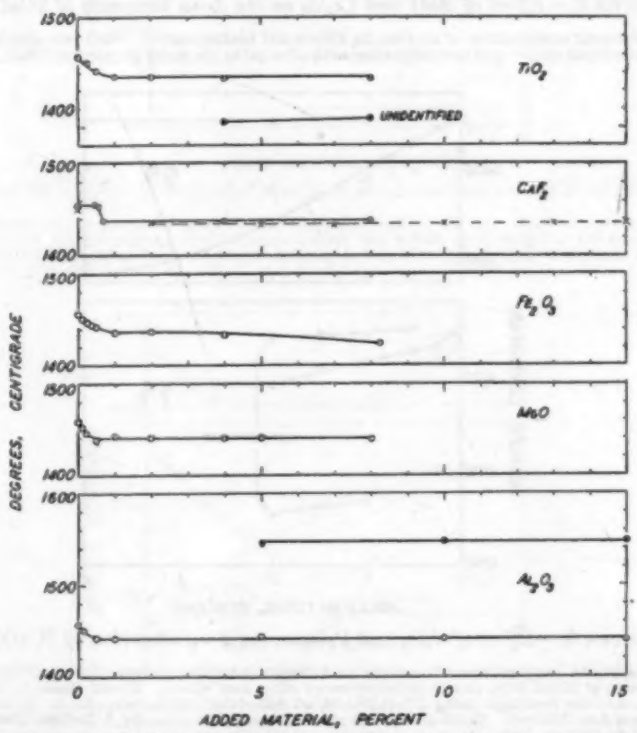

FIGURE 7.—*Effect of* Al_2O_3, MgO, Fe_2O_3, CaF_2, *and* TiO_2 *on the* $\beta \rightarrow \alpha$ *inversion of* $2CaO.SiO_2$

Points represent temperatures of maxima on differential heating curves. Open circles and squares represent the inversion of $2CaO.SiO_2$. Closed circles represent other heat effects, unidentified for TiO_2 and assumed to be the melting of the eutectic $2CaO.SiO_2$-$2CaO.Al_2O_3.SiO_2$ in the diagram for Al_2O_3. In the diagram for CaF_2, squares represent analyzed samples and crosses represent data given by S. Zerfoss. Thesis, The Pennsylvania State College, 1942.

one of these compounds lowered the temperature of inversion to approximately 1,440° C. As mentioned previously, SiO_2 also lowered this inversion temperature to approximately this same value. The

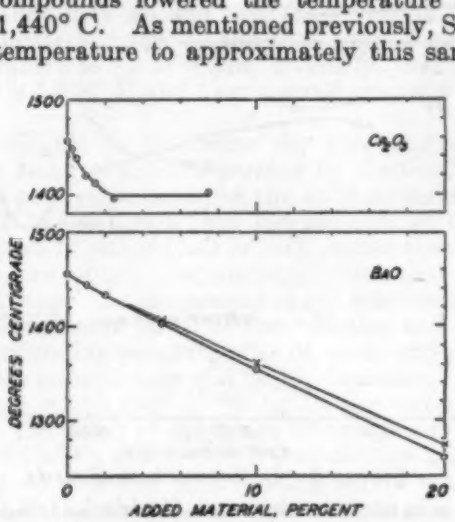

FIGURE 8.—*Effect of* BaO *and* Cr_2O_3 *on the* $\beta \rightarrow \alpha$ *inversion of* $2CaO.SiO_2$.

Points represent temperatures of maxima on differential heating curves. BaO was added both alone as the carbonate (open circles) and in combination with silica gel in the molar proportions $2BaO.SiO_2$ (crosses).

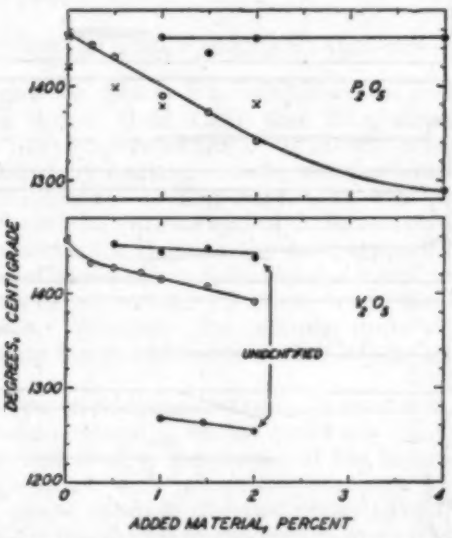

FIGURE 9.—*Effect of* V_2O_5 *and* P_2O_5 *on the* $\beta \rightarrow \alpha$ *inversion of* $2CaO.SiO_2$.

Points represent temperatures of maxima on differential heating curves. Open circles represent the $\beta \rightarrow \alpha$ inversion at $2CaO.SiO_2$; closed circles represent other heat effects. Closed circles in the diagram for P_2O_5 represent the invariant point $2CaO.SiO_2$-$3CaO.SiO_2$-$7CaO.2SiO_2.P_2O_5$. R. L. Barrett and W. I. McCaughey, Am. Mineral. 27, 680 (1942). Crosses represent data given by S. Zarfoss. Thesis, The Pennsylvania State College, 1942.

additions of larger amounts of TiO_2 or of Al_2O_3 caused the appearance of heat effects in addition to that caused by the $\alpha \rightleftarrows \beta$ inversion, and in this respect resembled the behavior of SiO_2. Additional heat

effects were not observed between 1,250° and 1,540° C for dicalcium silicate with the other added materials of this group. Under the conditions prevailing in these experiments, none of these compounds prevented the $\beta \rightarrow \gamma$ inversion of $2CaO.SiO_2$, or dusting.

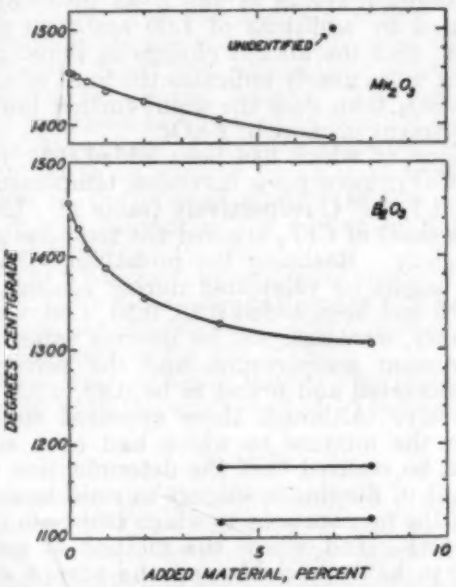

FIGURE 10.—*Effect of* B_2O_3 *and* Mn_2O_3 *on the* $\beta \rightarrow \alpha$ *inversion of* $2CaO.SiO_2$.

Points represent temperatures of maxima on differential heating curves. Open circles represent the $\beta \rightarrow \alpha$ inversion of $2CaO.SiO_2$; closed circles represent other heat effects, unidentified in the case of Mn_2O_3. In the diagram for B_2O_3 these heat effects are assumed to represent the melting of the ternary eutectic $2CaO.SiO_2$-$CaO.SiO_2$-$2CaO.B_2O_3$ at 1,118° C, and the disappearance of the phase $CaO.SiO_2$ at 1,176° C.

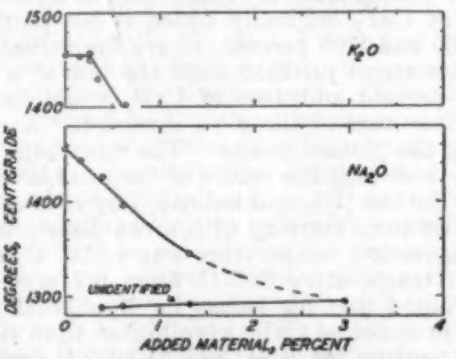

FIGURE 11.—*Effect of* Na_2O *and* K_2O *on the* $\beta \rightarrow \alpha$ *inversion of* $2CaO.SiO_2$.

Points represent temperatures of maxima on the differential heating curves. Open circles represent the $\beta \rightarrow \alpha$ inversion of $2CaO.SiO_2$, closed circles represent an unidentified heat effect. The compositions of these samples were determined by analysis after the heating curves were obtained.

Burdick [9], using heating curves, reported a maximum solubility of about 0.5 percent of Fe_2O_3 in dicalcium silicate and a lowering of the $\beta \rightarrow \alpha$ inversion temperature to 1,361° C. He also reported a ternary eutectic ($2CaO.SiO_2$-$3CaO.SiO_2$-$2CaO.Fe_2O_3$) melting at

1,414° C, and a eutectic between $2CaO.SiO_2$ and $2CaO.Fe_2O_3$ melting at 1,428° C. Heat effects corresponding to these phenomena were not observed in the present work.

It can be seen in figure 7 that additions of 4.00 and 8.25 percent of Fe_2O_3 caused a slight lowering of the $\beta \rightarrow \alpha$ inversion temperature beyond that caused by additions of 1.00 and 2.00 percent. It is believed, however, that the abrupt change in slope of the curve at about 1.00 percent more nearly indicates the limit of solid solution of Fe_2O_3 in α-$2CaO.SiO_2$ than does the slight further lowering with the addition of 4.00 percent or more of Fe_2O_3.

Four preparations, to which had been added 0.25, 0.50, 1.00, and 2.00 percent of CaF_2, gave $\beta \rightarrow \alpha$ inversion temperatures of 1,456°, 1,457°, 1,456°, and 1,442° C respectively (table 3). Larger additions (4.00 and 8.00 percent) of CaF_2 lowered the temperature of the $\beta \rightarrow \alpha$ inversion but slightly. Realizing the probability that some of the fluorine of CaF_2 might be volatilized during heating, the first four mixtures, to which had been added 0.25, 0.50, 1.00, and 2.00 percent of CaF_2, respectively, were analyzed for fluorine [4] after the determinations of the inversion temperature, and the percentage of CaF_2 remaining was calculated and found to be 0.49, 0.52, 0.58, and 0.70 percent, respectively. Although there appeared to be more CaF_2 (0.49 percent) in the mixture to which had been added but 0.25 percent, it should be realized that the determination of only 1 or 2 tenths of a percent of fluorine is subject to considerable error. The loss of fluorine in the preparations to which had been added 1.00 and 2.00 percent of CaF_2 (and where the method of analysis is more reliable) appears to be appreciable and the abrupt decrease in the $\beta \rightarrow \alpha$ inversion temperature consequently appears to be between 0.58 and 0.70 percent of CaF_2 (see table 3 and fig. 7) rather than between 1.00 and 2.00 percent. Hence, it is concluded that the limit of solubility of CaF_2 in $2CaO.SiO_2$ is about 0.7 percent. This abrupt change in $\beta \rightarrow \alpha$ inversion temperature is represented in figure 7 by squares. The percentage of CaF_2 originally added is not plotted in figure 7 except for the 4.00 and 8.00 percent, where the values are plotted as open circles. This seems justified since the loss of a portion of the 4 percent and 8 percent additions of CaF_2 would have little or no effect on the temperature of the $\beta \rightarrow \alpha$ inversion. A curve was then drawn connecting the plotted points. The right-hand portion of the curve agrees very well with the values of the $\alpha \rightleftarrows \beta$ inversion temperature obtained by Zerfoss [10], and indicated by crosses. The present investigation shows that, starting with a raw base mix of $2CaO.SiO_2$ where the $\beta \rightarrow \alpha$ inversion temperature was 1,458° C, the addition of CaF_2 lowers this temperature 20° C when 0.7 percent or more is added. Zerfoss noted that his values for the actual temperature of inversion in the presence of CaF_2 were higher than the temperature reported in the literature for $2CaO.SiO_2$ (1,420° C see [3]). Whether one concludes that the temperature of inversion is raised or lowered by addition of CaF_2 depends, therefore, on what temperature is accepted as that representing the $\alpha \rightleftarrows \beta$ inversion of $2CaO.SiO_2$, and shows the importance of fixing this temperature.

The data shown in figure 7 and in table 3 indicate maximum solubility limits for Al_2O_3, MgO, Fe_2O_3, CaF_2, and TiO_2 in α-$2CaO.SiO_2$ of approximately 0.5, 0.5, 1.0, 0.7, and 1.0 percent, respectively.

[4] The preparations were analyzed by R. B. Peppler.

2. $2BaO.SiO_2$ AND BaO

The effect of both barium orthosilicate, $2BaO.SiO_2$ and of BaO, on the $\beta \rightarrow \alpha$ inversion of $2CaO.SiO_2$ was investigated. For studying the effect of $2BaO.SiO_2$, the samples were prepared by adding $BaCO_3$ and silica gel to the dicalcium raw mix in the mole proportions of BaO and SiO_2 of 2:1. Toropow and Konowalow [11] have reported that barium orthosilicate forms a complete solid solution series with calcium orthosilicate, $2CaO.SiO_2$, basing their conclusions on measurements of refractive indices and density. The lowering of the $\beta \rightarrow \alpha$ temperature of inversion as obtained by heating curves (represented by crosses in fig. 8) confirms their work, since the temperature of this inversion continued to be lowered by all of the added increments of $2BaO.SiO_2$ made in the present study. It was found also that a similar lowering was caused by the adding of BaO (see the curve through the open circles in fig. 8).

The existence of a solid solution series of the substitution type was indicated by the X-ray diffraction patterns of β-$2CaO.SiO_2$ containing $2BaO.SiO_2$. These patterns showed a slight shift of some of the lines from their normal position for β-$2CaO.SiO_2$.

The additions of BaO, either as BaO or $2BaO.SiO_2$, did not prevent the $\beta \rightarrow \gamma$ inversion until the equivalent of 10 percent of BaO had been added (table 3).

3. Cr_2O_3

The temperature of the $\beta \rightarrow \alpha$ inversion of dicalcium silicate was lowered to about 1,400° C by Cr_2O_3 (fig. 8) and the limit of solubility in the α form, as indicated by the heating curves, was approximately 2.5 percent. Solid solution in the β form, indicated by the green color of the crystals, the inhibition of the $\beta \rightarrow \gamma$ inversion, and the raising of the refractive indices [12] must be less than 2.5 percent as the inversion temperature is lowered by the addition to the solute.

4. V_2O_5, P_2O_5, B_2O_3, AND Mn_2O_3

The oxides V_2O_5 and P_2O_5 (fig. 9) and B_2O_3 and Mn_2O_3 (fig. 10) resembled each other in their effects on dicalcium silicate. These oxides lowered the $\alpha \rightleftarrows \beta$ inversion temperature. They also prevented the $\beta \rightarrow \gamma$ inversion (dusting) and in this respect, resembled Cr_2O_3.

The heating curves of dicalcium silicate containing either V_2O_5, P_2O_5, B_2O_3, or Mn_2O_3, were characterized by one or more heat effects in addition to that caused by the inversion. The inversion temperatures of preparations containing V_2O_5 or P_2O_5 were lowered continuously by further increments of these oxides after the appearance of heat effects at higher temperatures. Normally, heat effects occurring above the inversion temperature, where α-$2CaO.SiO_2$ is the stable form, would indicate that the limit of solubility of the added substance in this form of $2CaO.SiO_2$ had been exceeded and further lowering of the $\alpha \rightleftarrows \beta$ inversion should not occur. The authors have not found a satisfactory explanation for the apparent contradiction in the cases of V_2O_5 and P_2O_5. Nevertheless, the first appearance of heat effect at temperatures above that of the $\alpha \rightleftarrows \beta$ inversion has been assumed to signify the limits of solubility. Therefore, from figures 9 and 10, the limits of solubility of V_2O_5, P_2O_5, B_2O_3, and Mn_2O_3, in $2CaO.SiO_2$ have been estimated not to exceed 0.5, 1.0, 8.0, and 8.0 percent, respectively.

That both B_2O_3 and Mn_2O_3 are soluble in β-$2CaO.SiO_2$ are indicated by the changes they produce in the refractive index of β-$2CaO.SiO_2$, by their prevention of the β to γ inversion, and, in the case of Mn_2O_3, the formation of colored crystals of β-$2CaO.SiO_2$. The appearance of additional heat effects (fig. 10) at temperatures below the $\beta \rightarrow \alpha$ inversion, where β-$2CaO.SiO_2$ is the stable form, indicates that the limit of solubility of B_2O_3 in β-$2CaO.SiO_2$ does not exceed 4.00 percent. The additional heat effects were caused by the melting of the ternary eutectic ($2CaO.SiO_2$-$CaO.SiO_2$-$2CaO.B_2O_3$) at 1,118° C [13], and the disappearance of the phase $CaO.SiO_2$ at 1,176° C.

A limit of solubility of Mn_2O_3 in β-$2CaO.SiO_2$ of not exceeding 4.00 percent was indicated by the presence of an additional phase among the greenish crystals of a preparation of β-$2CaO.SiO_2$ to which 4.00 percent of Mn_2O_3 had been added.

The present data indicate two minor changes in the ternary diagram of the sysem CaO-B_2O_3-SiO_2 as portrayed by Flint and Wells [13]. The solid-solution area shown in their report apparently should extend at least as far as the line joining $2CaO.SiO_2$ and B_2O_3, and the boundary between α- and β-$2CaO.SiO_2$ should curve somewhat more abruptly so as to cross the 1,300° C isotherm at about the intersection with $2CaO.SiO_2$-B_2O_3 tieline.

5. Na_2O AND K_2O

The alkalies, Na_2O and K_2O, were somewhat volatile under the conditions encountered in preparing the samples and obtaining the heating and cooling curves. The points in figure 11 are based on the percentage of alkali calculated from chemical analyses of the mixtures after the experiments had been completed. The data for K_2O are limited to a narrow range of composition because of the relatively large loss by volatilization. However, 0.6 percent of K_2O lowered the temperature of the $\beta \rightarrow \alpha$ inversion of $2CaO.SiO_2$ to 1,402° C. It was found that Na_2O lowered the temperature of the $\beta \rightarrow \alpha$ inversion to about 1,290° C where it became indistinguishable from another and unidentified heat effect. The limit of solubility of Na_2O in α-$2CaO.SiO_2$ is uncertain but probably exceeds 1.3 percent. The limit of solubility in β-$2CaO.SiO_2$ is less than 0.4 percent, as indicated by the appearance of the additional heat effect at 1,288° C.

VII. X-RAY DIFFRACTION PATTERNS

The X-ray diffraction patterns of samples containing BaO, P_2O_5, Na_2O, and K_2O showed slight shifts in certain lines of the X-ray pattern of β-$2CaO.SiO_2$, indicating that these materials form solid solutions of the substitution type. Shifts in the lines were not observed in patterns of dicalcium silicate containing Al_2O_3, TiO_2, Cr_2O_3, B_2O_3, Mn_2O_3, or V_2O_5. Because the β form of dicalcium silicate was not retained in quenched samples of the preparations to which had been added MgO, Fe_2O_3, CaO, or SiO_2, X-ray diffraction patterns were not prepared. Burdick [9] succeeded in preserving the β form of $2CaO.SiO_2$ in a preparation containing Fe_2O_3 by heating and dehydrating a mixture of Fe_2O_3 and the dicalcium silicate hydrate, $10CaO.5SiO_2.6H_2O$. The X-ray pattern of the resulting preparation showed a slight shift in the lines characterizing β-$2CaO.SiO_2$, and there-

fore confirmed the presence of a limited solid solution of Fe_2O_3 in dicalcium silicate.

VIII. $\beta \rightarrow \gamma$ INVERSION OF $2CaO.SiO_2$

The expansion accompanying the $\beta \rightarrow \gamma$ inversion of dicalcium silicate results in the crumbling to a fine powder, or "dusting," of portland cement clinker containing substantial quantities of unstabilized β-$2CaO.SiO_2$. The inversion of even a moderate amount causes sufficient expansion to produce cracking or disintegration of material such as blast furnace slag and dolomitic refractories.

In the case of portland cement clinker the γ form is undesirable since it has no hydraulic properties, and, consequently, does not contribute to the strength of the hardened cement, whereas β dicalcium silicate is a valuable constituent because of its hydraulic properties.

It has been observed [4] that Cr_2O_3, B_2O_3, P_2O_5, V_2O_5, and As_2O_5 prevent the $\beta \rightarrow \gamma$ inversion when present in comparatively small amounts. These materials have been termed chemical inhibitors of "dusting", and Mn_2O_3 should be added to this list. Zerfoss and Davis [4] have explained that such inhibitors prevent the $\beta \rightarrow \gamma$ inversion by entering into solid solution with dicalcium silicate, and that other substances may prevent this inversion by physically restraining the particles from expanding, or by isolating the crystals of β-$2CaO.SiO_2$ from points initiating the inversion. It is believed by many in the cement industry [14] that Al_2O_3, MgO, Fe_2O_3, or any material which is present as glass, may prevent dusting.

IX. SUMMARY AND CONCLUSIONS

Details were given of the application of differential heating and cooling curves to the determination of the temperature of the $\alpha \rightleftarrows \beta$ inversion of $2CaO.SiO_2$, and to the measurement of limits of solid solution of CaO, SiO_2, Al_2O_3, MgO, Fe_2O_3, TiO_2, CaF_2, BaO, Cr_2O_3, V_2O_5, P_2O_5, B_2O_3, Mn_2O_3, Na_2O, and K_2O in dicalcium silicate.

It was found that the $\alpha \rightleftarrows \beta$ inversion temperature is sensitive to variations from the molar ratio $2CaO:SiO_2$. By means of heating curves it was possible to observe not only the effects of chemically undetectible variations from the 2:1 molar ratio, but also the limits of solid solution of these oxides in α-$2CaO.SiO_2$, and the formation of additional crystalline phases.

As an increase in volume of about 10 percent accompanies the $\beta \rightarrow \gamma$ inversion of $2CaO.SiO_2$, and causes the so-called "dusting" of dicalcium silicate and may result in a destructive expansion of materials in which it is an ingredient, the effectiveness of these oxides in preventing this inversion was studied. Also, because γ-$2CaO.SiO_2$, in contrast with β-$2CaO.SiO_2$, has no hydraulic properties, it is not desired in portland cement clinkers.

It was emphasized that lowering of temperature of the $\alpha \rightleftarrows \beta$ inversion indicated greater solubility of the added material in the alpha form of dicalcium silicate than in the beta, and that the limit of solubility in the alpha form had been reached when the addition of more of the solute caused no further change in the temperature of the $\alpha \rightleftarrows \beta$ inversion.

The limits of solubility of Al_2O_3, MgO, Fe_2O_3, and TiO_2 in α-$2CaO.SiO_2$ were estimated to be 0.5, 0.5, 1.0, 0.7, and 1.0 percent, respec-

tively. The limits of solubility in β-$2CaO.SiO_2$ must be less, since the temperature of the inversion was lowered. None of the materials prevented dusting.

The limit of solubility of BaO or $2BaO.SiO_2$ in dicalcium silicate was not reached. Other investigators have reported that $2CaO.SiO_2$ and $2BaO.SiO_2$ form a complete solid solution series and the data obtained in this investigation (including X-ray diffraction patterns of β-$2CaO.SiO_2$ containing $2BaO.SiO_2$) support that conclusion in the range of compositions studied. The additions of BaO, either as BaO or $2BaO.SiO_2$, did not prevent the $\beta \rightarrow \gamma$ inversion (and "dusting") until the equivalent of 10 percent of BaO had been added.

The limits of solubility of Cr_2O_3, V_2O_5, P_2O_5, B_2O_3, and Mn_2O_3 were estimated to be 2.5, 0.5, 1.0, 8.0, and 8.0 percent, respectively. Preparations containing these materials gave evidences of their solubility in β-$2CaO.SiO_2$ by changes in color or refractive index, and the absence of dusting. The limits of solubility of both B_2O_3 and Mn_2O_3 in β-$2CaO.SiO_2$ were estimated not to exceed 4.0 percent.

The volatility of the alkalies, Na_2O and K_2O, hindered the study of their effects on $2CaO.SiO_2$ and no estimate of the solubility of K_2O was made. It was estimated that the limit of the solubility of Na_2O in α-$2CaO.SiO_2$ was slightly in excess of 1.3 percent, and that its solubility in the β form did not exceed 0.4 percent.

Limiting values of the solubility of TiO_2, B_2O_3, V_2O_5, Mn_2O_3, or Na_2O in β-$2CaO.SiO_2$ were shown by the presence of other phases in addition to $2CaO.SiO_2$. The additional phase was observed microscopically for Mn_2O_3; with the other oxides by inflections on heating and cooling curves in addition to the inflection caused by the $\alpha \rightleftarrows \beta$ inversion of dicalcium silicate.

This investigation has shown that most of the common oxides change the temperature of the $\alpha \rightleftarrows \beta$ inversion of $2CaO.SiO_2$ and that Mn_2O_3 should be added to the list of known chemical inhibitors that prevent dusting.

X. REFERENCES

[1] T. W. Parker and J. F. Ryder, J. Iron Steel Inst. (London) **146,** 21P (1942).
[2] G. E. Seil and staff, J. Am. Ceram. Soc. **20,** 1 (1941).
[3] G. A. Rankin and F. E. Wright, Am. J. Sci. [4] **39,** 1 (1915).
[4] S. Zerfoss and H. M. Davis, J. Am. Ceram. Soc. **26,** 302 (1943).
[5] E. S. Newman, J. Research NBS **27,** 191 (1941) RP1413.
[6] W. P. White, Am. J. Sci. [4] **28,** 453 (1909).
[7] H. S. Roberts, J. Opt. Soc. Am. & Rev. Sci. Inst. **11,** 171 (1925).
[8] W. F. Roeser and H. T. Wensel, BS J. Research **10,** 275 (1933) RP530.
[9] M. D. Burdick, J. Research NBS **25,** 475 (1940) RP1340.
[10] S. Zerfoss, Thesis. The Pennsylvania State College (1942).
[11] N. A. Toropow and P. F. Konowalow, Compt. rend. acad. sci. U. R. S. S. **22,** 663 (1938).
[12] P. H. Bates and A. A. Klein, BS Tech. Pap. 78 (1917).
[13] E. P. Flint and L. S. Wells, J. Research NBS **17,** 727 (1936) RP941.
[14] R. H. Bogue, private communication.

WASHINGTON, September 28, 1945.

U. S. Department of Commerce National Bureau of Standards

RESEARCH PAPER RP1697

Part of Journal of Research of the National Bureau of Standards, Volume 36, February 1946

REPRODUCIBILITY OF THE LEAD ELECTRODE AND THE ELECTROMOTIVE FORCE OF THE LEAD STICK-LEAD AMALGAM CELL AT 0° TO 60° C

By Roger G. Bates, Murray Edelstein, and S. F. Acree

ABSTRACT

The potentials of four types of solid lead electrodes with respect to saturated lead amalgam were obtained. Although lead anneals spontaneously, the surface condition has a profound effect upon the electromotive force. Untreated lead sticks were, in general, positive to lead the surface of which had been rendered strain-free. When etched in a mixture of nitric acid and lead nitrate, these lead sticks soon reached the same potential. Removal of air from the solutions improved the agreement among the electrodes.

Twelve sticks cast from National Bureau of Standards Standard Sample 49b and twelve cast from "spectroscopically pure" lead were etched and used to determine the difference of potential between stick lead and 8-percent lead amalgam at intervals of 5 degrees from 0° to 60° C. The results are given by the equation

$$E=0.005347+0.0000201t,$$

where E is the electromotive force in international volts and t is in degrees centigrade. Thermodynamic constants were computed from the temperature coefficient of electromotive force. No difference was found between the two kinds of lead.

CONTENTS

	Page
I. Introduction	159
II. Reproducibility of the lead electrode	161
1. Materials	161
2. Effect of surface condition on the potentials of lead electrodes	162
3. Effect of air on the potentials of lead electrodes	164
4. Comparison of various types of lead electrodes	165
III. Electromotive force between lead sticks and saturated lead amalgam at 0° to 60° C	165
1. Experimental procedures and results	166
2. Thermodynamic constants for lead and lead amalgam	168
IV. References	169

I. INTRODUCTION

Although the lead electrode has been the subject of a number of published investigations, its reproducibility and suitability for use in electromotive-force studies over a range of temperatures have not been clearly defined. In 1910, Lewis and von Ende [1][1] wrote " . . . all solid metals (give) an inconstant potential owing to uncontrollable surface variations." When a highly reproducible electrode reversible to a metallic ion is required, it has usually been necessary to use

[1] Figures in brackets indicate the literature references at the end of this paper.

amalgams. As a fairly soft metal, however, pure lead should readily lose the strains responsible for the erratic thermodynamic behavior of other harder metals. Inasmuch as reference electrodes reversible to bivalent anions can be used advantageously in certain types of electrometric pH work, and the lead-lead sulfate electrode appears to be the most suitable representative of this class, further studies of lead electrodes were undertaken. Furthermore, the lead electrode, together with the slightly soluble lead salts of weak acids, might be used to advantage in studies of the activity of these acids and their soluble salts in aqueous solution.

Active surface areas can sometimes be rendered strain-free, and reproducible electrodes obtained, by subjecting the metal to slow etching in acid for several days [2]. However, when Heller and others [3, 4, 5] immersed lead sticks in solutions of lead acetate to which nitric acid had been added, the metal was found to disintegrate slowly until only a gray powder remained. Electrolysis of lead sticks in nitric acid produced a similar deterioration [6]. This evidence of the existence of two or more allotropic forms of lead appeared to be confirmed by measurements of density [4]. In their study of the lead electrode, Lewis and Brighton [7] failed to find evidence of allotropism, and later work by Rawdon [8] led to the conclusion that the forms previously described as allotropic were only a granular condition of the ordinary form brought about by intercrystalline embrittlement. The impurities commonly occurring in lead are insoluble in the solid state and are found lodged between the grains of lead. Embrittlement is largely due to the behavior of these impurities when the metal is immersed in electrolyte. This conclusion was supported by the work of Thiel [9].

Gerke [10] measured the differences of potential between 5-percent lead amalgam and two electrodes formed of electrolyzed lead crystals in 1-*M* lead acetate at temperatures from 5° to 45° C. The potentials of four lead sticks, two of them immersed in a solution of lead acetate and two in lead perchlorate, were also measured between 20° and 50° C. The mean emf at 25° C was 0.0057 v. No statement was made concerning the method of preparing the lead sticks. The thermodynamic properties of electrolyzed crystals and of sticks appeared to be different. Carmody [11] found that five scraped sticks free of physical defects gave an average emf of 0.00584 ± 0.00002 v at 25° C with respect to a saturated lead amalgam. He observed that ". . . the potential was constant for about two hours. After this time a gray coating formed on the surface of the stick and the potential slowly lowered without again reaching a constant value." Although precautions had been taken to remove air from the solution of lead chloride, this observation suggests that traces of oxygen were actually present and were reacting at the surface of the lead, with the ultimate formation of basic lead salts. It seems likely that the susceptibility of the emf to oxygen can be diminished somewhat by the use of electrolytes containing high concentrations of lead ion and enough free acid to prevent the deposition of slightly soluble basic salts.

The number of lead electrodes studied has been insufficient to furnish a clear picture of the effect of surface treatment, air, and temperature changes upon the potential. In this investigation, sticks cast from NBS melting-point lead and from a sample of spectroscopically pure lead were etched with acid until further treatment caused

no change in potential. Twenty-four electrodes were then selected, and emf measurements with respect to saturated lead amalgams were made at intervals of 5 degrees from 0° to 60° C.

II. REPRODUCIBILITY OF THE LEAD ELECTRODE

The potentials of electrodes treated in various ways were measured at room temperature with respect to each other and to saturated lead amalgams. For this comparison, the electrodes were usually immersed in a 0.05-*M* solution of lead acetate containing sufficient nitric acid to discharge the turbidity. These comparisons were usually made in 1-liter flasks, that accommodated seven rubber stoppers. Twelve electrodes could thus be measured against the same amalgam.

1. MATERIALS

Reagent grades of lead acetate, lead carbonate, perchloric acid, and nitric acid were used without further purification. The mercury, stated to have a purity greater than 99.999 percent, was supplied by the Reagents and Platinum Metals Section of this Bureau. The nitrogen was purified by passage over soda-lime and over finely divided copper heated to 500° C.

Two samples of lead were used. The first was NBS Standard Sample 49b, which has a melting point of 327.4$_6$° C. The second was obtained from the laboratories of the American Smelting & Refining Co., Perth Amboy, N. J. Spectroscopic examination was said to reveal no impurity other than a trace of iron.

Lead amalgam, containing 8 percent of lead by weight, was used in all the work. Two amalgams, one prepared from each of the two samples of lead, were found to give the same potential, within experimental error. The NBS Standard Sample of lead was used in preparing the amalgam for all subsequent measurements. An analysis of the phase studies of Puschin [12] for the lead-mercury system indicated that an 8-percent amalgam consists of two phases between 0° and 60° C. Lead amalgam that contains 5 percent of lead has found most general use heretofore for emf measurements, even at temperatures as high as 50° C [10, 13], although one of the writers [14], in a study of solutions of lead bromide at temperatures from 5° to 40° C, found desirable the employment of a 10-percent amalgam. Puschin did not indicate as high accuracy for the freezing points of amalgams which contained less than 10 atom percent of lead as for those richer in lead, but it seems evident that the solid phase persists in an 8-percent amalgam to a temperature of 80° C. Haring, Hatfield, and Zapponi [15] found that lead is soluble in mercury to the extent of 0.0165 atom fraction (1.7 percent by weight) at 25° C.

The amalgam was prepared by heating together weighed quantities of stick lead and mercury in a small beaker at a temperature sufficiently high to insure homogeneity of the resulting amalgam. It was stored in the amalgam pipette shown in figure 1, in which it could be melted and from which it could be withdrawn into the evacuated cell vessels. The pipette was heated to 100° C in an oven before charging it with amalgam. It was then evacuated with an oil pump and the hot amalgam drawn in through stopcock *b*, care being taken to leave the dross behind. When the pipette had cooled to room temperature,

the vacuum was broken with pure nitrogen by rotating stopcock *a* through 180°.

Four types of lead electrodes were prepared. (1) The metal was melted in an alundum crucible and poured into glass or polystyrene tubes, fitted into holes in a graphite block (see fig. 1). Usually the ends of the stick were exposed and a portion of the glass or plastic left in the form of a sleeve over the electrode where it passed through the stopper in which it was later supported. (2) A few electrodes were prepared by electrolytic deposition of lead on platinum foils sealed in glass. The metal was obtained in a macrocystalline form from a solution of lead acetate, or as a smooth deposit from a solution of lead

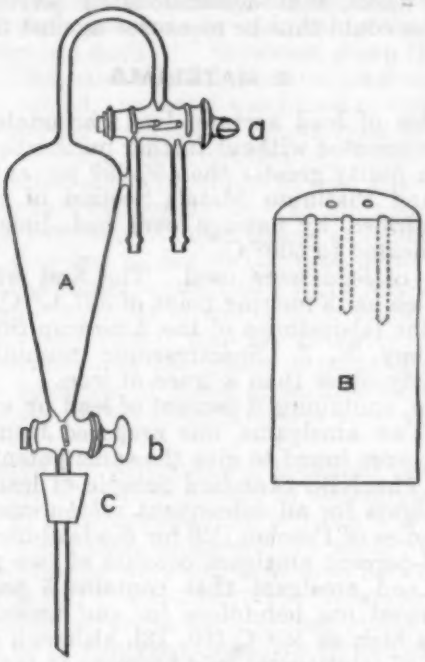

FIGURE 1.—*Amalgam pipette (A) and graphite block (B) in which the stick electrodes were cast.*

fluoborate furnished by the Electrochemistry (Plating) Section of this Bureau. (3) Lead sticks, 6 mm in length and 5 mm in diameter, were fused to platinum wires which, in turn, were sealed into short lengths of glass tubing. (4) Lead was cast in the graphite block shown in figure 1 to form sticks 7.5 cm in length and 5 mm in diameter. All four types of electrodes were mounted in pairs in rubber stoppers for subsequent treatment and study.

2. EFFECT OF SURFACE CONDITION ON THE POTENTIALS OF LEAD ELECTRODES

It is well known that lead, hardened by cold-working, anneals itself spontaneously at room temperature. Slightly deformed samples are the slowest to recover, but in most instances annealing is found to be complete in a few hours [16, 17]. It was evident early in this study,

however, that surface condition had a profound influence upon the potentials of samples of lead. Electrodes whose surfaces appeared smooth and bright usually differed in potential by 0.5 to 2.0 mv, or more, from electrodes that showed the dull-gray characteristic of a well-etched lead surface.

Slow attack of the lead surface was found to be desirable. For this purpose, several acidified solutions of lead salts were tried before a mixture 0.2 *M* in lead nitrate and 0.75 *M* in nitric acid was selected as the most suitable. The nature of the etching solution was apparently not critical, however. Electrodes that had been etched for a few hours often appeared to be in a stable condition, although several days was usually allowed, with occasional replacement of the etching solution. The rapid initial changes made it impracticable to attempt to follow the potential as a function of the time of etching, as has been done with zinc [2].

The effect of etching 12 lead electrodes of type 3 is shown by the emf values given in table 1. The electrodes were washed with dilute nitric acid and rinsed. Before etching, the mean potential was 3.12 mv more negative than the two-phase amalgam with which the electrodes were compared, and the standard deviation[2] of the mean of the 12 values was 0.27 mv. After the electrodes had been treated for 5 hours with dilute nitric acid, the mean emf was found to have risen to 5.84 mv, a value close to that found by Gerke [10] and Carmody [11]. The standard deviation of the mean had dropped to 0.07 mv. The comparisons were made in an acidified solution of lead acetate. Dissolved oxygen was not removed.

TABLE 1.—*Potentials of lead electrodes (type 3) in 0.05–M lead acetate before and after etching for 5 hours in dilute nitric acid; vs saturated lead amalgam at room temperature*

Number	Before etching	After etching
	mv	mv
1	4.74	5.88
2	4.56	5.90
3	2.72	5.97
4	2.80	6.03
5	2.46	6.16
6	3.01	5.88
7	2.60	5.97
8	3.26	5.90
9	3.83	5.82
10	1.22	5.04
11	2.77	5.78
12	3.44	5.73
Mean	3.12	5.84
Standard deviation of the mean	0.27	0.07

The emf values of 16 stick electrodes classified by visual examination as "well etched," of 7 classified as "poorly etched," and of one bright, new electrode *versus* saturated amalgam are given in table 2. The appearance of the electrode was found to provide an adequate index of the progress of the etching.

[2] The standard deviation of the mean is given by $\sqrt{\Sigma(E_i-E_m)^2/[n\ (n-1)]}$, where E_i is the emf of each individual electrode with respect to saturated amalgam, E_m is the mean emf of the group, and n is the number of observations from which E_m is derived.

TABLE 2.—*Potentials of lead stick electrodes (type 4) with different degrees of etching, in 0.05-M lead acetate at room temperature*

Number	Electromotive force versus saturated amalgam
BRIGHT, UNETCHED STICK	
1	mv 3.80
POORLY ETCHED STICKS	
2	5.52
3	5.36
4	5.40
5	5.43
6	5.55
7	5.16
8	5.19
Mean	5.37
WELL-ETCHED STICKS	
9	5.62
10	5.69
11	5.66
12	5.63
13	5.72
14	6.16
15	5.64
16	5.65
17	5.65
18	5.70
19	5.66
20	5.56
21	5.80
22	5.56
23	5.66
24	5.56
Mean	5.68

3. EFFECT OF AIR ON THE POTENTIALS OF LEAD ELECTRODES

Nitrogen was chosen in preference to hydrogen for removing dissolved air from the solutions in which lead electrodes were used. The danger of hydrogen polarization at the exposed platinum surfaces of electrodes of types 2 and 3 was thus avoided. Exclusion of air did not exert a large influence on the potential of well-etched electrodes immersed in acidified lead acetate solution but improved the agreement among individual electrodes of a set. Further, it is reasonable to suppose that side reactions were slowed and the life of the cell prolonged.

Table 3 illustrates the effect of passing nitrogen for 2 hours through a solution of lead acetate in which lead electrodes were being compared with a lead amalgam electrode. When most of the air had been replaced by nitrogen, the standard deviations of the means were reduced to one-third or one-half of their former values.

TABLE 3.—*Effect of air on the potentials of lead electrodes in 0.05-M lead acetate at room temperature*

Number	Electromotive force versus saturated amalgam, of—			
	Pb sealed to Pt (type 3)—		Etched Pb sticks (type 4)—	
	In air-containing solution	After removal of air	In air-containing solution	After removal of air
	mv	mv	mv	mv
1	6.19	5.72	5.93	5.92
2	6.43	5.95	5.69	5.91
3	6.26	5.85	5.71	5.92
4	6.05	5.70	5.49	5.85
5	5.85	5.87	5.44	5.91
6	5.80	5.70	5.28	5.91
7	5.52	5.76	5.34	5.86
8	5.73	5.81	5.57	5.97
9			5.30	5.61
Mean	5.98	5.80	5.53	5.87
Standard deviation of the mean	0.10	0.03	0.07	0.03

4. COMPARISON OF VARIOUS TYPES OF LEAD ELECTRODES

Of the four types of electrodes studied, lead in stick form (type 4) was found to be the most convenient and reproducible. Type 3, formed of lead sealed to platinum wire, was slightly less satisfactory. Electrodes of this type, and those prepared by the electrolytic deposition of lead upon platinum, frequently gave erratic potentials in the most acid solutions. Reaction of the lead with the acid solution, as a result of the low hydrogen overvoltage of the platinum, was a possible cause of this behavior. Lead deposited from the commercial fluoborate plating solution differed in potential from the purest forms by several tenths of a millivolt, and no further experiments were performed with smooth deposits. Electrolytic crystals appeared to give satisfactory results, but the crystals did not adhere well to the platinum support. Electrodes of type 1 were subject to the objection that the lead did not adhere tightly to the glass or polystyrene sleeve, with the result that etching solution passed into the sleeve and was not removed by subsequent washing.

Inasmuch as the partial free energy of lead in the amalgam is somewhat lower than the free energy of lead in the solid state, the lead electrode is more susceptible to oxidation than is a saturated lead amalgam. Further, sudden temperature changes, as will be seen in the succeeding section, sometimes effect disturbances of potential not found with amalgams. On the other hand, lead electrodes are more convenient to prepare and use than are amalgams and can be used more than once.

III. ELECTROMOTIVE FORCE BETWEEN LEAD STICKS AND SATURATED LEAD AMALGAM AT 0° TO 60° C

Gerke's study of the difference in potential between pure lead and two-phase amalgam has been extended by measurements with a set of reproducible lead electrodes over the range 0° to 60° C. These data yield a comparison of the potential of NBS Standard Sample 49b with

that of lead of nearly spectroscopic purity. They permit, as well, a recalculation of some of the thermodynamic constants for lead and saturated lead amalgam to be made.

1. EXPERIMENTAL PROCEDURES AND RESULTS

Lead sticks were cast from NBS Standard Sample 49b and from spectroscopically pure lead. All of them were etched for 1 week. Twelve well-etched sticks of each kind were selected for study.

Six cells of the type shown in figure 2 were employed. A pair of sticks cast from spectroscopically pure lead was rinsed and fixed in place in arm *A*. The amalgam pipette, heated in the oven to 80° to 100° C, was adjusted by means of the rubber stopper (*c*, fig. 1)

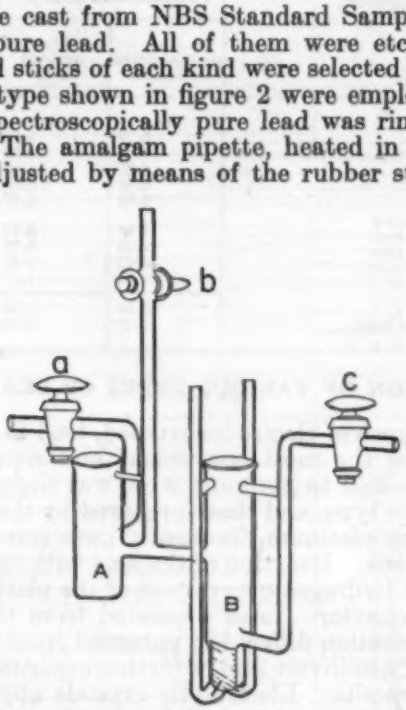

FIGURE 2.—*Cell vessel used for lead and lead amalgam electrodes.*

in the other arm (*B*) of the cell, the vessel evacuated through stopcock *c*, and molten amalgam drawn in to form the two amalgam electrodes at the bottom of *B*. When the amalgam had cooled, enough air-free solution was admitted from the solution flask (attached at *b*) to cover it, and the vacuum was then broken by admitting nitrogen through stopcock *a*.

With nitrogen escaping from the top of *B*, the amalgam pipette was replaced by a pair of sticks cast from NBS Standard Sample 49b. The cell was twice filled completely with electrolyte and emptied through the waste tube at *c* before the final portion of solution was admitted.

The first three cells contained 0.5–*M* lead perchlorate, prepared from lead carbonate and perchloric acid. The other three were filled with 0.5–*M* lead acetate to which a little acetic acid had been added.

At the outset of the experiments, the two amalgam electrodes in each cell agreed in potential, on the average, to 0.03 mv. The results are summarized in table 4. The emf was observed to increase

about 0.1 mv for an increase in temperature of 5 degrees. Occasionally, however, one or more electrodes were found to exhibit an increase of as much as five times the normal temperature effect, or even a decrease. This erratic behavior occurred most frequently with the "spectroscopic" lead at the low temperatures. Inasmuch as the abnormal deviations could readily be identified, these questionable observations were rejected.

The individual emf values are plotted in figure 3 as a function of temperature. The open circles represent potentials of electrodes cast from NBS Standard Sample 49b, and the dots represent the emf of sticks of the spectroscopically pure lead. The diameter of

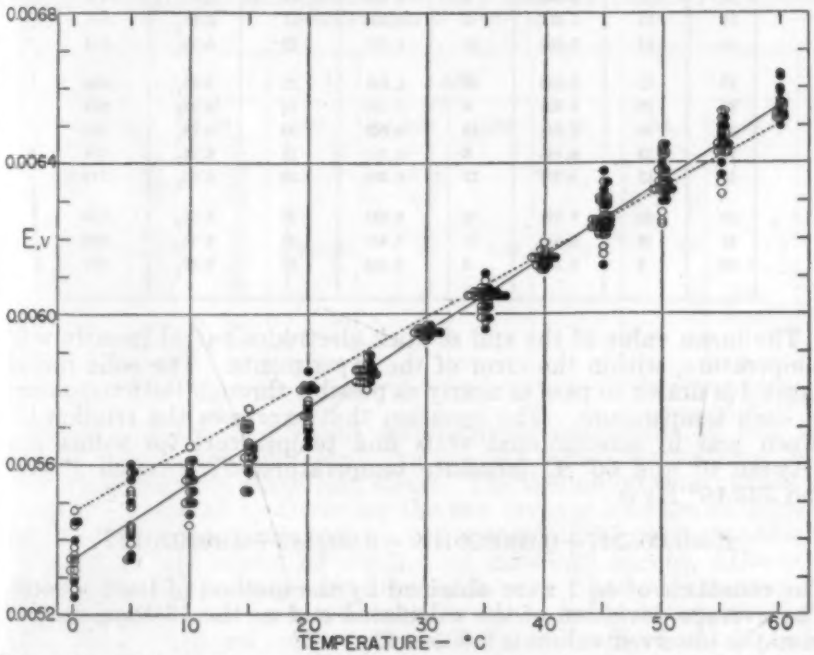

FIGURE 3.—*Electromotive force of the lead stick-lead amalgam cell at 0° to 60° C, as a function of temperature.*

Open circles represent NBS lead electrodes; dots represent "spectroscopically pure" lead. Diameter of circles corresponds to 0.02 mv. The slope of the dotted line differs from that of the solid line by three times the uncertainty assigned to the latter. All the measurements were made at multiples of 5 degrees centigrade. To minimize overlapping, however, some of the points have been plotted slightly to the right or left of the appropriate coordinate line.

each circle corresponds to 0.02 mv. It is evident that no real difference exists between lead from the two sources.

The mean emf values at 13 temperatures for the two kinds of lead are given in table 4, together with the over-all mean for all electrodes and the standard deviation. Two observations were recorded for some of the lead sticks at 35°, 45°, and 55° C. These measurements were obtained when a portion of the temperature range was repeated for check. The emf at 25° C, 0.00585 int v, is in excellent agreement with 0.00584 v found by Carmody [11].

TABLE 4.—*Electromotive force of the cell:* Pb *stick* |Pb^{++}| Pb (*2-phase amalgam*) *at 0° to 60° C*

t	Average emf of cells with—				Total number of electrodes	Mean emf	Standard deviation of the mean
	NBS lead sticks		"Spectroscopic" lead sticks				
	Number	emf	Number	emf			
°C		*Int. mv*		*Int. mv*		*Int. mv*	
0	11	5.362	6	5.330	17	5.35_1	0.020
5	12	5.437	7	5.480	19	5.45_2	.021
10	11	5.551	6	5.538	17	5.54_6	.013
15	12	5.651	5	5.618	17	5.64_2	.016
20	10	5.763	10	5.755	20	5.75_9	.013
25	11	5.845	10	5.849	21	5.84_7	.005
30	10	5.963	8	5.950	18	5.95_2	.003
35	20	6.041	18	6.045	38	6.04_1	.005
40	10	6.149	8	6.145	18	6.14_7	.004
45	17	6.257	17	6.268	34	6.26_2	.010
50	10	6.351	10	6.354	20	6.35_2	.010
55	16	6.443	17	6.457	33	6.45_0	.009
60	8	6.553	9	6.558	17	6.55_5	.010

The mean value of the emf of stick electrodes varied linearly with temperature, within the error of the experiments. The solid line of figure 3 is drawn to pass as nearly as possible through the average emf at each temperature. The equation that expresses the relation between emf in international volts and temperature for values of t between 0° and 60° C (absolute temperature, T, between 273.16° and 333.16° K) is

$$E=0.005347+0.0000201t=-0.000149+0.00002012T. \quad (1)$$

The constants of eq 1 were obtained by the method of least squares. The average deviation of the calculated emf at the 13 temperatures from the observed values is 0.005 mv.

2. THERMODYNAMIC CONSTANTS FOR LEAD AND LEAD AMALGAM

The differences of free energy, ΔF, of entropy, ΔS, and of heat content, ΔH, for the process: Pb (stick)=Pb (in saturated amalgam) are expressed in terms of the constants of eq 1 by the equations

$$\Delta F=-2(96{,}500)\ (-0.000149+0.00002012T). \quad (2)$$

$$\Delta S=2(96{,}500)\ (0.00002012). \quad (3)$$

$$\Delta H=2(96{,}500)\ (0.000149). \quad (4)$$

As a consequence of the linear variation of emf with respect to temperature, ΔS and ΔH are independent of temperature. The values of these three thermodynamic constants are given in table 5. The unit of energy in eq 2, 3, and 4 is the international joule. These quantities were expressed in defined calories by dividing by the conversion factor 4.1833.

An estimate of the probable uncertainties in the constants given in table 5 can be made with the use of the standard deviations of the mean emf values listed in table 4, namely, 0.02 mv at 0° C and 0.01 mv at 60° C. If the error is arbitrarily set at twice that indicated by the standard deviations of these two emf values, the uncertainty of the coefficient of t (or T) in eq 1 is estimated to be 1×10^{-6}. In this way, ΔF is assigned an uncertainty of 5 int. j, whereas ΔS and ΔH may be in error by 0.20 int. j/deg and 60 int. j, respectively. For comparison, it may be noted that the dotted line of figure 3 differs in slope from the solid line by 3×10^{-6}, or three times the estimated uncertainty in establishing the slope of the latter.

TABLE 5.—*Thermodynamic constants for the process:* Pb (*stick*)=Pb (*saturated amalgam*) *at 0° to 60° C*

t	$-\Delta F$		t	ΔS		t	ΔH	
°C	*Int. j*	*cal*	°C	*Int. j/deg*	*cal/deg*	°C	*Int. j*	*cal*
0	1,032	247						
5	1,051	251						
10	1,071	256						
15	1,090	261						
20	1,110	265						
25	1,129	270						
30	1,148	275	0 to 60	3.9	0.93	0 to 60	29	7
35	1,168	279						
40	1,187	284						
45	1,207	288						
50	1,226	293						
55	1,245	298						
60	1,265	302						

Gerke [10] found different termperature coefficients of emf for similar cells which contained, on the one hand, electrolyzed lead crystals and, on the other, lead sticks. The thermodynamic quantities at 25° C computed by Gerke for the two types of lead are as follows: For electrolyzed crystals, $\Delta F=-263$ cal; $\Delta S=0.97$ cal/deg; $\Delta H=26$ cal; and for lead sticks, $\Delta F=-263$ cal, $\Delta S=0.69$ cal/deg, $\Delta H=-57$ cal. The values computed from cells with electrodes formed of electrolyzed crystals agree well with the values found in this investigation: $\Delta F=-270$ cal; $\Delta S=0.93$ cal/deg; and $\Delta H=7$ cal. Gerke removed dissolved air from the solutions but makes no mention of etching the lead sticks. If the sticks were indeed untreated, it seems probable that the crystals represent the more stable modification. This conclusion would lend support to the values given in table 5.

IV. REFERENCES

[1] G. N. Lewis and C. L. von Ende, J. Am. Chem. Soc. **32,** 732 (1910).
[2] W. J. Clayton and W. C. Vosburgh, J. Am. Chem. Soc. **58,** 2093 (1936).
[3] H. Heller, Z. physik. Chem. **89,** 761 (1915).
[4] E. Cohen and W. D. Helderman, Verslag Akad. Wetenschappen **17,** 822 (1915).
[5] F. H. Getman, J. Am. Chem. Soc. **38,** 792 (1916); **40,** 611 (1918).
[6] H. J. M. Creighton, J. Am. Chem. Soc. **37,** 2064 (1915).
[7] G. N. Lewis and T. B. Brighton, J. Am. Chem. Soc. **39,** 1906 (1917).
[8] H. S. Rawdon, Sci. Pap. BS **16,** 215 (1920) S377.
[9] A. Thiel, Ber. deut. chem. Ges. **53,** 1052, 1066 (1920).
[10] R. H. Gerke, J. Am. Chem. Soc. **44,** 1684 (1922).

[11] W. R. Carmody, J. Am. Chem. Soc. **51**, 2905 (1929).
[12] N. A. Puschin, Z. anorg. Chem. **36**, 14 (1903).
[13] M. C. Hannan, Dissertation, The Catholic University of America (1936).
[14] R. G. Bates, J. Am. Chem. Soc. **64**, 1136 (1942).
[15] M. M. Haring, M. R. Hatfield, and P. P. Zapponi, Trans. Electrochem. Soc. **75**, 473 (1939).
[16] T. K. Rose, J. Inst. Metals **8**, 123 (1912).
[17] A. L. Norbury, Trans. Faraday Soc. **19**, 140 (1923).

WASHINGTON, September 25, 1945.

U. S. Department of Commerce National Bureau of Standards

RESEARCH PAPER RP1698

Part of Journal of Research of the National Bureau of Standards, Volume 36, February 1946

ENGINE TESTS WITH PRODUCER GAS

By Frederic A. Middleton and Clarence S. Bruce

ABSTRACT

Bench tests with a four-cylinder stationary engine were made with gasoline and producer gas from charcoal as the fuels. A comparison of their performance revealed that maximum power from producer gas from charcoal is about 55 percent of gasoline power, and that about 11.4 pounds of charcoal is equivalent to 1 gallon of gasoline. When operating an engine on producer gas the spark should be advanced beyond the setting for maximum power with gasoline.

CONTENTS

	Page
I. Scope and objective of investigation	171
II. Test equipment	171
III. Test procedure	173
1. Spark setting	173
2. Power and economy tests	174
3. Variations of power with speed	174
4. Fuel-gas analysis	175
5. Analysis of charcoal	175
IV. Test results	175
1. Spark setting	175
2. Power and economy tests	175
3. Variations of power with speed	180
4. Fuel-gas analysis	180
5. Analysis of charcoal	182
(a) Calorific value	182
(b) Ash	182
V. Operating characteristics of the charcoal burner	182
VI. Conclusions	183
VII. References	183

I. SCOPE AND OBJECTIVE OF INVESTIGATION

The work reported herein is a portion of an extensive investigation [1][1] of substitute motor fuels, conducted by the National Bureau of Standards for the Foreign Economic Administration. The objective of this phase of the investigation was the evaluation of charcoal as a fuel for automotive purposes and the determination of the performance both of the gas producer and of the engine when operating on producer gas from charcoal.

II. TEST EQUIPMENT

The engine used for this study was a four cylinder International Model U–4 with a displacement of 152.1 cubic inches. It was designed for multifuel uses and was supplied with a combination gas-

[1] Figures in brackets indicate the literature references at the end of this paper.

gasoline carburetor, a distillate carburetor, a manifold with heat control, and also cylinder head, piston and cylinder sleeve combinations to give compression ratios of 4.75, 5.9, 7.35, and 10.0. The 5.9 compression ratio was used in this work. Ignition was by an impulse-coupled magneto. A spark-advance indicator was added, and the range of adjustment of the ignition timing was increased to 50 degrees. An adjustable carburetor was used so that air-fuel ratios could be changed easily. The temperature of the cooling water was controlled by a regulator, no radiator or fan being used. Gasoline feed to the carburetor was by gravity, and a fuel-measuring

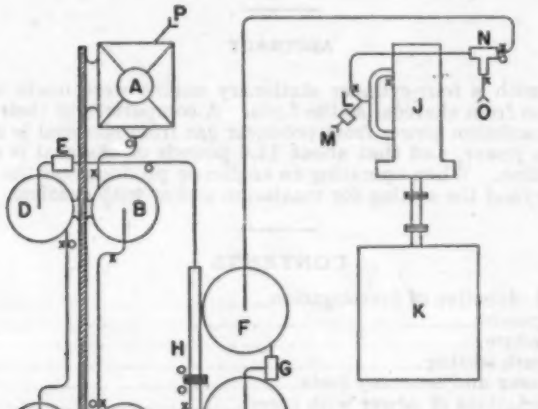

FIGURE 1.—*Schematic layout of test setup.*

A, Gas generator; *B*, cyclone filters; *C*, charcoal filter; *D*, radial-fin filter; *E*, security filter; *F*, buffer drums; *G*, centrifugal blower; *H*, orifice meter; *J*, engine; *K*, dynamometer; *L*, change-over valve; *M*, carburetor air intake; *N*, static mixer; *O*, mixer air intake; *P*, gas-generator air intake.

device was located in the fuel line. The engine was direct-connected to a Sprague electric dynamometer.

The gas producer was Gasogene model DR, a model made for export by the M & R Products Co., Inc., Brooklyn, N. Y. Designed for charcoal, it has a cross-draft fire zone, an air-cooled tuyere, and a means for admitting water to the primary air stream (not used in these tests). The gas generator itself is a steel container approximately 6 feet in height, 20 inches wide, and 27 inches deep, with an opening in the top for the admission of fuel, and an ash clean-out door at the bottom. The fire zone is well toward the bottom. The primary air enters from the front (see fig. 1) and passes through the tuyere into the fire zone and across to the take-off point at the back of the generator. From this point the gas passes through a system of filters for cooling and cleaning before entering the engine. The gas first passes through two cyclone filters that remove the entrained heavier fly ash and act as coolers. The gas next passes through a bed of charcoal, where additional filtering takes place as well as the removal of water that may be condensing. The gas is then conducted through a felt cloth filter which removes fine dust that may have passed through the other filters. This is known as the radial-fin

filter. It is followed by a security filter, which consists of a wire screen of very fine mesh. The purpose of this filter is to safeguard the engine in case of failure of the other filters. From this point the gas passes through an orifice meter, an electrically driven centrifugal blower, two 35-gallon oil drums (which act as a buffer to eliminate any pulsations that would be transmitted from the engine back to the orifice meter), then through the static mixer to the engine. Butterfly valves are located in the passages for air and for gas. and are interconnected. When the throttle control is operated both valves move together so that the mixture ratio is maintained approximately constant for all throttle settings. Means are provided for changing the air-inlet valve independently of the gas valve so that the air-fuel ratio can be varied. The use of the static mixer constitutes a change from the export design of the gas producer. The export equipment included a carbocharger, which is a centrifugal blower operated by a V-belt from a pulley on the water-pump shaft. This blower mixes the air and producer gas to form a combustible mixture and then forces it into the intake manifold under a slight, positive pressure. For the purposes of this study, it was found that when using a static mixer the gas pressures were easier to control than with the carbocharger. The gas is led from the mixer through a change-over valve to the intake manifold of the engine. One branch of the Y-shaped change-over valve is connected to the static mixer and the other branch to the carburetor. A movable vane at the junction of the two branches opens one passageway or the other to the intake manifold.

The amount of air used by the engine was measured by an air-flow indicator connected to the mixer intake. This air-flow indicator and the orifice meter in the gas line permitted air-fuel ratios to be determined for all operating conditions.

In order to weigh the amount of charcoal consumed during any period of operation, the generator end of the plant was slung between two beam scales. The generator and filters were mounted on a wooden framework so that their relative positions were approximately the same as they are on the truck for which the unit was designed. By weighing the entire generator end of the plant, a close record could be kept of the charcoal consumed.

Temperatures were taken by means of thermocouples located at numerous points around the plant.

It was necessary to know how the resistance to the flow of gas through the plant was changing during operation. By observing manometers connected to pressure taps at a number of points in the gas line, it was possible to tell when the fire bed or a certain filter was clogging sufficiently to require a cleaning. For sampling the producer gas, a take-off cock was located in the line just ahead of the mixer. A Shepherd gas analyzer [10] was used to determine the composition of the gas.

III. TEST PROCEDURE

1. SPARK SETTING

The optimum spark setting for the various engine speeds and load conditions was determined experimentally at speeds of 900, 1,200, 1,500, and 1,800 rpm at full load and at least two part-throttle conditions for both gasoline and producer gas. For both fuels the method

was the same—at a given engine speed and throttle setting, and with the air-fuel ratio for maximum power, the spark was advanced a few degrees at a time from an initially retarded position, where the power had fallen off, to an advanced setting, where the power again fell off. Constant engine speed was maintained by varying the electrical load on the dynamometer, and the scale reading at each spark setting was observed. Plotting the horsepower output against spark setting gave a curve for each set of engine conditions. From these curves the optimum spark settings were determined, and a curve was drawn giving the spark setting needed for any condition of load for that particular engine speed.

2. POWER AND ECONOMY TESTS

Tests were made with gasoline and with producer gas at engine speeds of 900 and 1,800 rpm, both at full load and at part-throttle settings giving approximately 75, 50, 25, and 15 percent of the maximum brake power. In the full-load tests, power and fuel-consumption readings were taken at a number of mixture ratios covering the range from lean to rich. As the power was maintained constant in the part-throttle tests, by suitable adjustment of the throttle, readings were taken of intake-manifold depression and fuel consumption at a series of mixture ratios. Power, or intake-manifold depression, and specific fuel consumption were then plotted against measured fuel flow, the latter being an index of mixture ratio.

When the mixture ratio is near that for maximum power, enriching the mixture increases the fuel consumption rapidly without changing the power much, hence it is not possible to determine accurately a "specific fuel consumption at maximum power" because the specific fuel consumption increases rapidly when a mixture near that for maximum power is enriched, although the power changes but little. To obviate these difficulties, it has been customary to use the specific fuel consumption at a lean-mixture ratio giving 99 percent of maximum power, which is in the range of service usage and is capable of rather precise determination. This has been done in the present work.

In the full-load runs, the observed indicated horsepower (sum of brake and friction horsepower) and the fuel consumption were corrected to standard conditions by the formula [2, 3]

$$P_c = P_o \frac{29.53}{B-h}\sqrt{\frac{T}{486.4}},$$

in which

P_o = observed power or fuel consumption
P_c = corrected power or fuel consumption
B = barometric pressure, inches of mercury
h = pressure of water vapor, inches of mercury
T = absolute temperature of air, degrees Fahrenheit.

3. VARIATIONS OF POWER WITH SPEED

The relationship of power to speed was derived from the mixture-ratio runs at constant speeds by plotting the power at optimum spark advance and best mixture ratio against speed.

4. FUEL-GAS ANALYSIS

Samples for analysis were collected in a gas-sampling pipette by mercury displacement. The system was flushed twice, the third filling being retained for analysis. Samples were taken only after the gas generator had been in operation for several hours.

5. ANALYSIS OF CHARCOAL

Samples were collected from a number of bags of each grade of charcoal, and were pulverized and thoroughly mixed. Ash determinations were made on each sample. The heat of combustion of a composite sample was determined in the bomb calorimeter.

IV. TEST RESULTS

1. SPARK SETTING

Upon an inspection of the spark-advance curves, figure 2, two features are at once apparent. The curves for the producer gas indicate the optimum spark advance to be considerably greater than for

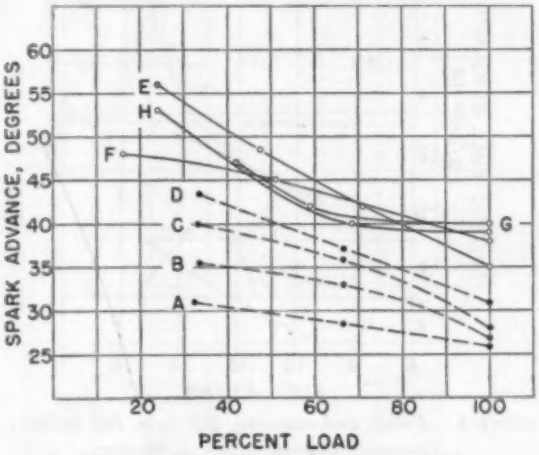

FIGURE 2.—*Spark setting versus load.*

900 rpm, curves A and E; 1,200 rpm, B and F; 1,500 rpm, C and G; 1,800 rpm, D and H; ———— Charcoal. ---------- Gasoline.

gasoline. These curves also lack the consistency of the curves for gasoline. The former observation is in general agreement with other studies [4, 5] and is probably due to the slow-burning characteristics of the fuel. The irregularity and lack of consistency in the curves for producer gas is undoubtedly due to the difficulty experienced in maintaining the best mixture ratio during these runs. The significant fact is that an engine operating on producer gas requires a spark advance greater than that for gasoline.

2. POWER AND ECONOMY TESTS

The maximum power developed with charcoal as the fuel compared to that with gasoline varies from 59 percent at 900 rpm to 55 percent at 1,800 rpm. This percentage agrees generally with studies made elsewhere [4, 6]. Figures 3 and 4 show power and economy curves

for full-throttle conditions at the engine speeds of 900 rpm and 1,800 rpm, respectively, with both fuels. Differences in the peaks of the power curves illustrate the loss of power when operating on charcoal. Figure 5 shows the differences in manifold depressions between the two fuels when the engine is operating at part throttle and constant power output. The peaks of these curves represent a condition of minimum throttle opening or the most powerful mixture of air and

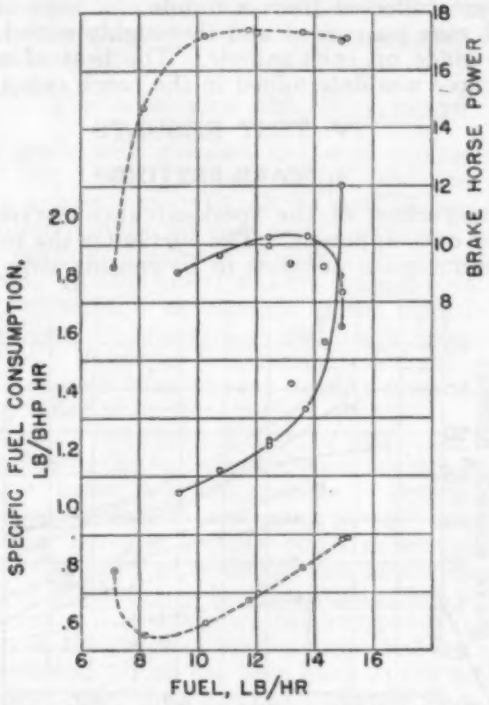

FIGURE 3.—*Power and economy, 900 rpm, full throttle.*
——— Charcoal. ..... Gasoline.

fuel. From this type of graph the specific fuel consumption was derived for all the part-throttle conditions.

The data obtained in tests at engine speeds of 900 rpm and 1,800 rpm are shown in figures 6 and 7, in which specific fuel consumption is plotted against percentage of maximum load. To illustrate the relative performance of gasoline and charcoal more graphically, these data were used to calculate the road performance of a light truck, which might logically be powered by the International U–4 engine used in the tests. The following pertinent truck specifications were assumed: Projected frontal area, 25 ft²; weight (empty) 3,000 lb, (loaded) 6,000 lb; tires, 6.00×16; rear-axle ratio, 4.16:1. Converting the two engine speeds to road speeds, 1,800 rpm equal 36 mph and 900 rpm equal 18 mph. To compute the horsepower required to propel this truck under the selected conditions of weight and speed, it was reasoned that the load imposed on an automotive engine when propelling a vehicle on a

level road at constant speed is composed of frictional resistance in the power-transmission system, including the tires, and of air resistance to the motion of the vehicle and the rotation of its wheels. An unpublished study of car-resistance measurements made here and elsewhere by Donald B. Brooks, of this Bureau shows that the total resistance can be approximated closely by the formula

$$P=0.0000042\,7As^3+0.000000333\,Ws^2+0.000333\,Ws,$$

in which

P=horsepower required to propel vehicle
A=projected frontal area of vehicle, ft²
W=weight of vehicle, lb
s=vehicle speed, mph.

Although no formula can represent all vehicles accurately, because of the differences in the coefficients of air and frictional resistance

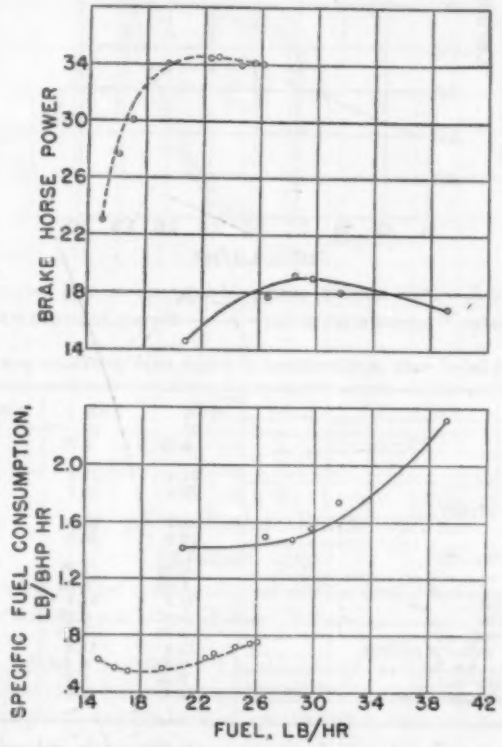

FIGURE 4.—*Power and economy, 1,800 rpm, full throttle.*
——— Charcoal. ---------- Gasoline.

this formula is a sufficiently good approximation to forecast maximum road speeds within 2 mph in the majority of cases, when used in conjunction with the engine-power curve. Knowing the power available for these engines speeds, figure 8, the percentages of load were determined. Table 1 is a compilation of this calculated road performance.

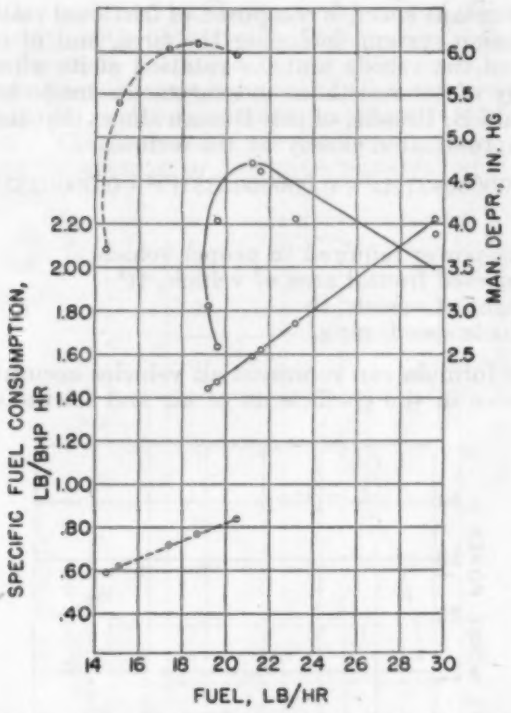

FIGURE 5.—*Part throttle, manifold depression, and economy.*

.....Gasoline, 71 percent of full power; ————charcoal, 70 percent of full power.

TABLE 1.—*Calculated road performance of truck with producer gas and gasoline*

Weight of truck, lb	3,000	3,000	6,000	6,000
Miles per hour	36	18	36	18
Horsepower required	9.88	2.75	14.76	4.67
Horsepower available:				
Gasoline	34.4	17.3	34.4	17.3
Charcoal	19.0	10.2	19.0	10.2
Percentage of power available:				
Gasoline	28.7	15.8	43.0	26.2
Charcoal	52.0	26.9	77.8	47.8
Fuel consumption (lb/bhp hr):				
Gasoline	0.99	1.31	0.80	0.96
Charcoal	1.80	2.36	1.51	1.73
Miles per gallon, gasoline	23.2	31.7	19.3	24.2
Miles per pound, gasoline	3.87	5.28	3.22	4.03
Miles per pound, charcoal	2.03	2.78	1.63	2.13
Pounds of charcoal per gallon of gasoline	11.4	11.4	11.8	11.4
Pounds of charcoal per ton mile	0.330	0.240	0.203	0.156
Ton miles per pound, charcoal	3.03	4.17	4.93	6.41
Ton miles per gallon, gasoline	34.8	45.6	57.9	72.6

Considering the truck performance at 36 mph when loaded to a gross weight of 6,000 lb, it can be seen that 14.76 horsepower is required. This is 43.0 percent of the gasoline power available, but 77.8 percent of the charcoal or producer-gas power available. The respective fuel consumptions are 0.80 lb/bhp hr and 1.51 lb/bhp hr, which is about the best figure for charcoal but considerably poorer than the best for gasoline. The reserve power, needed for acceleration and hill climbing, would be 19.64 hp for gasoline and 4.24 hp for charcoal, which indicates that when operating on charcoal the truck would have

very poor performance. This illustrates one of the serious drawbacks to charcoal as a substitute fuel, the loss of about 45 percent of gasoline power, and at the same time suggests a remedy, the use of a larger or supercharged engine. However, where the engine is capable of developing more power with gasoline than is ever likely to be needed, as with most passenger-car engines, the loss of power when operating

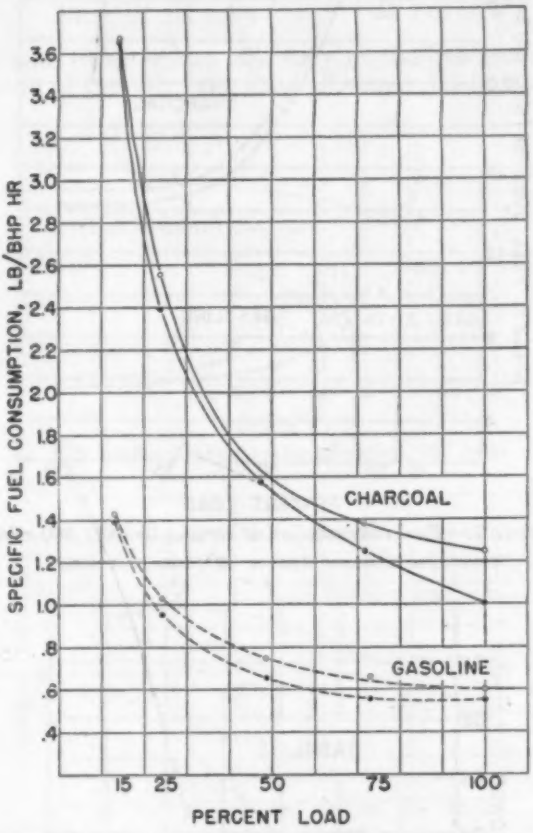

FIGURE 6.— *Fuel consumption at various loads, 900 rpm.*
○Economy at 99 percent of power. ●Maximum economy.

on charcoal is not as serious. Commerical vehicles, whose power plants are frequently required to perform at or near their rated capacity, would find a proportionate loss of power a serious handicap.

3. VARIATIONS OF POWER WITH SPEED

The curves shown in figure 8 illustrate the differences in the power available with gasoline and with charcoal. The power with charcoal varies from 59 percent of that with gasoline at 900 rpm to 55 percent at 1,800 rpm.

4. FUEL-GAS ANALYSIS

Gas samples were collected under a variety of conditions of engine speed and load. The following shows the principal constituents

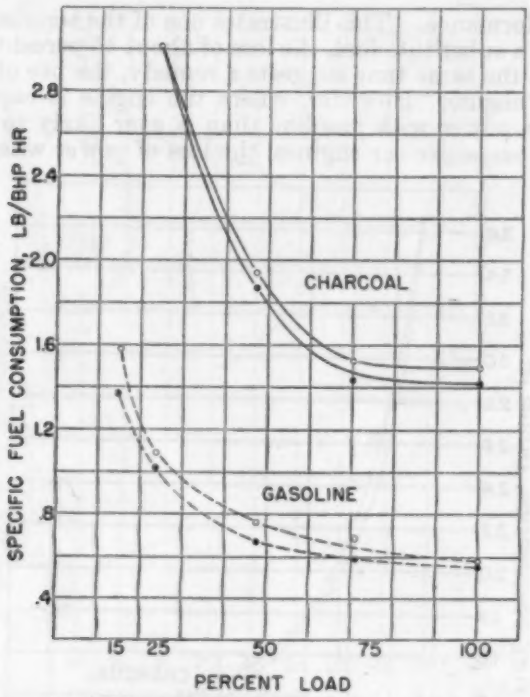

FIGURE 7.—*Fuel consumption at various loads, 1,800 rpm.*

○Economy at 90 percent of power. ●Maximum economy.

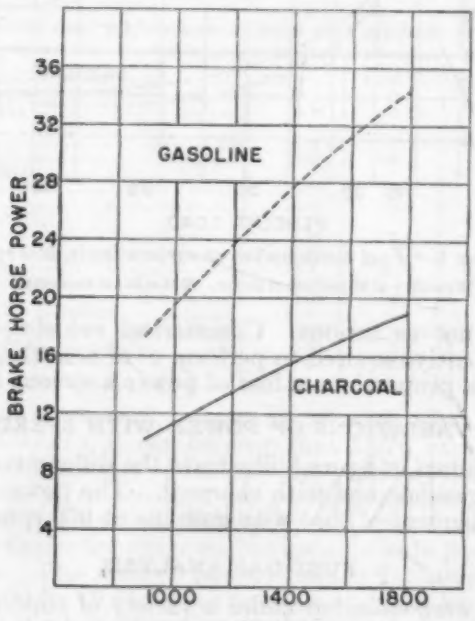

FIGURE 8.—*Full-throttle speed and power.*

found in the producer gas, their average percentage by volume, and the spread, as determined from 12 analyses:

Gas	Average	Spread
CO_2	1.8	0.8 to 4.1
O_2	1.4	.1 to 2.3
H_2	5.2	.3 to 13.0
CH_4	1.8	.0 to 7.0
CO	28.2	21.3 to 30.4
N_2	62.0	52.7 to 67.9

Figures 9 and 10 show the efficiency of the gas generator plotted against pounds of fuel per hour, the efficiency being the ratio of the

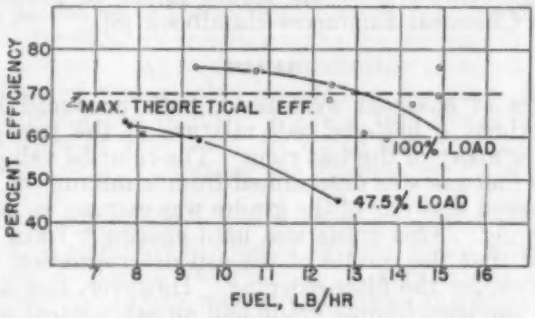

FIGURE 9.—*Gas-generator efficiency, 900 rpm.*

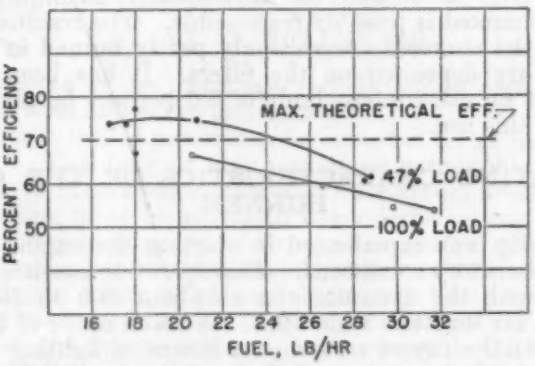

FIGURE 10.—*Gas-generator efficiency, 1,800 rpm.*

heating value of the gas divided by the heating value of the charcoal consumed to produce the gas. Examination of these curves indicates that in most cases the efficiency improves as the mixture ratio is made leaner. The reversal of the positions of the part-throttle curves with respect to the full-throttle curves for the two engine speeds may result from the fact that at 1,800 rpm, full throttle, the fire bed was quite extensive with a resulting decrease in the beneficial insulating effects of the surrounding charcoal.

In computing the theoretical efficiencies shown in the above figures it was assumed that the carbon burns entirely to carbon monoxide [7]. A ratio between the heats of combustion of CO and C will give this

theoretical maximum efficiency value of 70 percent. Efficiencies in excess of this figure may be explained by the presence of other combustibles in the gas, such as H_2 and CH_4.

5. ANALYSIS OF CHARCOAL

(a) CALORIFIC VALUE

From the composite sample the calorific value of the charcoal was established at 13,880 Btu/pound. This value is believed to be correct within 0.5 percent. It is higher than the values 13,325 to 13,487 Btu/pound reported by the National Research Council of Canada. It is also high compared to the values 12,000 to 13,000 Btu/pound given in the Chemical Engineers Handbook [8].

(b) ASH

Two grades of charcoal were used, both produced by the same company. About a half-and-half mixture of the two grades made up the fuel for many of the test runs. The calorific value of the charcoal and the fuel gas was determined from a mixture of the two, but it was discovered that one of the grades was causing an undue amount of filter clogging. This grade was used sparingly from then on. It was expected that the results of the ash determination would reveal the explanation for the filter-clogging. However, this determination showed that the troublesome grade had an ash content of 1.7 percent and that the other grade had an ash content of 7.0 percent. As the ash content does not account for the difficulty, incomplete carbonization of the charcoal is possibly responsible. The residual tarry products left in the charcoal are still only partly burned in the gas producer, and are deposited on the filters. It has been proposed in Canada that an ash-content limit of 3.0 percent be placed on wood charcoal for this use.

V. OPERATING CHARACTERISTICS OF THE CHARCOAL BURNER

No difficulty was experienced in starting the engine on producer gas under laboratory conditions. This operation consisted of cranking the engine with the dynamometer at about 300 to 500 rpm, with the gas and air throttles wide open. A torch made of twisted newspaper held at the tuyere served as a means of lighting the charcoal. As soon as the fuel was ignited the operator would slowly open and close the air butterfly. In less than 2 minutes enough gas was generated and delivered to the engine to make it possible to set the air throttle to give a combustible mixture. From then on a common throttle linkage was used to control the engine, with only slight adjustments of the air valve to maintain a good mixture.

It was found after several experiences that when the radial-fin filter cloth was new or well cleaned its ability to function as a filter was poor, in which case the following security filter would always clog and throttle the engine. After some dirt had collected on the cloth its filtering action would return to normal, and then the security would require very little service.

The nature of the charcoal appeared to be the controlling factor in the clogging of the filters. On one occasion the cyclone filters were

operated for more than 50 hours before being cleaned, yet at another time, with a different grade of charcoal, the same filters were completely clogged after only 3 hours and 20 minutes. A different grade of charcoal was used in these two instances. No serious effort was ever made to investigate the causes of this behavior. Apparently the makeup of the charcoal has a great deal to do with the satisfactory operation of the plant. Regardless of the nature of the fuel, however, the filters will become dirty in time and impede the flow of gas sufficiently to cause a serious loss of power. Water manometers across the filters made an excellent means of showing the state of the filters. When the radial-fin filter was not performing as it should and the dirt was being passed on to the security filter, it was impossible to observe the manometer steadily creeping up as the security filter became more and more clogged. At such times another clean security filter was kept nearby and was quickly inserted in the place of the dirty one without stopping the engine. Usually this would not be repeated more than three or four times, by which time the radial fin would be acting satisfactorily. Cleaning the filters is very dirty work but cannot be avoided.

One difficulty that was entirely unforeseen, and which could never be overlooked, was that the metal tuyeres would melt away at their tips when left in the fire overnight. A very simple solution was at once adopted—the tuyere was removed from the generator at the end of the day's run. Most of the trouble was with the 1-inch metal tuyeres; the ¾-inch metal and the silicon carbide tuyeres did not melt so extensively.

VI. CONCLUSIONS

Charcoal may be used as a successfully automotive fuel if its limitations and weaknesses are understood.

A 45-percent loss of power can be expected on an unmodified gasoline engine. This may or may not prove permissible, depending on the amount of excess power available over actual needs.

Spark timing must be advanced beyond the setting for gasoline.

Servicing requirements would make the use of gas producers impractical for the average automobile owner in this country, but for commercial uses where a fleet of vehicles was being operated, trained servicemen could handle this problem satisfactorily.

In general, the gas-generating plant performed satisfactorily. The difficulty experienced with the tuyeres melting at their tips is a subject that should be investigated.

This work shows that although different lots of charcoal vary in their suitability as producer fuel, the ash content is not a satisfactory criterion of performance.

VII. REFERENCES

[1] Donald B. Brooks, Single-cylinder engine tests of substitute motor fuels J. Research NBS **35,** 1 (1945) RP1660.

[2] Donald B. Brooks, Correcting engine tests for humidity, BS J. Research **3,** 795 (1925) RP118.

[3] D. B. Brooks and E. A. Garlock, The effect of humidity on engine power at altitude, Nat. Adv. Comm. Aeron. Rep. 426 (1932), Eighteenth Annual Report of NACA.

[4] E. A. Alcutt, Producer gas for motor transport, Automotive and Aviation Ind. **89,** 39 (August 15, 1943).
[5] A. E. Burstall and M. W. Woods, Experiments on a high-speed producer gas engine, Engineer **167,** 642 (May 26, 1939).
[6] J. Spiers, The performance of a converted petrol engine on producer gas, Proc. Inst. Automobile Engrs. (London) **36,** 117 (1941–42).
[7] Harold C. Weber, Theory of gas producers, Mechanical Engineers' Handbook (McGraw-Hill Book Co., Inc., New York, N. Y., 4th ed., p. 372 1941).
[8] Harry A. Curtis, Solid fuels, Chemical Engineers' Handbook (McGraw-Hill Book Co., Inc., New York, N. Y., 2d ed., p. 2341, 1941).
[9] E. A. Allcut and R. H. Patten, Gas producers for motor vehicles, National Research Council of Canada, No. 1220, p. 69, Ottawa (1944).
[10] Martin Shepherd, Improved apparatus and methods for analysis of gas mixtures by combustion and absorption, BS J. Research **6,** 121 (1931) RP266.

WASHINGTON, November 14, 1945.

U. S. DEPARTMENT OF COMMERCE NATIONAL BUREAU OF STANDARDS

RESEARCH PAPER RP1699

Part of Journal of Research of the National Bureau of Standards, Volume 36, February 1946

PHASE EQUILIBRIUM RELATIONS IN A PORTION OF THE SYSTEM Na_2O-CaO-Al_2O_3-SiO_2

By Kenneth T. Greene and R. H. Bogue

ABSTRACT

A study of a portion of the system Na_2O-CaO-Al_2O_3-SiO_2 has been made as a step in the solution of the problem of the state of combination of Na_2O in portland cement clinker. Quenching data are given for compositions in the tetrahedron formed by $2CaO.SiO_2$, CaO, $Na_2O.Al_2O_3$, and Al_2O_3, and phase diagrams are shown for three composition planes through the space model. Five invariant points were located approximately, at one of which $2CaO.SiO_2$, $3CaO.SiO_2$, $3CaO.Al_2O_3$, and $Na_2O.8CaO.3Al_2O_3$ are in equilibrium with liquid. This point, which is not a eutectic, occurs at 1,440° ± 10°C and has a composition of 3.5 percent Na_2O, 55.2 percent CaO, 31.0 percent Al_2O_3, and 10.3 percent SiO_2. Evidence was obtained of the formation, under favorable conditions, of a solid solution between $3CaO.Al_2O_3$ and $Na_2O.8CaO.3Al_2O_3$ at temperatures below that of liquid formation. Present information indicates that Na_2O may be present in clinker in several possible forms: (1) in glass, (2) as $Na_2O.8CaO.3Al_2O_3$ or a solid solution of this compound and $3CaO.Al_2O_3$, (3) in solid solution in $2CaO.SiO_2$, (4) as inclusions of a soda-bearing phase in β-$2CaO.SiO_2$ produced by ex-solution on inversion from α-$2CaO.SiO_2$.

CONTENTS

	Page
I. Introduction	185
II. Experimental method	187
III. Phase equilibria	189
1. General discussion	189
2. The plane $2CaO.SiO_2$-CaO-($Na_2O+6Al_2O_3$)	197
3. The plane $2CaO.SiO_2$-CaO-($Na_2O+3Al_2O_3$)	198
4. The system $2CaO.SiO_2$-CaO-$Na_2O.Al_2O_3$	200
5. Additional compositions, located between the $2CaO.SiO_2$-CaO-($Na_2O+6Al_2O_3$) and $2CaO.SiO_2$-CaO-($Na_2O+3Al_2O_3$) planes	201
IV. Discussion	202
1. Crystallization in the system	202
2. Solid solutions	203
3. Applications to portland cement clinker	205
V. Summary	206
VI. References	207

I. INTRODUCTION

In order to understand the state of chemical combination of the various component oxides of portland cement, it is necessary first to study the interrelations of these oxides as systems of few components, gradually extending the scope of the investigations to include other oxides and, consequently, more complicated systems, as more and more data become available. The phase equilibrium relations of the major oxides of portland cement, CaO, SiO_2, Al_2O_3, Fe_2O_3, and MgO have been rather thoroughly determined and the results are well known. However, it is only within the last few years that a systematic

attempt has been made to study the effect of such minor components as SO_3, K_2O, Na_2O, TiO_2, etc., upon the constitution of portland cement clinker. This paper represents part of an investigation undertaken to determine the manner in which one of these minor components, Na_2O, combines with the other oxides of clinker.

The quaternary system Na_2O-CaO-Al_2O_3-SiO_2 is one of several which have a direct bearing on the effect of Na_2O on the phase composition of portland cement clinker. It is probably the most important of these systems, since it contains the three oxides which are usually in greatest abundance, CaO, SiO_2, and Al_2O_3. Ferric oxide is the only major component of clinker that is likely to have any radical effect on the phase relations as determined in the Na_2O-CaO-Al_2O_3-SiO_2 system, since MgO has been shown to exist in clinker essentially uncombined [1, 2, 3].

One of the four ternary systems bounding the four-component system, which has been determined, is the system CaO-Al_2O_3-SiO_2 originally studied by Rankin and Wright [4]. Portions of the other three ternary systems, each of which contains Na_2O as a component, have also been studied. However, the only earlier work which has a direct application to portland cement compositions is that of Brownmiller and Bogue on the system Na_2O-CaO-Al_2O_3 [5]. They investigated the region of the smaller ternary system $Na_2O.Al_2O_3$-CaO-Al_2O_3. The most important result of this work was the discovery of a compound having the formula, $Na_2O.8CaO.3Al_2O_3$, and being capable of existing in equilibrium with $3CaO.Al_2O_3$. As $3CaO.Al_2O_3$ is a constituent of portland cement clinker, it appeared that this compound had a possibility of existence in clinkers containing Na_2O. However, the behavior of $Na_2O.8CaO.3Al_2O_3$ in the presence of the calcium silicates, $3CaO.SiO_2$, and $2CaO.SiO_2$, had not yet been determined.

Certain limited portions of the quaternary system have also been investigated, but the ranges of composition of these are mostly far removed from the region of interest from the standpoint of portland cement. Consequently, such data will not be considered here. A previous paper from this laboratory by one of the present authors [6] dealt with solid solutions which the compound $2CaO.SiO_2$ may form under suitable conditions in the system Na_2O-CaO-Al_2O_3-SiO_2, as well as in the system Na_2O-CaO-Fe_2O_3-SiO_2. It was shown that these solid solution phases have a hexagonal crystal structure and that this structure very likely is fundamentally that of the α form of $2CaO.SiO_2$. The relation of these phases to the $2CaO.SiO_2$ of commercial portland cement clinker was discussed at some length in this paper.

To determine whether $Na_2O.8CaO.3Al_2O_3$ is the compound of Na_2O which is stable in mixtures of Na_2O, CaO, Al_2O_3, and SiO_2 in which these oxides are present in the same proportions as in portland cement, it was necessary to study in some detail the phase equilibria in that part of the quaternary system which contains the compounds $3CaO.SiO_2$, $2CaO.SiO_2$, $3CaO.Al_2O_3$, and $Na_2O.8CaO.3Al_2O_3$. For this purpose the portion of the system consisting of compositions which may be made up of the four compounds $2CaO.SiO_2$, CaO, $Na_2O.Al_2O_3$, and Al_2O_3 was chosen. When a regular tetrahedron is used to represent the larger oxide system Na_2O-CaO-Al_2O_3-SiO_2, the four compounds $2CaO.SiO_2$, CaO, $Na_2O.Al_2O_3$, and Al_2O_3 are at the apexes of a tetrahedron of unequal dimensions which occupies a space within the larger tetrahedron.

Various methods are possible for representing the space relations in the model of a four-component system. The ultimate purpose is to define the limits of the regions of primary crystallization of the various phases, called primary phase volumes, and to determine the temperature relations within the primary phase volumes and particularly on the surfaces, along the lines, and at the points where two, three, or four primary phase volumes adjoin one another. It is customary to select various lines or planes through the space model and to determine the manner in which these intersect the primary phase volumes. The lines or planes may represent binary or ternary systems within the quaternary system, they may represent joins which are not true binary or ternary systems, or they may depict planes having arbitrary compositional relationships. An example of the latter type is a series of planes parallel to one face of the tetrahedron, each plane containing a certain constant percentage of the fourth component. Lea and Parker [7] and Schairer [8] discuss in detail methods of studying quaternary systems, and give diagrams to illustrate the manner in which the data may be presented.

In the present investigation, the phase equilibrium relations of three composition planes through the tetrahedral space model have been studied, as well as a number of extra compositions situated between the planes. Each plane, which is triangular in shape, has the compounds $2CaO.SiO_2$ and CaO at two of its apexes. The third apex represents a mixture of Na_2O and Al_2O_3 in a certain definite proportion. All compositions in the same plane therefore contain Na_2O and Al_2O_3 in a constant molar ratio. One of the planes corresponds to one side of the smaller tetrahedron $2CaO.SiO_2$-CaO-$Na_2O.Al_2O_3$-Al_2O_3, whereas the other two occupy positions within it. They may be represented as follows:

$$2CaO.SiO_2\text{-}CaO\text{-}(Na_2O+6Al_2O_3)$$
$$2CaO.SiO_2\text{-}CaO\text{-}(Na_2O+3Al_2O_3)$$
$$2CaO.SiO_2\text{-}CaO\text{-}Na_2O.Al_2O_3$$

The planes are arranged in order of increasing proportion of Na_2O.

Each of the first two planes is a section through the quaternary system, in which one of the three components is an arbitrary mixture of Na_2O and Al_2O_3. In the third plane, however, the corresponding component is the definite chemical compound, sodium aluminate. Figure 1 shows the relation of these planes and of the smaller tetrahedron $2CaO.SiO_2$-CaO-$Na_2O.Al_2O_3$-Al_2O_3 to the tetrahedron representing the complete Na_2O-CaO-Al_2O_3-SiO_2 system.

II. EXPERIMENTAL METHOD

The quenching method of thermal study was used throughout this investigation. The procedure followed was in general similar to that described in previous publications of this laboratory pertaining to alkali systems [5, 9, 10]. In certain cases minor changes were made, as dictated by the conditions encountered.

As in the earlier work with alkalies, volatilization was a problem, particularly in compositions having a relatively high percentage of Na_2O. For this reason most of the mixtures were given no preliminary heat treatment prior to making the quenching determinations, and the time held at constant temperature was kept as short as possible

consistent with the attainment of equilibrium. By this means the volatilization of Na_2O was kept at a minimum, and in the great majority of cases it was not found necessary to add an excess of soda to compensate for this loss.

To test the extent of loss of Na_2O by volatilization, and also the accuracy of proportioning of the raw materials, several representative mixes were analyzed chemically for Na_2O after heating for one-half hour at temperatures near those of the quenching experiments. The samples analyzed cover a rather large range of Na_2O percentages, and the results indicate that, with the exception of those relatively

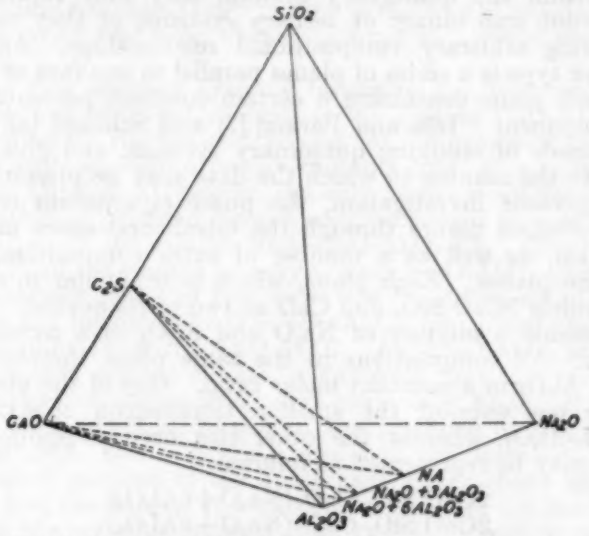

FIGURE 1.—*Tetrahedron* $2CaO.SiO_2$-CaO-$Na_2O.Al_2O_3$-Al_2O_3 *in relation to system* Na_2O-CaO-Al_2O_3-SiO_2.

high in Na_2O, the volatilization is negligible and the amounts of Na_2O are close to those desired. The data are tabulated below.

Mix number	Na_2O desired %	Na_2O found %
19	11. 34	10. 99
24	3. 78	3. 79
60	1. 69	1. 63
101	5. 90	5. 89
204	3. 88	3. 97

The omission of preliminary heatings and grindings of the samples used in the quenching furnace made it essential that the raw materials be very thoroughly mixed the first time. This was accomplished by prolonged grinding together of the ingredients in an agate mortar. The distribution of solid phases in the quenched charges, as observed microscopically, indicated that satisfactory mixing had been obtained.

The presence of vapors of Na_2O in the quenching furnace made it necessary to recalibrate the thermocouple frequently. This was done at times against a standard couple, but more often checks were made against the known melting points of the pure compounds $CaO.MgO.2SiO_2$ (1,391.5° C) and $BaO.2SiO_2$ (1,418° C).

III. PHASE EQUILIBRIA

1. GENERAL DISCUSSION

The data on the phase equilibrium relations, as determined by the quenching procedure, are presented in tables 1, 2, 3, and 4. These contain those critical determinations that furnish information necessary to the interpretation of the system. However, they represent only a fraction of the total number of quenching experiments performed. In order to reduce the length of the tables, many data that do not contribute essential information have been omitted. For example, in cases where it was desired to show only which crystalline phase is primary, the results of only one quench are given. Near invariant points or where the liquidus temperatures were determined, data on more than one quench are recorded. In the tables and diagrams the following abbreviations are used:

$C_3S = 3CaO.SiO_2$
$C_2S = 2CaO.SiO_2$
$C_3A = 3CaO.Al_2O_3$
$NC_8A_3 = Na_2O.8CaO.3Al_2O_3$
$C_5A_3 = 5CaO.3Al_2O_3$ [1]
$C_2AS = 2CaO.Al_2O_3.SiO_2$
$CA = CaO.Al_2O_3$
$C_3A_5 = 3CaO.5Al_2O_3$
$N_2C_3A_3 = 2Na_2O.3CaO.5Al_2O_3$
$N_2C_3A_3ss = 2Na_2O.3CaO.5Al_2O_3$ solid solution with $Na_2O.Al_2O_3$
$NA = Na_2O.Al_2O_3$
Tr. = Trace
Amt. = Amount.

TABLE 1.—*Quenching data for compositions in the* $2CaO.SiO_2$-CaO-$(Na_2O+6Al_2O_3)$ *plane*

No.	Composition							Time	Temperature	Phases present
	Oxides				Components					
	Na_2O	CaO	Al_2O_3	SiO_2	C_2S	CaO	$(Na_2O+6Al_2O_3)$			
CaO PRIMARY										
	%	%	%	%	%	%	%	*hr*	°*C*	
191	4.1	55.0	40.9	------	------	55.0	45.0	¼	1,530	CaO, glass.
								½	1,520	C_3A, tr. CaO, glass.
192	3.7	56.0	36.8	3.5	10.0	49.5	40.5	¼	1,520	CaO, glass.
								¼	1,515	C_3A, CaO, glass.
193	3.3	57.0	32.7	7.0	20.0	44.0	36.0	¼	1,485	CaO, glass.
								¼	1,475	CaO, C_3A, tr. NC_8A_3, glass.
194	2.9	58.0	28.6	10.5	30.0	38.5	31.5	¼	1,510	Tr. CaO, tr. C_2S, glass.
								¼	1,480	CaO, C_2S, glass.

[1] That the results of this investigation might be compared more readily with the literature on the CaO-Al_2O_3-SiO_2 system, the formula $5CaO.3Al_2O_3$ is used throughout the paper, although it is recognized that strong evidence has been presented by various authors indicating that the correct formula is $12CaO.7Al_2O_3$ [18, 19, 20, 21].

TABLE 1.—*Quenching data for compositions in the* $2CaO.SiO_2$-CaO-$(Na_2O+6Al_2O_3)$ *plane*—Continued

No.	Composition							Time	Temperature	Phases present
	Oxides				Components					
	Na_2O	CaO	Al_2O_3	SiO_2	C_2S	CaO	$(Na_2O+6Al_2O_3)$			
	C_3S PRIMARY									
	%	%	%	%	%	%	%	*hr*	°C	
196	2.7	58.5	26.6	12.2	40.0	33.0	27.0	½	1,525	C_2S, tr. CaO, glass.
								½	1,485	C_2S, CaO, glass.
197	3.0	56.3	30.2	10.5	30.0	36.8	33.2	½	1,475	Small amt. C_2S, tr. CaO, glass.
								½	1,460	C_3S, tr. CaO, tr. C_2S, glass.
								½	1,450	C_3S, C_2S, C_3A, glass.
199	3.0	56.6	29.1	11.3	32.5	35.4	32.1	½	1,475	C_3S, tr. C_2S, glass.
								½	1,470	C_3S, C_2S, glass.
								½	1,450	C_3S, C_2S, C_3A, glass.
	C_2S PRIMARY									
120	2.8	45.6	27.2	24.4	70.0	------	30.0	½	1,510	Tr. C_2S, glass.
								½	1,500	C_2S, C_2AS, glass.
132	1.8	59.0	18.2	21.0	60.4	19.6	20.0	½	1,360	C_2S, glass.
								½	1,355	C_2S, CA_2, glass.
133	2.8	51.6	27.2	18.4	52.8	17.2	30.0	½	1,450	C_2S, glass.
134	3.7	44.2	36.3	15.8	45.3	14.7	40.0	½	1,450	All glass.
								½	1,410	C_2S, glass.
								½	1,400	C_2S, C_2AS, glass.
143	3.2	54.5	31.8	10.5	30.0	35.0	35.0	½	1,440	Small amt. C_2S, glass.
								½	1,435	C_3S, C_3A, glass.
146	3.0	55.3	29.5	12.2	35.0	32.5	32.5	½	1,440	C_2S, glass.
								½	1,435	C_2S, small amt. C_3A, glass.
								½	1,375	C_2S, glass.
153	3.5	51.0	35.0	10.5	30.0	31.5	38.5	½	1,373	C_2S, NC_3A_2, glass.
								½	1,370	C_2S, C_3A_2,NC_3A_2, glass.
								½	1,360	Almost completely crystalline.
156	3.9	47.5	38.1	10.5	30.0	28.0	42.0	½	1,370	C_2S, glass.
								½	1,365	C_2S, C_3A_2, glass.
165	3.7	50.5	36.2	9.6	27.5	32.6	39.9	½	1,375	C_2S, glass.
170	3.9	45.5	38.4	12.2	35.0	22.7	42.3	½	1,375	Do.
184	4.1	43.5	40.9	11.5	33.0	22.0	45.0	½	1,350	Tr. C_2S, glass.
								½	1,345	C_2S, C_3A_2, glass.
195	2.5	59.1	24.5	13.9	40.0	33.0	27.0	½	1,525	C_2S, C_3S, glass. Probably near boundary.
198	2.8	57.0	28.0	12.2	35.0	34.1	30.9	½	1,475	C_2S, tr. C_3S, glass.
								½	1,460	C_2S, C_3S, glass.
								½	1,450	C_2S, C_3S, C_3A, glass.
								½	1,445	C_2S, C_3A, glass.
	C_3A PRIMARY									
140	4.6	50.0	45.4	------	------	50.0	50.0	½	1,450	C_3A, glass.
141	4.1	51.5	40.9	3.5	10.0	45.0	45.0	½	1,505	Small amt. C_3A, glass.
142	3.7	53.0	36.3	7.0	20.0	40.0	40.0	½	1,465	All glass.
								½	1,460	Tr. C_3A, glass.
								½	1,450	All glass.
145	3.4	53.8	34.1	8.7	25.0	37.5	37.5	¼	1,445	C_3A, glass.
								¼	1,430	C_3A, tr. C_2S, glass.
								½	1,445	All glass.
147	3.3	54.2	32.9	9.6	27.5	36.3	36.2	½	1,440	C_3A, tr. C_2S, glass.
								½	1,450	All glass.
160	4.3	49.3	42.9	3.5	10.0	42.7	47.3	½	1,440	C_3A, glass.
								⅛	1,425	All glass.
161	3.9	51.0	38.1	7.0	20.0	38.0	42.0	⅛	1,410	C_3A, glass.
								½	1,420	All glass.
162	3.6	51.9	35.8	8.7	25.0	35.6	39.4	½	1,415	C_3A, tr. C_2S, glass.

TABLE 1.—*Quenching data for compositions in the* $2CaO.SiO_2$-CaO-$(Na_2O+6Al_2O_3)$ *plane*—Continued

No.	Composition							Time	Temperature	Phases present
	Oxides				Components					
	Na_2O	CaO	Al_2O_3	SiO_2	C_2S	CaO	$(Na_2O+6Al_2O_3)$			
	NC_3A_2 PRIMARY									
	%	%	%	%	%	%	%	*hr*	*°C*	
152	4.0	49.0	40.0	7.0	20.0	36.0	44.0	½	1,400	All glass.
								½	1,390	Tr. NC_3A_2, tr. C_3A_2, glass.
								½	1,385	NC_3A_2, C_3A_2, glass.
								½	1,375	Tr. NC_3A_2, glass.
154	3.8	50.0	37.5	8.7	25.0	33.7	41.3	½	1,370	NC_3A_2, C_3A_2, C_2S, glass.
								½	1,365	C_3A_2, C_2S, prob. NC_3A_2 and C_3A, small amt. glass.
								½	1,360	Almost completely crystalline.
	C_3A_2 PRIMARY									
150	5.1	45.0	49.9	.....	.....	45.0	55.0	½	1,450	All glass.
								½	1,445	C_3A_2, glass.
151	4.5	47.0	45.0	3.5	10.0	40.5	49.5	½	1,425	All glass.
								½	1,420	C_3A_2, glass.
156	5.0	42.5	49.0	3.5	10.0	36.0	54.0	½	1,440	All glass.
								½	1,435	C_3A_2, glass.
157	4.4	45.0	43.6	7.0	20.0	32.0	48.0	½	1,410	All glass.
								½	1,405	Tr. C_3A_2, glass.
159	4.1	46.3	40.9	8.7	25.0	30.0	45.0	½	1,390	Do.
163	4.2	47.0	41.8	7.0	20.0	34.0	46.0	½	1,400	Perhaps tr. C_3A_2, glass.
								½	1,395	C_3A_2, glass.
164	4.0	48.1	39.2	8.7	25.0	31.9	43.1	½	1,370	Do.
								½	1,365	C_3A_2, C_2S, glass.
168	4.8	41.0	47.2	7.0	20.0	28.0	52.0	½	1,390	All glass.
								½	1,380	C_3A_2, glass.
169	4.2	44.0	41.3	10.5	30.0	24.5	45.5	½	1,375	All glass.
								½	1,360	C_3A_2, glass.
175	5.1	38.7	49.9	6.3	18.0	27.0	55.0	½	1,400	All glass.
								1¼	1,390	C_3A_2, perhaps tr. CA, glass.
181	4.6	41.3	45.4	8.7	25.0	25.0	50.0	½	1,370	All glass.
								½	1,365	C_3A_2, glass.
183	4.6	40.4	45.4	9.6	27.5	22.5	50.0	½	1,350	Tr. C_3A_2, glass.
								½	1,345	C_3A_2, tr. C_2AS, glass.
	C_2AS PRIMARY									
122	4.6	32.6	45.4	17.4	50.0	.....	50.0	½	1,510	All glass.
								½	1,505	C_2AS, glass.
128	4.8	30.9	47.7	16.6	52.5	.....	47.5	¼	1,500	Tr. C_2AS, glass.
135	4.6	36.9	45.4	13.1	37.7	12.3	50.0	½	1,475	All glass.
								½	1,460	C_2AS, glass.
137	5.1	33.2	49.9	11.8	34.0	11.0	55.0	½	1,450	Tr. C_2AS, glass.
180	5.1	34.0	49.9	11.0	31.5	13.5	55.0	½	1,425	C_2AS, glass.
182	4.6	39.5	45.4	10.5	30.0	20.0	50.0	½	1,375	Tr. C_2AS, glass.
185	4.1	41.6	40.9	13.4	38.5	16.5	45.0	½	1,395	C_2AS, glass.
186	4.1	42.5	40.9	12.5	35.8	19.2	45.0	½	1,375	All glass.
								½	1,350	C_2AS, glass.
187	4.4	41.5	43.1	11.0	31.5	21.0	47.5	½	1,350	C_2AS, glass.

TABLE 1.—*Quenching data for compositions in the* $2CaO.SiO_2$-CaO-($Na_2O+6Al_2O_3$) *plane*—Continued

No.	Composition							Time	Temperature	Phases present
	Oxides				Components					
	Na_2O	CaO	Al_2O_3	SiO_2	C_2S	CaO	(Na_2O+6Al_2O_3)			
	CA PRIMARY									
	%	%	%	%	%	%	%	hr	°C	
171	5.5	33.0	54.5	7.0	20.0	20.0	60.0	¼	1,425	CA, tr, $N_3C_1A_2$, glass.
								½	1,410	CA, $N_3C_1A_2$, glass.
172	5.1	37.2	49.9	7.8	22.5	22.5	55.0	¼	1,400	CA, glass.
173	5.5	34.4	54.5	5.6	16.0	24.0	60.0	½	1,435	Tr. CA, glass.
								¼	1,430	CA, tr. $N_3C_1A_2$, glass.
176	5.5	31.6	54.5	8.4	24.0	16.0	60.0	¼	1,450	Tr. CA, glass.
179	5.1	35.6	49.9	9.4	27.0	18.0	55.0	¼	1,400	CA, glass.
189	6.0	30.1	59.0	4.9	14.0	21.0	65.0	½	1,465	All glass.
								¼	1,455	Tr. CA, glass.
	$N_3C_1A_2$ PRIMARY									
155	5.5	40.0	54.5	------	------	40.0	60.0	½	1,470	All glass.
								¼	1,465	$N_3C_1A_2$,C_1A_2, glass.
166	6.0	35.0	59.0	------	------	35.0	65.0	¼	1,475	$N_3C_1A_2$, glass.
167	5.4	38.0	53.1	3.5	10.0	31.5	58.5	¼	1,425	All glass.
								¼	1,420	Tr. $N_3C_1A_2$, glass.
174	5.5	35.8	54.5	4.2	12.0	28.0	60.0	½	1,435	$N_3C_1A_2$, glass.
188	6.0	31.3	59.0	3.7	10.5	24.5	65.0	¼	1,475	All glass.
								¼	1,465	$N_3C_1A_2$, glass.
	C_1A_2 PRIMARY									
123	5.5	26.1	54.5	13.9	40.0	------	60.0	¼	1,550	C_1A_2, glass.
124	6.4	19.5	63.6	10.5	30.0	------	70.0	¼	1,600	Do.
126	5.1	29.3	49.9	15.7	45.0	------	55.0	¼	1,475	Do.
136	5.5	29.5	54.5	10.5	30.2	9.8	60.0	¼	1,460	Do.
177	5.5	30.2	54.5	9.8	28.0	12.0	60.0	¼	1,450	Do.
178	5.5	30.9	54.5	9.1	26.0	14.0	60.0	¼	1,440	C_1A_2, tr. CA, glass.
								¼	1,435	C_1A_2, CA, glass.
190	6.0	28.9	59.0	6.1	17.5	17.5	65.0	¼	1,460	C_1A_2, glass.
	Al_2O_3 PRIMARY									
125	6.9	16.3	68.1	8.7	25.0	------	75.0	½	1,600	α-Al_2O_3, C_1A_2, glass.
								¼	1,550	α-Al_2O_3, more C_1A_2, glass. Probably in Al_2O_3 field.

TABLE 2.—*Quenching data for compositions in the* $2CaO.SiO_2$-CaO-$(Na_2O + 3Al_2O_3)$ *plane*—Continued

No.	Composition: Oxides Na_2O	CaO	Al_2O_3	SiO_2	Components C_2S	CaO	$(Na_2O+3Al_2O_3)$	Time	Temperature	Phases present
					CaO PRIMARY					
	%	%	%	%	%	%	%	*hr*	°C	
78	8.4	50.0	41.6	------	------	50.0	50.0	½	1,510	Small amt. CaO, glass.
								½	1,500	NC_3A_2, glass.
79	8.4	48.3	41.6	1.7	5.0	45.0	50.0	½	1,500	Tr. CaO, glass.
								½	1,490	NC_3A_2, tr. CaO, glass.
90	7.6	51.2	37.4	3.8	11.0	44.0	45.0	½	1,500	CaO, glass.
								½	1,490	NC_3A_2, CaO, glass.
100	6.7	53.0	33.3	7.0	20.0	40.0	40.0	½	1,485	CaO, glass.
								½	1,465	NC_3A_2, CaO, glass.
101	5.9	54.5	29.1	10.5	30.0	35.0	35.0	½	1,450	CaO, glass.
								½	1,440	NC_3A_2, CaO, glass.
102	5.1	56.1	24.9	13.9	40.0	30.0	30.0	½	1,500	CaO, tr. C_2S, glass.
								½	1,485	CaO, C_2S, glass. Near boundary.
								½	1,450	CaO, glass.
105	5.5	55.3	27.0	12.2	35.0	32.5	32.5	¾	1,445	CaO, tr. C_2S, tr. C_2S, glass.
								1	1,440	NC_3A_2, C_2S, CaO, glass.
								1	1,445	Tr. CaO, glass.
107	5.7	53.7	28.4	12.2	35.0	30.9	34.1	½	1,440	CaO, tr. C_2S, glass.
								½	1,435	C_2S, NC_3A_2, glass.
					C_2S PRIMARY					
109	4.8	56.5	23.9	14.8	42.5	28.8	28.7	⅗	1,525	C_2S, C_2S, glass. Near boundary.
					C_2S PRIMARY					
50	1.7	58.6	8.3	31.4	90.0	------	10.0	½	1,500	C_2S, glass.
51	3.4	52.1	16.6	27.9	80.0	------	20.0	½	1,500	Do.
								½	1,375	C_2S, C_2AS, glass.
52	5.1	45.6	24.9	24.4	70.0	------	30.0	½	1,450	C_2S, glass.
								1	1,400	C_2S, C_2AS, glass.
60	1.7	66.3	8.3	23.7	67.9	22.1	10.0	½	1,500	C_2S, C_2S, small amt. glass. Probably in C_2S field.
61	3.4	59.0	16.6	21.0	60.4	19.6	20.0	½	1,500	C_2S, glass.
62	5.1	51.6	24.9	18.4	52.8	17.2	30.0	½	1,500	Do.
63	6.7	44.2	33.3	15.8	45.3	14.7	40.0	½	1,340	Do.
								½	1,325	C_2S, $N_3C_2A_3$ ss, glass.
66	7.6	40.5	37.4	14.5	41.5	13.50	45.0	½	1,350	Tr. C_2S, glass.
70	6.7	41.2	33.3	18.8	54.0	6.0	40.0	½	1,390	C_2S, glass.
								½	1,375	C_2S, tr. C_2AS, glass.
73	7.6	39.1	37.4	15.9	45.5	9.5	45.0	½	1,340	All glass.
								½	1,330	Tr. C_2S, glass.
								½	1,320	C_2S, C_2AS, glass.
88	6.0	52.1	29.7	12.2	35.0	29.2	35.8	½	1,440	Tr. C_2S, glass.
								½	1,435	C_2S, NC_3A_2, glass.
89	5.6	53.1	27.4	13.9	40.0	27.0	33.0	½	1,440	C_2S, glass.
								½	1,425	C_2S, NC_3A_2, glass.
92	7.6	43.5	37.4	11.5	33.0	22.0	45.0	½	1,375	Tr. C_2S, glass.
95	6.8	48.2	33.6	11.4	32.6	27.0	40.4	½	1,375	C_2S, glass.
								½	1,350	C_2S, NC_3A_2, glass.
103	4.2	57.6	20.8	17.4	50.0	25.0	25.0	½	1,525	C_2S, tr. C_2S, glass.
106	4.6	56.8	22.9	15.7	45.0	27.5	27.5	½	1,550	Tr. C_2S, glass.
								½	1,525	C_2S, tr. C_2S, glass.
					NC_3A_2 PRIMARY					
74	9.3	45.0	45.7	------	------	45.0	55.0	½	1,470	NC_3A_2, glass.
75	9.3	43.4	45.7	1.6	4.5	40.5	55.0	½	1,450	All glass.
								½	1,445	NC_3A_2, small amt. $N_3C_2A_3$, glass. Near boundary.
80	8.4	46.5	41.6	3.5	10.0	40.0	50.0	½	1,460	All glass.
								½	1,455	NC_3A_2, glass.
81	8.4	44.8	41.6	5.2	15.0	35.0	50.0	½	1,425	All glass.
								½	1,420	NC_3A_2, glass.
85	7.4	49.0	36.6	7.0	20.0	36.0	44.0	½	1,460	Tr. NC_3A_2, glass.
87	6.5	51.0	32.0	10.5	30.0	31.5	38.5	¼	1,450	All glass.
								½	1,440	NC_3A_2, glass.

TABLE 2.—*Quenching data for compositions in the* $2CaO.SiO_2$-CaO-$(Na_2O+3Al_2O_3)$ *plane*—Continued

No.	Composition							Time	Temperature	Phases present
	Oxides				Components					
	Na_2O	CaO	Al_2O_3	SiO_2	C_2S	CaO	$(Na_2O+3Al_2O_3)$			
	C_3A_3 PRIMARY									
	%	%	%	%	%	%	%	*hr*	°C	
91	7.6	45.4	37.4	9.6	27.5	27.5	45.0	¼	1,375	All glass.
								½	1,360	Tr. C_3A_3 glass.
								¾	1,355	C_3A_3, NC_3A_3, glass.
93	7.6	44.4	37.4	10.6	30.3	24.7	45.0	¼	1,360	C_3A_3, tr. C_2S, glass.
								½	1,345	C_3A_3, C_2S, $N_2C_3A_3$ ss, glass.
								¾	1,335	All crystalline.
94	7.8	44.4	38.4	9.4	26.9	26.9	46.2	¼	1,370	All glass.
								½	1,360	C_3A_3, glass.
	C_3AS PRIMARY									
53	6.7	39.1	33.3	20.9	60.0	.....	40.0	¼	1,430	All glass.
								½	1,420	C_3AS, glass.
54	8.4	32.6	41.6	17.4	50.0	.....	50.0	¼	1,420	All glass.
								½	1,415	C_3AS, glass.
59	7.6	35.8	37.4	19.2	55.0	.....	45.0	¼	1,435	All glass.
								½	1,425	C_3AS, glass.
72	7.6	37.7	37.4	17.3	49.5	5.5	45.0	¼	1,395	All glass.
								½	1,385	C_3AS, glass.
	$N_2C_3A_3$ SOLID SOLUTION PRIMARY									
55	10.1	26.1	49.9	13.9	40.0	.....	60.0	½	1,500	Tr. $N_2C_3A_3$ ss, glass.
56	11.8	19.5	58.2	10.5	30.0	.....	70.0	¼	1,565	Tr. $N_2C_3A_3$ ss, glass.
								½	1,525	$N_2C_3A_3$ ss, tr. "unstable" C_3A_3 glass.
58	9.3	29.3	45.7	15.7	45.0	.....	55.0	¼	1,425	Tr. $N_2C_3A_3$ ss, glass.
64	8.4	36.8	41.6	13.2	33.7	12.3	50.0	¼	1,405	All glass.
								½	1,400	Tr. $N_2C_3A_3$ ss, glass.
65	10.1	29.5	49.9	10.5	30.2	9.8	60.0	¼	1,550	All glass.
								½	1,525	$N_2C_3A_3$ ss, glass.
71	8.4	34.3	41.6	15.7	45.0	5.0	50.0	¼	1,400	All glass.
								½	1,375	Tr. $N_2C_3A_3$ ss, glass.
76	9.3	41.9	45.7	3.1	9.0	36.0	55.0	½	1,410	$N_2C_3A_3$ss , glass.
77	9.3	37.1	45.7	7.9	22.5	22.5	55.0	¼	1,400	$N_2C_3A_3$ ss, NC_3A_3, glass.
								½	1,450	$N_2C_3A_3$ ss, glass.
82	8.4	43.0	41.6	7.0	20.0	30.0	50.0	¼	1,400	Tr. $N_2C_3A_3$ ss, glass.
83	8.4	41.3	41.6	8.7	25.0	25.0	50.0	¼	1,375	$N_2C_3A_3$ ss, C_3A_3, glass.
								½	1,410	Tr. $N_2C_3A_3$ ss, glass.
	Al_2O_3 PRIMARY									
57	13.5	13.0	66.5	7.0	20.0	.....	80.0	¼	1,600	βAl_2O_3, glass.
								½	1,575	βAl_2O_3, $N_2C_3A_3$ ss, glass.
								¾	1,550	βAl_2O_3, $N_2C_3A_3$ ss, "unstable" C_3A_3 glass.

TABLE 3.—*Quenching data for compositions in the system* $2CaO.SiO_2$-CaO-$Na_2O.Al_2O_3$

No.	Composition							Time	Temperature	Phases present
	Oxides				Components					
	Na_2O	CaO	Al_2O_3	SiO_2	C_2S	CaO	NA			
					CaO PRIMARY					
	%	%	%	%	%	%	%	hr	°C	
37	3.8	68.0	6.2	22.0	63.0	27.0	10.0	½	1,550	CaO, C_2S, glass.
								1	1,500	Do.
39	7.6	60.5	12.4	19.5	56.0	24.0	20.0	½	1,550	CaO, tr. C_2S, glass.
								½	1,500	CaO, tr. NA, glass.
41	11.3	52.9	18.7	17.1	49.0	21.0	30.0	½	1,550	Small amt. CaO, quench growths, glass.
								½	1,500	CaO, NA, quench growths, glass.
					C_2S PRIMARY					
18	7.6	59.0	12.4	21.0	60.4	19.6	20.0	½	1,600	C_2S, quench growths, glass.
								½	1,550	C_2S, small amt. C_2S, glass.
20	5.7	62.6	9.3	22.4	64.1	20.9	15.0	½	1,550	C_2S, small amt. C_2S, tr. CaO, glass.
								1	1,500	C_2S, small amt. C_2S and CaO, glass.
					C_2S PRIMARY					
12	3.8	58.6	6.2	31.4	90.0	------	10.0	½	1,500	C_2S, small amt. glass.
13	7.6	52.1	12.4	27.9	80.0	------	20.0	½	1,550	C_2S, glass.
14	11.3	45.6	18.7	24.4	70.0	------	30.0	½	1,550	Tr. C_2S, quench growths, glass.
24	3.8	61.8	6.2	28.2	81.0	9.0	10.0	¼	1,600	C_2S, C_2S, tr. CaO, glass.
								½	1,550	C_2S, tr. CaO, glass.
25	7.6	54.9	12.4	25.1	72.0	8.0	20.0	1	1,500	C_2S, glass.
					C_2S PRIMARY					
26	11.3	48.0	18.7	22.0	63.0	7.0	30.0	1	1,500	C_2S, glass.
28	13.2	42.3	21.8	22.7	65.0	------	35.0	¼	1,500	Tr. C_2S, glass.
								½	1,410	C_2S, quench growths, glass.
								½	1,400	All crystalline.
								¼	1,475	Tr. C_2S, glass.
29	14.2	40.7	23.3	21.8	62.5	------	37.5	½	1,410	C_2S, NA, quench growths. Evidence of melting.
								½	1,400	All crystalline.
32	7.6	57.7	12.4	22.3	64.0	16.0	20.0	¼	1,600	C_2S, CaO, quench growths, glass.
34	5.7	61.3	9.3	23.7	68.0	17.0	15.0	¼	1,600	C_2S, CaO, glass.
35	9.4	54.1	15.6	20.9	60.0	15.0	25.0	¼	1,550	C_2S, glass.
36	4.7	63.1	7.8	24.4	70.0	17.5	12.5	½	1,550	C_2S, small amt. C_2S and CaO, glass.
					NA PRIMARY					
15	15.1	39.1	24.9	20.9	60.0	------	40.0	¼	1,460	All glass.
								½	1,450	NA, glass.
								½	1,415	Small amt. glass.
								½	1,400	All crystalline.
16	18.9	32.6	31.1	17.4	50.0	------	50.0	½	1,550	NA, quench growths, glass.
19	11.3	51.6	18.7	18.4	52.8	17.2	30.0	½	1,550	Glass, quench growths.
								½	1,500	NA, quench growths, glass.
								¾	1,400	NA, CaO, quench growths, glass.
								1	1,350	All crystalline.
27	15.1	41.2	24.9	18.8	54.0	6.0	40.0	¼	1,450	NA, glass.
30	13.2	44.6	21.8	20.4	58.5	6.5	35.0	¼	1,450	Small amt. NA, glass.
								½	1,500	NA, glass.
33	11.3	50.5	18.7	19.5	56.0	14.0	30.0	1	1,360	NA, C_2S, glass.
								1	1,350	All crystalline.

TABLE 4.—*Quenching data for additional compositions located between the* $2CaO.SiO_2$-CaO-$(Na_2O+6Al_2O_3)$ *and* $2CaO.SiO_2$-CaO-$(Na_2O+3Al_2O_3)$ *planes*

No.	Composition								Time	Temperature	Phases present
	Oxides				Components						
	Na_2O	CaO	Al_2O_3	SiO_2	C_2S	CaO	$(Na_2O+6Al_2O_3)$	$(Na_2O+3Al_2O_3)$			
	%	%	%	%	%	%	%	%	hr	°C	
200	4.4	53.7	29.7	12.2	35.0	30.9	17.1	17.0	½	1,435	C_2S, glass.
									½	1,430	C_2S, small amt. NC_3A_2, glass.
201	3.8	53.7	30.3	12.2	35.0	30.9	25.6	8.5	½	1,425	C_2S, glass.
									½	1,420	C_2S, tr. NC_3A_2, glass.
									½	1,415	C_2S, NC_3A_2, glass.
									¼	1,450	C_2S, CaO, tr. C_3S, glass.
202	4.2	55.3	28.3	12.2	35.0	32.5	16.3	16.2	¼	1,440	C_2S, small amt. NC_3A_2, tr. C_3S, glass. C_3A not observed.
									¼	1,435	C_2S, NC_3A_2, glass. C_3A not observed.
203	3.6	55.3	28.9	12.2	35.0	32.5	24.4	8.1	¼	1,445	C_2S, glass.
									¼	1,440	C_2S, C_3A, glass.
									¼	1,435	C_2S, C_3A, NC_3A_2, glass.
									¼	1,445	All glass.
204	3.9	54.4	31.1	10.5	30.0	35.0	26.3	8.7	¼	1,440	NC_3A_2, possibly C_3A, glass.
									¼	1,435	NC_3A_2, C_2S, possibly C_3A, glass.
205	3.8	55.3	30.6	10.3	29.5	36.0	25.9	8.6	¼	1,450	Tr. C_3S, tr. CaO, glass.
									¼	1,445	C_3S, tr. CaO, glass.
									¼	1,435	C_2S, NC_3A_2, probably C_3A, glass.
206	3.5	55.2	31.0	10.3	29.5	36.0	30.2	4.3	¼	1,450	Small amt. C_3A, tr. C_2S, tr. CaO, glass.
									½	1,440	C_2S, C_3A, C_3S, NC_3A_2, glass.
									½	1,430	C_2S, C_3A, NC_3A_2, glass.

The phase equilibria in the various composition planes studied can be represented by diagrams that resemble those used for ternary systems. However, it must be borne in mind that the information which can be obtained from the diagram of an arbitrary plane through a quaternary system is in general much more limited than that which can be derived from the diagram of a true ternary system. The course of crystallization upon cooling a given melt can be followed on the diagram of a ternary system, but in general this is not possible for a plane through a quaternary system. This is due to the fact that the liquids and crystalline phases in equilibrium at various temperatures usually have compositions outside of the original plane.

When a plane is passed through the tetrahedron representing a quaternary system, it intersects the boundary surfaces defining the various primary phase volumes within the tetrahedron. This gives a diagram showing a field or region for each primary phase as a result of the intersection of the corresponding phase volume. Diagrams of this type are shown in figures 3, 4, and 5, for the planes studied in this investigation. In order that the relation to the ternary system CaO-Al_2O_3-SiO_2 may be more evident, the corresponding portion of this system is reproduced from Rankin and Wright in figure 2. The diagrams of figures 2, 3, 4, and 5 thus form a series that illustrates the effect of substituting successively increasing amounts of Na_2O for Al_2O_3 in the system CaO-Al_2O_3-SiO_2. As mentioned previously, the ratio of Na_2O to Al_2O_3 remains constant in any particular plane.

As the calcium silicates $2CaO.SiO_2$ and $3CaO.SiO_2$ are major crystalline phases of portland cement clinker, the interpretation of

the system Na_2O-CaO-Al_2O_3-SiO_2 in relation to cement is simplified by keeping $2CaO.SiO_2$ and CaO at two of the apexes of each composition plane.

2. THE PLANE $2CaO.SiO_2$-CaO-($Na_2O+6Al_2O_3$)

The diagram of this plane is shown in figure 3, and is based on the data of table 1. There is considerable resemblance to the corresponding part of the CaO-Al_2O_3-SiO_2 system (fig. 2), with the difference that two additional crystalline phases have made their appearance. These are the Na_2O-bearing compounds, $Na_2O.8CaO.3Al_2O_3$ and $2Na_2O.3CaO.5Al_2O_3$. A total of 11 primary phase regions are indicated. The others are those of CaO, $3CaO.SiO_2$, $2CaO.SiO_2$, $3CaO.Al_2O_3$, $5CaO.3Al_2O_3$, $2CaO.Al_2O_3.SiO_2$, $CaO.Al_2O_3$, $3CaO.5Al_2O_3$, and α-Al_2O_3.

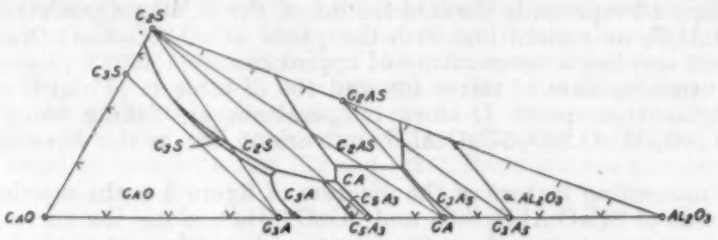

FIGURE 2.—*Part of system* CaO-Al_2O_3-SiO_2.

The area in which $Na_2O.8CaO.3Al_2O_3$ is the primary phase is seen to be very narrow. In the neighborhood of points A and B (fig. 3) the fields of four crystalline phases meet nearly in a single point. The composition where this actually occurs is the invariant point for $2CaO.SiO_2$, $3CaO.Al_2O_3$, $5CaO.3Al_2O_3$, $Na_2O.8CaO.3Al_2O_3$, and liquid. It is located slightly outside the plane of the diagram in the direction of lower Na_2O/Al_2O_3 ratios. The composition of this point, designated invariant point 4, is estimated to be 3.5 percent Na_2O, 50.2 percent CaO, 37.6 percent Al_2O_3, and 8.7 percent SiO_2. The temperature is 1,365 °±10° C. It is not a eutectic. Mix 154 of table 1 is near its composition. The temperature of 1,365° C for point 4 is worthy of note, as it is higher, rather than lower, than the corresponding ternary invariant point in the system CaO-Al_2O_3-SiO_2. The $2CaO.SiO_2$-$3CaO.Al_2O_3$-$5CaO.3Al_2O_3$ eutectic in the CaO-Al_2O_3-SiO_2 system is at 1,335° C [4]. The explanation for this appears to be the fact that the $5CaO.3Al_2O_3$ in the quaternary system is not

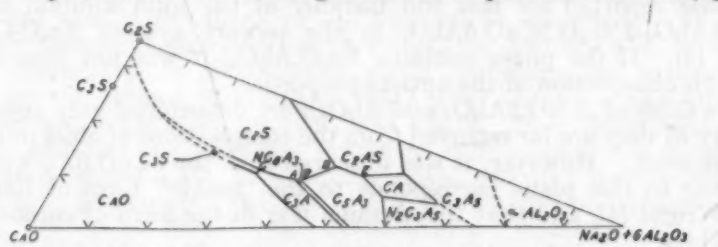

FIGURE 3.—*Composition plane* $2CaO.SiO_2$-CaO-($Na_2O+6Al_2O_3$).

pure, but contains Na_2O in solid solution. An analogous situation was found by Brownmiller and Bogue in the ternary system Na_2O-CaO-Al_2O_3 [5].

The important invariant point, not a eutectic, where $2CaO.SiO_2$, $3CaO.SiO_2$, $3CaO.Al_2O_3$, and $Na_2O.8CaO.3Al_2O_3$ are in equilibrium with liquid, designated invariant point 1, also lies outside of this plane, but in the direction of higher Na_2O/Al_2O_3 ratios. Its composition and temperature were established by determinations on supplementary mixtures and will be presented later in this report. Point C of figure 3 represents the intersection of the $2CaO.SiO_2$-$3CaO.SiO_2$-$3CaO.Al_2O_3$ univariant line with the plane $2CaO.SiO_2$-CaO-$(Na_2O+6Al_2O_3)$, and has a temperature of approximately 1,450° C, based on the quenching data of mixes 198 and 199 of table 1. Point C must be higher than point 1, since temperatures are falling along the $2CaO.SiO_2$-$3CaO.SiO_2$-$3CaO.Al_2O_3$ univariant line in the direction of point 1.

An interesting feature of the diagram of figure 3 is the meeting of the fields of $2CaO.Al_2O_3.SiO_2$ and $5CaO.3Al_2O_3$ along the curve DE. This is unexpected as these two compounds are incompatible in the system CaO-Al_2O_3-SiO_2, as is evident in figure 2. One possible explanation for this behavior is the taking up in solid solution of about 1 percent of Na_2O by the $5CaO.3Al_2O_3$, as reported by Brownmiller and Bogue [5]. However, such an explanation is not necessarily the true one, as the mere presence of Na_2O as a fourth component may be sufficient to cause both $2CaO.Al_2O_3.SiO_2$ and $5CaO.3Al_2O_3$ to be mutually stable in the presence of liquid.

The primary phase crystallizing in the region labeled $2Na_2O.3CaO.5Al_2O_3$ in figure 3 has optical properties corresponding to those reported for this end member of the solid solution series $Na_2O.Al_2O_3$-$2Na_2O.3CaO.5Al_2O_3$ in the ternary system Na_2O-CaO-Al_2O_3 [5]. If the phase contains $Na_2O.Al_2O_3$, it was not detectable through observation of the optical properties.

The fields of $3CaO.5Al_2O_3$ and Al_2O_3 were determined only approximately as they are far removed from the compositions of chief interest in this work. However, it was observed that the $3CaO.5Al_2O_3$ crystallizing in this plane corresponds to the "stable" form of Rankin and Wright [4], and that the alumina was in the form of corundum, or αAl_2O_3.

3. THE PLANE $2CaO.SiO_2$-CaO-$(Na_2O+3Al_2O_3)$

Figure 4 shows the equilibrium diagram for this plane. It is constructed from the data of table 2. A number of marked changes in the primary phase regions have occurred in comparison to the preceding plane. Eight crystalline phases are indicated on the diagram, as follows: CaO, $3CaO.SiO_2$, $2CaO.SiO_2$, $Na_2O.8CaO.3Al_2O_3$, $5CaO.3Al_2O_3$, $2CaO.Al_2O_3.SiO_2$, $2Na_2O.3CaO.5Al_2O_3$ solid solution, and β-Al_2O_3.

The composition of the compound $Na_2O.8CaO.3Al_2O_3$ is located on the CaO-$(Na_2O+3Al_2O_3)$ side, but as this phase melts incongruently to CaO and liquid, it is in the CaO primary phase area. The field of $Na_2O.8CaO.3Al_2O_3$ is displaced away from the CaO apex, and extends from the CaO-$(Na_2O+3Al_2O_3)$ side toward the $2CaO.SiO_2$ apex. It may be observed that $Na_2O.8CaO.3Al_2O_3$exists in equilibrium with $2CaO.SiO_2$ and liquids whose compositions lie on the curve FG. The

perimental results indicate that the $3CaO.SiO_2$ field narrows to a point not indicated in figure 4, slightly to the left of point F, since $3CaO.SiO_2$ and $Na_2O.8CaO.3Al_2O_3$ were not observed to exist together in equilibrium with liquid in any of the quenched charges. It is probable, therefore, that $3CaO.SiO_2$ crystallizing from compositions in this plane decomposes upon cooling into $2CaO.SiO_2$ and CaO just before the crystallization of $Na_2O.8CaO.3Al_2O_3$ begins.

It follows from the near meeting of the fields for the four compounds CaO, $3CaO.SiO_2$, $2CaO.SiO_2$, and $Na_2O.8CaO.3Al_2O_3$, that an invariant point for these phases and liquid must be located near point F, but at a slightly smaller Na_2O/Al_2O_3 ratio. Point F has a composition very close to that of mix 107, table 2, and the invariant point, which will be referred to as point 3, is estimated to have the following composition: 5.0 percent Na_2O, 54.1 percent CaO, 28.6 percent Al_2O_3, and 12.3 percent SiO_2. It has a temperature estimated to be 1,445° ± 10° C, based on data for mixes 105 and 107. Point 3 is not a eutectic.

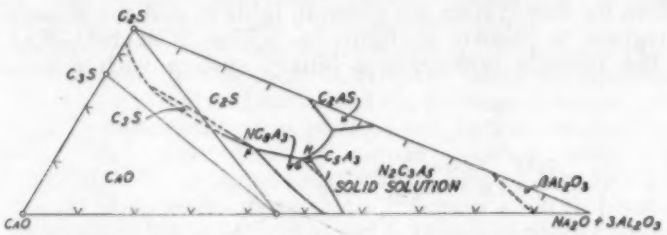

FIGURE 4.—*Composition plane* $2CaO.SiO_2$–CaO–$(Na_2O+3Al_2O_3)$.

It will be noted that the primary phase area of $5CaO.3Al_2O_3$ is very small, and that if the plane of the diagram be imagined to swing gradually toward higher Na_2O/Al_2O_3 ratios, the points G, H, and I would converge on a single point which represents the invariant point for the phases $2CaO.SiO_2$, $Na_2O.8CaO.3Al_2O_3$, $5CaO3Al_2O_3$, $2Na_2O.3CaO.5Al_2O_3$ solid solution, and liquid. It is designated as point 5, and has the following estimated composition: 8.0 percent Na_2O, 46.1 percent CaO, 35.5 percent Al_2O_3, and 10.4 percent SiO_2. Point 5 must be a eutectic as it lies within the composition tetrahedron formed by $2CaO.SiO_2$, $Na_2O.8CaO.3Al_2O_3$, $5CaO.3Al_2O_3$, and $2Na_2O.3CaO.5Al_2O_3$. It is a eutectic, regardless of the amount of $Na_2O.Al_2O_3$ in solid solution in $2Na_2O.3CaO.5Al_2O_3$. The temperature of point 5, based on data for mix 93, is estimated to be 1,340° ±10° C.

The composition of point 5 lies close to the $2CaO.SiO_2$-$Na_2O.8CaO.3Al_2O_3$-$2Na_2O.3CaO.5Al_2O_3$ join, which means that the percentage of $5CaO.3Al_2O_3$ at complete crystallization will be very small, provided that the compounds are pure. On this basis the phase composition was calculated to be 29.8 percent $2CaO.SiO_2$, 34.8 percent $Na_2O.8CaO.3Al_2O_3$, 34.8 percent $2Na_2O.3CaO.5Al_2O_3$ and 0.6 percent $5CaO.3Al_2O_3$. However, it is known that the $5CaO.3Al_2O_3$ contains about 1 percent Na_2O in solid solution, which would increase the $5CaO.3Al_2O_3$ to 1.0 percent. Moreover, if the $2Na_2O.3CaO.5Al_2O_3$ in equilibrium at the eutectic temperature contains $Na_2O.Al_2O_3$ in solid solution, as is indicated by a lowering of the mean index of refraction from 1.592 to about 1.587, the proportion of $5CaO.3Al_2O_3$ will be

further increased. Since the actual amount of this latter solid solution is not known, it is not possible to calculate the exact phase composition resulting from complete crystallization of a melt of the composition of point 5.

The compound $3CaO.5Al_2O_3$ was not observed as a primary phase in the plane $2CaO.SiO_2$-CaO-$(Na_2O+3Al_2O_3)$. However, the form of $3CaO.5Al_2O_3$ termed "unstable" by Rankin and Wright [4] occurs as a secondary phase in mix 56, and as a tertiary phase in mix 57. It appears to be in a state of stable equilibrium in these charges. The crystals have an index of refraction of about 1.67 and a low double refraction.

The form of Al_2O_3 which crystallizes from mixtures in this plane is βAl_2O_3, which appears to be in stable equilibrium. The optical properties agree with those reported by Brownmiller and Bogue [5].

4. THE SYSTEM $2CaO.SiO_2$-CaO-$Na_2O.Al_2O_3$

The data for this system are given in table 3, and the phase equilibrium diagram is shown in figure 5. The $2CaO.SiO_2$-$Na_2O.Al_2O_3$ side of the triangle represents a binary system with a eutectic at

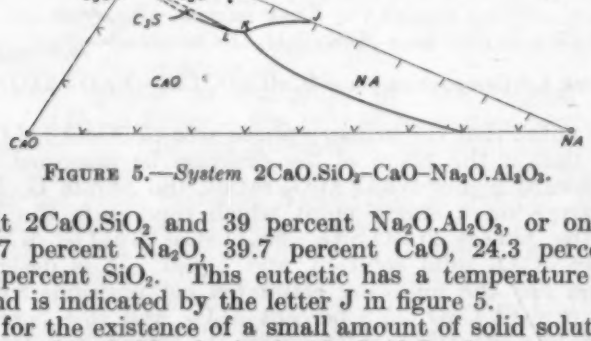

FIGURE 5.—*System* $2CaO.SiO_2$–CaO–$Na_2O.Al_2O_3$.

61 percent $2CaO.SiO_2$ and 39 percent $Na_2O.Al_2O_3$, or on an oxide basis, 14.7 percent Na_2O, 39.7 percent CaO, 24.3 percent Al_2O_3, and 21.3 percent SiO_2. This eutectic has a temperature of 1,405° ±10°C and is indicated by the letter J in figure 5.

Except for the existence of a small amount of solid solution in the $2CaO.SiO_2$, and probably also in the $Na_2O.Al_2O_3$, the system $2CaO.SiO_2$-CaO-$Na_2O.Al_2O_3$ is ternary. Due to experimental difficulties the phase relations as determined are not considered to be as accurate as those obtained with mixture of lower Na_2O/Al_2O_3 ratios. Not only is the rate of volatilization of Na_2O higher, but the time required for the attainment of equilibrium, particularly in charges containing crystalline $3CaO.SiO_2$, is much increased. This compound was found to form extremely slowly by reaction of $2CaO.SiO_2$ and CaO. Increasing the temperature does not appreciably accelerate the combination as the CaO tends to form large, unreactive crystals. Consequently, for charges where $3CaO.SiO_2$ was expected as a stable phase, the original mixes were prepared with $3CaO.SiO_2$ instead of $2CaO.SiO_2$ and CaO. In this way it is believed that a nearer approach to equilibrium was attained.

The results indicate that the phase equilibrium relations are in general as shown in figure 5. Point K is a ternary eutectic for $2CaO.SiO_2$, CaO, $Na_2O.Al_2O_3$, and liquid. It occurs at a compound composition of approximately 56 percent $2CaO.SiO_2$, 16 percent CaO,

and 28 percent $Na_2O.Al_2O_3$, or in terms of oxides, 11 percent Na_2O, 42 percent CaO, 17 percent Al_2O_3, and 20 percent SiO_2. The temperature, based on data for mix 33, table 3, is $1{,}355 \pm 10°C$.

It will be noticed that the primary field of $3CaO.SiO_2$ in figure 5 is drawn as narrowing to a point at L. The basis for this is the fact that $3CaO.SiO_2$ was never observed in charges containing crystalline $Na_2O.Al_2O_3$. The solid phases in equilibrium with $Na_2O.Al_2O_3$ were always $2CaO.SiO_2$ and CaO. Accordingly, point L represents an invariant point for $3CaO.SiO_2$, $2CaO.SiO_2$, CaO, and liquid, and indicates a lower temperature limit of stability for $3CaO.SiO_2$ in this system. Thus $3CaO.SiO_2$ should decompose into $2CaO.SiO_2$ and CaO when the temperature is lowered below that of point L. A partial decomposition of $3CaO.SiO_2$ was observed for several charges in the system, but attempts to locate the temperature of point L were not successful because of the slowness of the reaction. When once formed, $3CaO.SiO_2$ tends to persist in the melt, although held at constant temperature for many hours. According to the phase diagram, point L should have a temperature above 1,355°C.

This behavior of $3CaO.SiO_2$ is interesting in the light of the work of Carlson [11], who found that $3CaO.SiO_2$ tends to dissociate into $2CaO.SiO_2$ and CaO when heated at temperatures between 1,000° and 1,300° C. The possibility was pointed out by Jänecke [12] that with a suitable third component, a ternary system with CaO and $2CaO.SiO_2$ might be obtained in which the field of $3CaO.SiO_2$ narrows to a point at both ends, meeting the boundary curve between CaO and $2CaO.SiO_2$ at an invariant point. It is interesting to note that Eitel has since reported that such a situation exists in the system $2CaO.SiO_2$-CaO-CaF_2 [13]. It appears from the present work that $Na_2O.Al_2O_3$ also is such a component. The theoretical considerations involved in a limited temperature range of stability for $3CaO.SiO_2$ are discussed by Lea and Parker [7].

The $2CaO.SiO_2$ phase which was observed in the binary system $2CaO.SiO_2$-$Na_2O.Al_2O_3$ has the optical properties of the β form. This was confirmed by X-ray diffraction patterns.[2] If there is any solid solution in the β-$2CaO.SiO_2$ it must be very small. However, in several compositions in the interior of the system the $2CaO.SiO_2$ phase corresponded in properties to one of the α-$2CaO.SiO_2$ solid solutions described in a previous paper [6]. The extent of this solid solution was not determined and the relation which it may bear to the stability of the $3CaO.SiO_2$ has not been investigated. A somewhat similar situation with regard to solid solution appears to exist for the $Na_2O.Al_2O_3$. Along the join $2CaO.SiO_2$-$Na_2O.Al_2O_3$ the properties agree with those of the pure compound, but in compositions containing added CaO a slight increase in the indices of refraction indicate that the phase may be one in the solid solution series $Na_2O.Al_2O_3$-$2Na_2O.3CaO.5Al_2O_3$.

5. ADDITIONAL COMPOSITIONS LOCATED BETWEEN THE $2CaO.SiO_2$-CaO-($Na_2O+6Al_2O_3$) AND $2CaO.SiO_2$-CaO-($Na_2O+3Al_2O_3$) PLANES

To locate invariant point 1 at which $2CaO.SiO_2$, $3CaO.SiO_2$, $3CaO.Al_2O_3$, and $Na_2O.8CaO.3Al_2O_3$ are in equilibrium with liquid, it became necessary to investigate a number of mixtures not included in

[2] All X-ray patterns were made by H. F. McMurdie.

the original composition planes. The additional data are given in table 4. They show that mix 206 is approximately the composition of point 1. The phases, $2CaO.SiO_2$, $3CaO.SiO_2$, $3CaO.Al_2O_3$, $Na_2O.8CaO.3Al_2O_3$, and glass, were identified in a charge of mix 206 quenched at 1,440° C. The composition is therefore placed at 3.5 percent Na_2O, 55.2 percent CaO, 31.0 percent Al_2O_3, and 10.3 percent SiO_2, and the temperature at 1,440° ±10° C. Point 1 is not a eutectic, and therefore a mixture of this composition does not become completely crystalline on cooling when 1,440° is reached, but continues to contain liquid down to 1,340°, the temperature of point 5, the only quaternary eutectic in this part of the system.

One other quaternary invariant point, not a eutectic, is located near point 1. This is the point for CaO, $3CaO.SiO_2$, $3CaO.Al_2O_3$, $Na_2O.8CaO.3Al_2O_3$, and liquid. Using figures 3 and 4, it is estimated by interpolation that this point, referred to as point 2, has a composition only slightly higher in CaO and lower in SiO_2 than point 1, or approximately 3.5 percent Na_2O, 56.0 percent CaO, 31.0 percent Al_2O_3, and 9.5 percent SiO_2. According to theory, point 2 must have a higher temperature than point 1, but it can be only slightly higher, since both points must have temperatures below that of point 3, which has been determined as 1,445° ±10° C. To indicate this relationship point 2 is accordingly given the temperature 1,442° ±10° C.

IV. DISCUSSION

1. CRYSTALLIZATION IN THE SYSTEM

For purposes of discussion and comparison, the data obtained for the five quaternary invariant points determined in this investigation are grouped together in table 5. Of these only point 5 is a eutectic. The others are reaction points, and melts of these compositions upon complete equlibrium crystallization consist of sets of solid phases differing from those in equilibrium with liquid at the respective invariant points. A melt of the composition of point 2 when cooled under equilibrium conditions becomes completely crystalline at 1,365° C, the temperature of point 4, and consists of $2CaO.SiO_2$, $3CaO.Al_2O_3$, $5CaO.3Al_2O_3$, and $Na_2O.8CaO.3Al_2O_3$. Melts having compositions of points 1, 3, and 4 become completely crystalline at 1,340° C, the temperature of point 5, and consist of $2CaO.SiO_2$, $5CaO.3Al_2O_3$, $Na_2O.8CaO.3Al_2O_3$, and $2Na_2O.3CaO.5Al_2O_3$ solid solution.

The existence of invariant point 1 shows that the compounds $2CaO.SiO_2$, $3CaO.SiO_2$, $3CaO.Al_2O_3$, and $Na_2O.8CaO.3Al_2O_3$ may be final products of crystallization in mixtures of Na_2O, CaO, Al_2O_3, and SiO_2 approaching in composition that of portland cement clinker. Such mixtures are located in the tetrahedron formed by the compositions of the four solid phases in equilibrium at point 1. When these mixtures are heated, the first stable liquid is produced at 1,440° C, and this liquid has the composition of point 1. Conversely, when melts in this tetrahedron are cooled under equilibrium conditions, the last liquid (of the composition of point 1) disappears at 1,440° C.

TABLE 5.—*Quaternary invariant points in the system* Na_2O-CaO-Al_2O_3-SiO_2

Point	Temperature	Solid phases	Composition			
			Na_2O	CaO	Al_2O_3	SiO_2
	° C ±10°		%	%	%	%
1	1,440	C_2S, C_3S, C_3A, NC_3A_3	3.5	55.2	31.0	10.3
2	1,442	CaO, C_3S, C_3A, NC_3A_3	3.5	56.0	31.0	9.5
3	1,445	CaO, C_3S, C_2S, NC_3A_3	5.0	54.1	28.6	12.3
4	1,365	C_2S, C_3A, C_3A_2, NC_3A_3	3.5	50.2	37.6	8.7
5	1,340	C_2S, C_3A_2, NC_3A_3, $N_2C_3A_3$	8.0	46.1	35.5	10.4

The various possible courses of crystallization are many and complex for mixtures in the $2CaO.SiO_2$-$3CaO.SiO_2$-$3CaO.Al_2O_3$-Na_2O.-$8CaO.3Al_2O_3$ tetrahedron. However, the liquids of all such compositions eventually arrive at point 1 as the melt is cooled. In some melts the liquid composition passes through point 2 before point 1 is reached. $3CaO.Al_2O_3$ and $Na_2O.8CaO.3Al_2O_3$ do not crystallize out together until either point 2 or point 1 is reached. In melts whose course of crystallization passes through point 2, $3CaO.Al_2O_3$ appears before $Na_2O.8CaO.3Al_2O_3$ when the Na_2O/Al_2O_3 ratio of the original mixture is less than that of point 2. Likewise, in melts whose course of crystallization does not pass through point 2, but arrives at point 1 directly, $3CaO.Al_2O_3$ crystallizes before $Na_2O.8CaO.3Al_2O_3$ when the Na_2O/Al_2O_3 ratio of the original mixture is less than that of point 1. Since points 1 and 2 have the same Na_2O/Al_2O_3 ratio within experimental error, this ratio determines whether $3CaO.Al_2O_3$ or $Na_2O.8CaO.$-$3Al_2O_3$ is first to crystallize on cooling the melts under discussion. On a weight basis, the Na_2O/Al_2O_3 ratio of points 1 and 2 is 0.11. Therefore in mixtures which have Na_2O/Al_2O_3 ratios less than 0.11, $3CaO.Al_2O_3$ appears before $Na_2O.8CaO.3Al_2O_3$, whereas in those which have Na_2O/Al_2O_3 ratios greater than 0.11, $Na_2O.8CaO.3Al_2O_3$ precedes $3CaO.Al_2O_3$.

2. SOLID SOLUTIONS

Although it has been demonstrated by the present work that $3CaO.Al_2O_3$ and $Na_2O.8CaO.3Al_2O_3$ may exist together as distinct phases in stable equilibrium with liquid at the invariant point where $2CaO.SiO_2$ and $3CaO.SiO_2$ are also present, the data thus far reported do not give any information concerning the relation between these compounds below the temperature of liquid formation. Previous data of this laboratory have indicated that, with slow cooling or prolonged heating at lower temperatures, $3CaO.Al_2O_3$ and $Na_2O.8CaO.3Al_2O_3$ form a complete solid solution series in the ternary system Na_2O-CaO-Al_2O_3 [14]. In order to test the possibility of the formation of similar solid solutions in the quaternary system, a mix was made up which was calculated to have the following potential compound composition: 39.9 percent $3CaO.Al_2O_3$, 40.1 percent $Na_2O.8CaO.3Al_2O_3$, and 20.0 percent $2CaO.SiO_2$. A sample of this mixture was given two 30-minute heatings at 1,425° C, with intermediate grinding, and was examined microscopically and a portion taken for X-ray analysis.

Under the microscope the charge appeared to consist of a large amount of material having a mottled gray interference color, along with a small amount of $2CaO.SiO_2$. No glass was detected. The double refraction of the predominant material was appreciably less

than that of $Na_2O.8CaO.3Al_2O_3$. No distinct grains of either $3CaO.Al_2O_3$ or $Na_2O.8CaO.3Al_2O_3$ could be identified. Although the double refraction did not appear to be entirely uniform, there was definite evidence that a reaction had taken place to produce a phase or phases that were neither pure $3CaO.Al_2O_3$ nor pure $Na_2O.8CaO.3Al_2O_3$.

Unfortunately, the powder diffraction patterns of both $3CaO.Al_2O_3$ and $Na_2O.8CaO.3Al_2O_3$ are very similar. By comparing the data of McMurdie [15] for $3CaO.Al_2O_3$ with that of Brownmiller and Bogue [5] for $Na_2O.8CaO.3Al_2O_3$, only minor differences are seen. The pattern for the mixture of $3CaO.Al_2O_3$, $Na_2O.8CaO.3Al_2O_3$ and $2CaO.SiO_2$ mentioned in a previous paragraph, is also very similar, but resembles that of $Na_2O.8CaO.3Al_2O_3$ more than that of $3CaO.Al_2O_3$. It contains a number of pairs of lines located close together. Such pairs occur also with $Na_2O.8CaO.3Al_2O_3$, but to a lesser extent, while in the pattern of $3CaO.Al_2O_3$ only single lines occur. In table 6 are shown the interplanar spacings calculated for the charge prepared from the mixture, in comparison to the more important lines of $3CaO.Al_2O_3$ and $Na_2O.8CaO.3Al_2O_3$.

TABLE 6.—*Powder diffraction patterns of* $3CaO.Al_2O_3$, $Na_2O.8CaO.3Al_2O_3$, *and a mixture of* $3CaO.Al_2O_3$, $Na_2O.8CaO.3Al_2O_3$, *and* $2CaO.SiO_2$ *after heating to 1,425° C*

[VS=very strong, S=strong, M=medium, W=weak, VW=very weak]

$3CaO.Al_2O_3$ (McMurdie)		$3CaO.Al_2O_3$-$Na_2O.8CaO.3Al_2O_3$-$2CaO.SiO_2$ mixture [1]		$Na_2O.8CaO.3Al_2O_3$ (Brownmiller and Bogue)	
dÅ	Estimated intensity	dÅ	Estimated intensity	dÅ	Estimated intensity
3.34	VW	3.41	W	3.37	W
		3.33	VW		
2.70	VS	2.69	VS	2.68	VS
2.39	W	2.42	W	2.41	W
		2.37	W	2.37	W
2.258	VW	2.27	VW		
2.200	M	2.196	M	2.20	S
2.039	VW	2.036	W	2.03	W
1.984	VW				
1.951	VW	1.958	VW		
1.907	S	1.918	S	1.915	S
		1.888	M	1.888	S
1.826	VW	1.745	VW	1.746	W
1.556	S	1.564	S	1.558	VS
		1.547	M		
1.346	M	1.356	W	1.347	M
		1.346	M		
1.206	M	1.213	M	1.210	M
		1.197	W		
1.106	W	1.102	W	1.103	W
1.023	M	1.023	M	1.019	[2] M
		1.015	M		

[1] Lines corresponding to those of $2CaO.SiO_2$ are omitted.
[2] Very broad.

These microscopical and X-ray data are limited, but it seems justifiable to conclude that at temperatures below that of liquid formation in the system Na_2O-CaO-Al_2O_3-SiO_2, $3CaO.Al_2O_3$, and $Na_2O.8CaO.3Al_2O_3$ may combine under suitable conditions to form a solid solution phase having intermediate optical properties and a crystal structure similar to that of $Na_2O.8CaO.3Al_2O_3$.

In the majority of the compositions studied in this investigation the $2CaO.SiO_2$ possessed optical properties corresponding to those of the β form. In a few cases, however, as in the sytem $2CaO.SiO_2$-

aO-$Na_2O.Al_2O_3$, the $2CaO.SiO_2$ appeared to be one of the α-$2CaO.SiO_2$ olid solutions described in a previous paper [6]. No definite region f occurrence for this phase in contrast to β-$2CaO.SiO_2$ was observed, nd the amounts of Na_2O and Al_2O_3 in solid solutions were not deter- ined. Consequently in the tables and diagrams the two forms of $CaO.SiO_2$ are not differentiated.

Measurements of indices of refraction have indicated that solid olution of Na_2O and Al_2O_3 may occur to a limited extent in $2CaO.SiO_2$ [6]. There is evidence that such solid solution may lso take place in the ternary system Na_2O-CaO-SiO_2. Preliminary xperiments with compositions along the join $2CaO.SiO_2$-$Na_2O.$- $aO.SiO_2$ have given apparently a single phase up to a molar ratio f 1 $Na_2O.CaO.SiO_2$ to 14 $2CaO.SiO_2$. It was at first thought that his might represent a new ternary compound of the approximate ormula $Na_2O.29CaO.15SiO_2$. It has a complexly twinned structure ery similar to that of the $K_2O.23CaO.12SiO_2$ phase described by aylor [16]. However, the powder diffraction patterns obtained for he Na_2O phase have always corresponded to that of β-$2CaO.SiO_2$, ith a slight shift of some of the lines. Consequently, it must be oncluded that it is not a distinct compound but rather a solid solution hase. As mentioned in the previous paper [6], it is probable that he twinning results from the inversion of the $2CaO.SiO_2$ from the to the β form.

3. APPLICATIONS TO PORTLAND CEMENT CLINKER

The results of this investigation are limited in their application o commercial portland cement by the fact that one of the major omponents of clinker, Fe_2O_3, has been excluded. Furthermore, he exact effect of a number of the minor components is not yet known. Nevertheless, on the basis of present information, it is possible to each a much more definite conclusion than heretofore regarding the tate of the Na_2O in clinker. A number of possibilities are indicated, epending not only on the composition of the clinker, but perhaps even ore on the heat treatment which it receives.

If cooling has been rapid so that glass is present in the clinker, some f the Na_2O will always be found in this glass. The percentage of Na_2O occurring in this manner will depend upon individual conditions, ut some indication may be obtained from the phase equilibrium ata for the Na_2O-CaO-Al_2O_3-SiO_2 system. For example, a glass esulting from the quenching of a liquid near in composition to that f point 1 contains approximately 3.5 percent Na_2O. However, if his same melt is allowed to crystallize independently until the com- osition of the remaining liquid approaches that of point 5, and then s quenched, the resulting glass will contain upward of 8 percent Na_2O.

The results thus far obtained indicate that when the cooling takes lace at a slower rate, some of the Na_2O in a clinker may crystallize as he compound $Na_2O.\ 8CaO.3Al_2O_3$, or more likely as a solid solution hase of this compound and $3CaO.Al_2O_3$. It is probable that this hase is closely related to the "prismatic dark interstitical" material ound in some commercial portland cement clinkers. The compound, $Na_2O.8CaO.3Al_2O_3$ has been observed in the present work to form rismatic crystals when the cooling rate was suitable, and Taylor [17] has shown that the dark prismatic phase of clinker is closely related to

$3CaO.Al_2O_3$. Although he found no proportionality between the percentage of alkali in a clinker and the amount of the dark prismatic phase which may be produced, the presence of either Na_2O or K_2O appears to be necessary for its formation.

The fact that $2CaO.SiO_2$ can form solid solutions containing Na_2O makes this another possible manner of occurrence in clinker. The opinion was expressed in a previous paper [6] that because of their instability, the α-$2CaO.SiO_2$ solid solutions which may be formed at clinkering temperatures, probably are not present in normaly cooled clinker. However, since the material held in solid solution at the higher temperature is precipitated as inclusions in the $2CaO.SiO_2$ grains when they invert to the β form, some of the Na_2O will be contained in these inclusions. This fact may be of importance in the hydration of cement, since β-$2CaO.SiO_2$ hydrates slowly and the alkali imbedded in the grains might be protected from the action of the water for considerable lengths of time.

Addition of Na_2O to the system CaO-Al_2O_3-SiO_2 was found to result in an enlargement of the primary phase region of CaO. This is evident from an examination of figures 2, 3, 4, and 5. This is important since it means that certain compositions in the alkali-free system would not contain free CaO at clinkering temperatures, but after addition of Na_2O would contain stable CaO. In this way Na_2O can affect adversely the combination of the CaO in the cement mix.

V. SUMMARY

The portion of the quaternary system Na_2O-CaO-Al_2O_3-SiO_2 of importance to portland cement technology has been studied by the quenching method. The phase equilibrium data are presented in the form of tables and phase diagrams, and features of interest are discussed.

Mixtures located in three definite composition planes passing through the four-component tetrahedron, as well as a number of additional compositions, were investigated. A total of 12 crystalline compounds were observed to have primary phase volumes within this portion of the system.

Five of the quaternary invariant points occurring in this part of the system have been located approximately. Of these only one is a eutectic; the other four are reaction points. It was found that $2CaO.SiO_2$, $3CaO.SiO_2$, $3CaO.Al_2O_3$, and $Na_2O.8CaO.3Al_2O_3$ are capable of coexisting with liquid at one of these reaction points. The temperature of this point is 1,440° ±10°C and the composition is 3.5 percent Na_2O, 55.2 percent CaO, 31.0 percent Al_2O_3, and 10.3 percent SiO_2.

Evidence was obtained indicating that at temperatures below that of liquid formation, $3CaO.Al_2O_3$ and $Na_2O.8CaO.3Al_2O_3$ may combine under suitable conditions to form a solid solution phase of intermediate properties and crystal structure.

Based on present information, and necessarily ignoring the effect of Fe_2O_3 and minor components, it is concluded that the Na_2O in portland cement clinker may occur in several possible ways, depending on individual conditions:

1. As a component of glass.

2. As $Na_2O.8CaO.3Al_2O_3$ or a solid solution of that compound with $3CaO.Al_2O_3$. Such a phase may be associated with the prismatic dark interstitial material frequently observed in clinker.

3. As a solid solution of a soda-bearing phase in $2CaO.SiO_2$.

4. As inclusions of a soda-bearing phase in β-$2CaO.SiO_2$ produced by ex-solution on inversion from α-$2CaO.SiO_2$.

VI. REFERENCES

[1] W. C. Hansen, J. Am. Chem. Soc. **50,** 3081 (1928).
[2] H. F. McMurdie and H. Insley, J. Research NBS **16,** 467 (1936) RP884.
[3] H. Insley and H. F. McMurdie, J. Research NBS **20,** 173 (1938) RP1074.
[4] G. A. Rankin and F. E. Wright, Am. J. Sci. [4] **39,** 1 (1915).
[5] L. T. Brownmiller and R. H. Bogue, BS J. Research 8, 289 (1932) RP414; Am. J. Sci. [5] **23,** 501 (1932).
[6] K. T. Greene, J. Research NBS **32,** 1 (1944) RP1570.
[7] F. M. Lea and T. W. Parker, Trans. Roy. Soc. (London) [A] **234,** 1 (1934).
[8] J. F. Schairer, J. Am. Ceram. Soc. **25,** 241 (1942).
[9] L. T. Brownmiller, Am. J. Sci. [5] **29,** 260 (1935).
[10] W. C. Taylor, J. Research NBS **21,** 315 (1938) RP1131.
[11] E. T. Carlson, BS J. Research **7,** 893 (1931) RP381.
[12] E. Jänecke, Zement **21,** 377 (1932).
[13] W. Eitel, Physicalische Chemie der Silikate, 2d ed., p. 735, (J. A. Barth, Leipzig, 1941).
[14] R. H. Bogue, Symposium on the Chemistry of Cements, p. 65 (Royal Sweedish Institute for Engineering Research, Stockholm, 1938).
[15] H. F. McMurdie, J. Research NBS **27,** 499 (1941) RP1437.
[16] W. C. Taylor, J. Research NBS **27,** 311 (1941) RP1421.
[17] W. C. Taylor, J. Research NBS **30,** 329 (1943) RP1536.
[18] W. Bussem and A. Eitel, Z. Krist. [A] **95,** 175 (1936).
[19] K. Lagerquist, A. Wallmark and A. Westgren, Z. anorg. allgem. Chem. **234,** 1 (1937).
[20] W. Bussem, Symposium on the Chemistry of Cements, p. 149 (Stockholm, 1938).
[21] T. Thorvaldson and W. G. Schneider, Canadian J. Research **19,** 109 (1941).

WASHINGTON, October 18, 1945.

○